

**Antifouling Tuneable Functional Copolymers for Optimized
Hydrophilic-Hydrophobic Characteristics for Biomedical
Applications**



By

Aimon Qureshi

(Registration No: 00000327776)

Department of Materials Engineering

School of Chemical and Materials Engineering

National University of Sciences & Technology (NUST)

Islamabad, Pakistan

(2024)

Antifouling Tuneable Functional Copolymers for Optimized Hydrophilic-Hydrophobic Characteristics for Biomedical Applications



By

Aimon Qureshi

(Registration No: 00000327776)

A thesis submitted to the National University of Sciences and Technology, Islamabad,

in partial fulfillment of the requirements for the degree of

Master of Science in
Materials Engineering

Supervisor: Dr. Nasir M. Ahmad

Co Supervisor: Dr. Talha Masood

School of Chemical and Materials Engineering

National University of Sciences & Technology (NUST)

Islamabad, Pakistan

(2024)



THESIS ACCEPTANCE CERTIFICATE

Certified that final copy of MS thesis written by Ms **Aimon Qureshi** (Registration No 00000327776), of School of Chemical & Materials Engineering (SCME) has been vetted by undersigned, found complete in all respects as per NUST Statues/Regulations, is free of plagiarism, errors, and mistakes and is accepted as partial fulfillment for award of MS degree. It is further certified that necessary amendments as pointed out by GEC members of the scholar have also been incorporated in the said thesis.

Signature: _____

Name of Supervisor: **Dr Nasir M. Ahmad**

Date: _____

06-May-2024

Signature (HOD): _____

Date: _____

4/5/24

Signature (Dean/Principal): _____

Date: _____

8-5-2024



Form TH-1

National University of Sciences & Technology (NUST)

MASTER'S THESIS WORK

Formulation of Guidance and Examination Committee (GEC)

Name: Aimon Qureshi NUST Reg No: 00000327776
 Department: Department of Materials Engineering Specialization: Master of Science in Nanoscience and Engineering
 Credit Hour Completed: 24.0 CGPA: 3.25

Course Work Completed

S/No:	Code:	Title:	Core/Elective:	CH:	Grade:
1.	RM-898	Research Methodology	Additional	2.0	Q
2.	NSE-813	Essentials of Nanoscience and Engineering	Compulsory	3.0	B
3.	CHE-815	Nano Catalysis	Compulsory	3.0	B
4.	MSE-854	Characterization Of Materials	Compulsory	3.0	C
5.	MSE-856	Nano Material and Processing	Compulsory	3.0	B
6.	MSE-872	Composite Materials	Elective	3.0	B+
7.	MSE-954A	Advanced Characterization Of Materials	Elective	3.0	B
8.	MSE-854	Characterization Of Materials	Improve	3.0	B+
9.	NSE-812	Environmental Nanotechnology	Elective	3.0	A
10.	CHE-816	Molecular Nanotechnology	Elective	3.0	B

Date 12 - Dec - 2022

Student's Signature

Thesis Committee

- Name: Nasir Mahmood Ahmad (Supervisor)
Department: Department of Materials Engineering
- Name: Muhammad Talha Masood (Cotutor)
Department: Department of Materials Engineering
- Name: Mohsin Saleem (Internal)
Department: Department of Materials Engineering
- Name: Farhan Javaid (Internal)
Department: Department of Materials Engineering
- Name: Asad Ullah Khan (Internal)
Department: Department of Chemical Engineering

Signature

Signature

Signature

Signature

Signature

Date: 12 - Dec - 2022

Signature of Head of Department:

APPROVAL

Date: 12 - Dec - 2022

Signature of Dean/Principal:



National University of Sciences & Technology (NUST)

FORM TH-4

MASTER'S THESIS WORK

We hereby recommend that the dissertation prepared under our supervision by
Regn No & Name: 00000327776 Aimon Qureshi

Title: Antifouling Tunable Functional Copolymer for Optimized Hydrophobic/Hydrophilic
Characteristics for Bio Medical Applications.

Presented on: 25 Apr 2024 at: 1430 hrs in SCME Seminar Hall

Be accepted in partial fulfillment of the requirements for the award of Masters of Science
degree in Nano Science & Engineering.

Guidance & Examination Committee Members

Name: Dr Mohsin Saleem

Signature: Mohsin

Name: Dr Farhan Javaid

Signature: Farhan Javaid

Name: Dr Asad Ullah Khan

Signature: Asad Ullah Khan

Name: Dr M. Talha Masood (Co-Supervisor)

Signature: M. Talha Masood

Supervisor's Name: Dr Nasir M. Ahmad

Signature: Nasir M. Ahmad

Dated: 30th April 2024

fo
Head of Department

Date 02-05-24

AS
Dean/Principal

Date 2.5.2024

School of Chemical & Materials Engineering (SCME)

AUTHOR'S DECLARATION

This is to certify that “Antifouling tuneable functional Copolymer for optimized hydrophobic/hydrophilic characteristics”, submitted by Aimon Qureshi in partial fulfilment of requirement of degree of Master of science in Nano science Engineering At National university of science and engineering is an original and independent work carried out under the supervision of Dr.Nasir M Ahmed.

The work presented in this thesis has not been submitted for any other degree or qualification at any other institute All sources used or referred to in thesis have been duly cited and acknowledged. All material reproduce from other sources have been appropriately reference.

Aimon Qureshi

NUST 2024

PLAGIARISM UNDERTAKING

I solemnly declare the research work presented in the thesis titled “**Antifouling Tuneable Functional Copolymers for Optimized Hydrophilic-Hydrophobic Characteristics for Biomedical Applications**” is solely my research work with no significant contribution from any other person. Small contribution/help wherever taken has been duly acknowledged and that complete thesis has been written by me.

I understand the zero-tolerance policy of the HEC and university “**National University of Sciences and Technology**” towards plagiarism. Therefore, I as an Author of the above titled thesis declare that no portion of my thesis has been plagiarized and any material used as reference is properly referred/cited.

I undertake that if I am found guilty of any formal plagiarism in the above titled thesis even after award of MS degree, the university reserves the right to withdraw/revoke my MS degree and that HEC and the university has the right to publish my name on the HEC/ University Website on which names of students are placed who submitted plagiarized thesis.

Student / Author Signature:



Name: **Aimon Qureshi**

DEDICATION

This thesis is dedicated to my family for their tremendous support and cooperation led me to this wonderful accomplishment.

ACKNOWLEDGEMENTS

All praises to Almighty Allah, the authority of knowledge and creator of resources, skills and opportunities.

First, I would like to express my gratitude to my Supervisor Dr. Nasir M. Ahmed for their invaluable guidance, support throughout my journey of research work.

I am deeply thankful to my family for their unwavering love, encouragement and understanding during this challenging journey, Their belief in me kept me motivated to strive for excellence

I am grateful to the friends and colleagues for their support and encouragement and valuable discussion throughout the process.

Lastly, I would like to acknowledge the countless researcher, scholars and authors whose work has paved the way for this study.

TABLE OF CONTENTS

ACKNOWLEDGEMENTS	ix
LIST OF TABLES	xiv
LIST OF FIGURES	xv
LIST OF ABBREVIATIONS	xvii
ABSTRACT	xviii
CHAPTER 1: INTRODUCTION	1
1.1 Background	1
1.2 Antibiofouling Materials	2
1.3 Amphiphilic Copolymer as Antifouling Polymer	2
1.4 Layer by Layer (SAMs) as Antimicrobial	3
1.5 Problem Statement	3
1.6 Research Framework	4
<i>1.6.1 Part 1</i>	4
<i>1.6.2 Part 2</i>	4
<i>1.6.3 Part 3</i>	4
1.7 Aims & Objectives	5
CHAPTER 2: LITERATURE REVIEW	6
2.1 Fouling	6
2.2 Bio Fouling	6
2.3 Mechanism of Biofouling	6
2.4 Fields Susceptible to Biofouling	7
2.5 Main Factors Affecting Biofouling	8
<i>2.5.1 Surface Condition</i>	8
<i>2.5.2 Fouling Settlement</i>	9
<i>2.5.3 Biofilm Composition</i>	9

2.6 Antifouling Copolymers	10
2.7 Chemical Nature of Antifouling Polymer	11
2.7.1 <i>Hydrophilic Polymer</i>	11
2.7.2 <i>Amphiphilic Polymers</i>	12
2.7.3 <i>Zwitterionic Polymers</i>	13
2.8 Free Radical Polymerization	13
2.8.1 <i>Initiation</i>	14
2.8.2 <i>Propagation</i>	14
2.8.3 <i>Termination</i>	14
2.9 Methods to Incorporate Antifouling Properties	15
2.10 Mechanism of Antifouling Polymers	16
2.10.1 <i>Bio Passive / Static Copolymer</i>	16
2.10.2 <i>Bio Active Copolymer</i>	18
2.11 Components used in Copolymerization	19
2.11.1 <i>Acrylic Acid (AA)</i>	19
2.11.2 <i>Methyl Methacrylate (MMA)</i>	19
2.11.3 <i>Tetrahydrofuran (THF) Solvent</i>	20
2.11.4 <i>2,2-Azobisisobutyronitrile (AIBN)</i>	20
2.12 Layer by Layer Self Assembly	21
2.12.1 <i>Thin Films Properties</i>	22
2.12.2 <i>Advantage of Thin Film</i>	22
2.13 Polyelectrolytes	23
2.13.1 <i>Classification of Polyelectrolyte</i>	23
i. Strong polyelectrolyte:	23
ii. Weak polyelectrolyte:.....	23
2.14 pH Sensitive Behavior of Poly (Acrylic Acid) (PMMA-co-PAA) and Poly (DADMAC) (PAH)	23

CHAPTER 3: METHODOLOGY AND CHARACTERIZATION	26
3.1 Materials	26
3.1.1 <i>For Bacterial Growth</i>	26
3.2 Equipment and Characterization Tool for Copolymerization	26
3.3 Methods	27
3.3.1 <i>Synthesis of Copolymer P(MM-Co-AA)</i>	27
3.3.2 <i>Work Scheme</i>	28
3.4 LBL (SAMS) Dip Coating Method	29
3.4.1 <i>Materials used for thin film Fabrication</i>	30
3.4.2 <i>Fabrication of Thin Film</i>	32
3.4.2.1 <i>Cleaning of Glass Substrate</i>	32
3.4.2.2 <i>General Process for LBL Assembly</i>	32
3.5 pH Responsive Behavior of Model PAA	32
3.6 Sample Preparation for Thin Film Fabrication	33
3.7 Characterizations	35
3.7.1 <i>Characterization of Copolymer</i>	35
3.7.1.1 <i>FTIR</i>	35
3.7.1.2 <i>TGA (Thermogravimetric Analysis)</i>	36
3.7.1.3 <i>DSC (Differential Scanning Calorimetry)</i>	36
3.8 Characterization of Thin Films	36
3.8.1 <i>Antimicrobial Testing</i>	36
3.8.2 <i>Optical Microscopy</i>	37
3.8.3 <i>Optical Profilometry</i>	37
3.8.4 <i>Contact Angle Measurement</i>	38
CHAPTER 4: RESULTS AND DISCUSSIONS	39
4.1 ATR-FTIR	39
4.2 Thermo Gravimetric Analysis (TGA)	42

4.3 Differential Scanning Calorimetry (DSC)	45
4.5 Contact Angle Measurement	49
4.6 Optical Profilometry	57
4.7 Optical Microscopy	65
4.8 Antimicrobial Testing of the Thin Films	67
<i>4.8.1 Bacteria Repulsion and Attraction Study on Switchable Surface Coatings:</i>	69
<i>4.8.2 Bacterial repellent thin films on the basis of surface charge and Ionization degree:</i>	69
<i>4.8.3 Bacterial attraction thin films:</i>	69
CHAPTER 5: CONCLUSION AND FUTURE RECOMENDATIONS	72
5.1 Conclusion	72
5.2 Future Recommendations	72
BIBLIOGRAPHY	73

LIST OF TABLES

Table 2.3: Active Action Polymers for The Antimicrobial Applications[12].	18
Table 3.2: Depicting the Structural Formulas of Polymers Being Used in Thin Film Fabrication	31
Table 3.3: Characterizations Done for Copolymer and for Thin Film SAMs.	35
Table 4.1: Melting Temperature of Common Polymers.	48
Table 4.2: 15 BL Samples (PAH Top Layer shows less Hydrophilicity).	51
Table 4.3: 15 BL Samples (PDAC as the Top Layer).	52
Table 4.4: 15 BL Samples (PP50 as the Top Layer provide Lowest Contact Angle Values with more Hydrophilicity)	53

LIST OF FIGURES

Figure 1.1: Schematic illustration of Amphiphilic copolymer as Antimicrobial	3
Figure 2.2: Describe Various Surface Parameter That Effect Bacterial Attachment.	8
Figure 2.3: Zoospores with flagella on polymeric membrane by scanning electron micrograph at a voltage of 20kv[28].	9
Figure 2.4: The Five Stages of Biofilm Development.	10
Figure 2.5: Fouling Resistant Hydrophilic Functional Groups[42].	12
Figure 2.6: Amphiphilic Pegylated Fluoroalkyl Block Copolymer Side Chains With The Antifouling Property [44].	12
Figure 2.7: Fouling resistant groups of zwitterions[48].	13
Figure 2.8: Three different approaches to provide a surface with the antifouling properties: 1) surface chemistry modification, 2) topography of surface, and 3) architecture[54].	16
Figure 2.9: The Schematic of The Reaction Mechanisms of Active Action And Passive Action of Antimicrobial Polymer[12].	16
Figure 2.10: Structural Formula of Acrylic Acid (AA)	19
Figure 2.11: Structural Formula of MMA.	20
Figure 2.12: Structural Formula of AIBN[66].	20
Figure 2.13: The Mechanism of Electrostatic LBL Self-Assembly on 2-D Substrates and 3-D Nano Templates.	21
Figure 3.1: Chemical Reaction of Copolymerization between AA and MMA.	28
Figure 3.2: Polymerization Setup.	29
Figure 3.3: General Process Describing the Thin Film Fabrication on Surface Material [68]	30
Figure 3.6: LBL Self Assembly at Different (3,7,10) pH with PDAC at Top Layer	33
Figure 3.7: LBL Self Assembly at Different (3,7,10) pH with PP50 at Top Layer	34
Figure 3.8: LBL at Different pH (3,7,10) with PAH at Top Layer.	34
Figure 3.9: ATR-FTIR (BRUKER ALPHA II FTIR).	35
Figure 3.10: Optical Microscope (Optica B-600 MET) was Used to Analyze the Adsorption of Polymer Chain.	37
Figure 3.11: Contact angle measurement device.	38
Figure 3.12: Image J* Low Bond Axisymmetric Drop Shape Analysis.	38
Figure 4.1: ATR-FTIR Spectra for Copolymer Compositions.	39

Figure 4.2: Schematic representation of the model formation of hydrophilic PMMA-co-PAAS composite films as adopted from sources.	42
Figure 4.3: TGA Spectra for Copolymer Compositions.	43
Figure 4.4: DSC Spectra for Copolymer Compositions.	45
Figure 4.5: Structural Formula of Poly (Acrylic Acid) and Poly (Di-Acrylic Acid).	46
Figure 4.6: Depicting Specific volume w.r.t temperature. On cooling from liquid melt, total amorphous (Curve A, semicrystalline (Curve B), and crystalline (Curve C) polymers observed.	47
Figure 4.7: Normal Melting and Glass Transition Temperature.	47
Figure 4.8: The Young Equation Represented on an Ideal Surface, Together with The Equilibrium (Or Static) Contact Angle θ_E	49
Figure 4.9: Depicting by Increasing No of Bilayers, The Value of Contact Angle Decreased.	50
Figure 4.10: Shows Increasing the Value of pH (10) Contact Angle Value Decreased.	52
Figure 4.19: By Increasing number of LBL Bilayers, the Average Roughness Value Increased.	62
Figure 4.20: 10 BL Samples (PAA50 as the Top Layer)	62
Figure 4.21: 10 BL Samples (PDAC as the Top Layer)	63
Figure 4.22: Bilayers Effect on Surface Roughness of The Self-Assembled Multilayers Films.	64
Figure 4.23: Tuneable pH Effect on The Surface Roughness of The Self-Assembled Multilayers Films.	64
Figure 4.24: Optical Microscopic (OM) Images of 1, 5 and 10 BL at 100X Magnification.	67
Figure 4.25: More Negative Charge Toward Substrate Produces More Repulsive Substrate for Microbial Attachment and Vice Versa.	68
Figure 4.26: Number Of Bacterial Attachments Increases with The Number of Bilayers as Bacterial Get More Surface Area to Attached to Substrate.	68
Figure 4.27: PMMA-Co-PAA Polymer-Based Thin Film Antimicrobial Mechanisms Illustrate the Role of Attractive and Repulsive Nature. With Increase in PMMA Amount in Copolymers, There is a Possibility of More Adhesion; At Higher pH with Highly Charged Anionic Chain can Perform Repulsive Action to Foulants.	71

LIST OF ABBREVIATIONS

CDC	Centre of disease control
BL	Bilayers
LBL	Layer by Layer
S. aureus	Staphylococcus aureus
E.coli	Escherichia coli
°C	Degree centigrade
Rpm	Rotations per minute
OM	Optical Microscopy
OP	Optical Profilometry
SEM	Scanning Electron Microscopy
AFM	Atomic Force Microscopy
µm	Micrometer
mV	Millivolts
mM	Millimolar
Mg	Milligram
SAMu	Self-assembled multilayers
+ve	Positive
-ve	Negative
PAA	Poly (acrylic acid)
PAH	Poly (allylamine hydrochloride)
APTMS	3-aminopropyltrimethoxysilane toluene
PDADMAC	Poly (diallyldimethyl ammonium chloride)

ABSTRACT

Present project aims a molecular fabrication approach to study the behaviour of foulants on planar surfaces at specifically controlled pH for the polymeric thin films coatings fabricated by electrostatic layer-by-layer (LBL) assembly methods. Copolymers of polymethyl methacrylate PMMA and Poly (acrylic acid) (PAA, a weak polyanion) were synthesized with various compositions as PMMA-co-AA 70, 50 and 30%. These are employed as polyanion with poly(diallyl dimethylammonium chloride) (PDADMAC, a strong polycation) were used to build up the bulk films. The PDADMAC and in certain cases PAH was applied as a top layer in bacterial adhesive thin films. Surface charge tuning was accomplished by controlling the level of ionization of the weak polyelectrolytes at different pH values and subsequent manipulation of the amount of polyelectrolyte deposited in the one preceding the last and last layers, respectively. The prepared films were investigated for their antimicrobial and bacterial surface characteristics and role of hydrophilic and hydrophobic characteristics were discussed. The fouling behaviour of bacteria on the LBL films with similar hydrophilicity and roughness but different surface charge densities was studied. Antimicrobial activity of coated glass slides was evaluated against *Escherichia coli* (E. coli, ATCC# 8739) and *Staphylococcus aureus* (S. aureus, ATTC# 6538). The switchable thin films coatings developed allows achieving optimal microbial growth both in terms of repelling and adhesion performances at the specific pH values of the environment. The surface characteristics of the foulants as well as the bacterial adhesive thin films can be used to switchable attach or repel and detect control concentration of bacterial strains.

Keywords: Copolymerization, Polymeric thin films, Electrostatic layer-by-layer (LBL) assembly method, Polyelectrolytes, Surface charge tuning, Bacterial adhesive thin films, Antimicrobial coatings, Hydrophilicity.

CHAPTER 1: INTRODUCTION

1.1 Background

Polymers are large macromolecules made up of small repeating units known as monomers[1]. Polymers are naturally occurring and synthetic as well, plastic is one form of synthetic polymer. Several biological, synthetic and hybrid polymers are employed in a variety of medicinal applications. Polymers based on their composition classified into homopolymer & copolymer [2].

Copolymers which contain hydrophobic and hydrophilic part in them are called amphiphilic Copolymer [3].Amphiphilic copolymers effectively suppress bacterial development; they are acknowledged as significant biomaterials and are employed as antibacterial agents. Amphiphilic copolymers are attractive candidate for variety of applications particularly in medical field [3], [4].

Biofouling cause adverse effects on many applications like marine, industrial & particularly in medical field. Biofouling in medical field involves the formation of biofilm so this phenomenon is serious health and cost concern. Implant rejection, biosensor malfunction and propagation of infectious diseases are among the issue [5].

For both patients and medical staff, hospital-acquired infections resulting from implanted polymeric medical devices continue to be a significant concern. These infections frequently result from biofilm buildup on the device, which is challenging to remove and typically calls for both antibiotic treatment and device removal.

The National Healthcare Safety Network of the Centres for Disease Control and Prevention [6](CDC) revealed 1 out of 25 patients reports HAIs (Healthcare-associated infections), furthermore it is estimated that UTIs (urinary tract infection) represent 30–40% of healthcare-associated infections (HAIs) globally.

There is need to create functional polymeric coatings/devices with antimicrobial or antifouling qualities that inhibit or kill bacteria in close proximity to the device surface, or that restrict the initial attachment of proteins and bacteria, thereby limiting the formation of biofilms and subsequent infections.[7].

One of the choices to inhibit microbes on some surface is to use the biocides[6]. Bio active substances are commonly used for inhibition of microbes but they have adverse effect associated with them they target other cell with the microbes so they may be the root cause of other diseases as well and they are also poorly degradable [8] .Bacteria and proteins are charged entities so it is important to study electrostatic interaction in order to minimize their attachment on a substrate or it can be a basic requirement to prepare low fouling materials [9].

Electrostatic LBL (SAMs) is a convenient, cost effective and environmentally friendly method to prepare polymer films with desirable surface characteristics. Antimicrobial material can be synthesized by LBL films. surface properties of materials can be modified by taking suitable material choice and by adjusting the surface parameter of which the material is to be deposited[10].

1.2 Antibiofouling Materials

Biofouling is unwanted growth of microorganism protein & cells on a substrate, due to adverse effect of biofouling, Researchers try to develop such materials which have ability to stop them in their earlier stage by killing them or by stopping their attachment on substrate.

Recent publications have included evaluations on the creation and use of antifouling surfaces, including synthetic polymers like PEG (poly ethylene glycol), zwitterionic polymers & fouling release coatings. Despite the fact that materials with strong antibiofouling properties are documented but limitations are still associated with them as well like they lost their functionality with any physical (detachment) & chemical change (deterioration with oxygen & water), therefore development of long lasting antibiofouling is crucial [11].

1.3 Amphiphilic Copolymer as Antifouling Polymer

Different polymers have been developed for gram positive & negative bacteria, yeast & viruses [12]. Antimicrobial have garnered a lot of interest in clinical studies. Antimicrobial polymers to their small molecular counterparts, the former demonstrated higher efficacy, less toxicity, fewer environmental concerns, and enhanced resistance[13].

As for now, amphiphilic polymers with antifouling behavior are in practice [14].

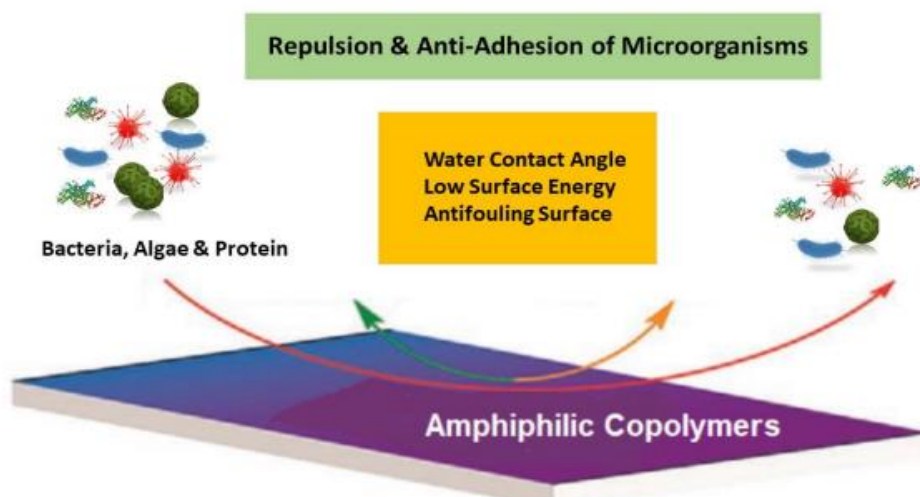


Figure 1.1: Schematic illustration of Amphiphilic copolymer as Antimicrobial

1.4 Layer by Layer (SAMs) as Antimicrobial

Layer by layer SAMs are used to deposit oppositely charged materials on their surface. Different approaches now made to study the effect of surface charge on fouling properties [10], [15]. Physical parameters can also be manipulated like mechanical properties, thickness and surface charges by altering the parameter like pH and ionic strength of solution. According to one of study Poly (allylamine hydrochloride)/ Poly (acrylic acid) (PAH/PAA) thin multilayers were prepared at high & low pH.

Those PAH/PAA multilayers who prepared at low pH shows swelling in physiological conditions and produce significant hydrated surfaces[9], [16], [17]. Generally , LBL films are charge balance and the top layer is used to promote or demote the protein adsorption by electrostatic interaction .it is reported that positive charges are used to kill bacteria[18]. Importantly, present strategy allows achieving optimal antimicrobial performance of a given material taking into account at specific pH values that has not yet been demonstrated in detail.

1.5 Problem Statement

Antifouling polymers are the material that resist the microorganisms attack on their surface, particularly those materials which are amphiphilic in nature they stop biofilm

formation. As the adverse effect of biofouling already been discussed so the idea was to develop functional antifouling system, because many fouling organisms share similar properties, particularly surface characteristics, it is a well-established fact from the research literature that an anti-fouling system effective against one type of microorganism, like bacteria, they may also be effective against other species, like fungus or algae.

In Pakistan biofouling covers all areas of life like food, water & bio medical so the idea was to develop such antifouling polymeric materials & surfaces which are functional, economic and nontoxic.

Secondly to produce coatings on planar LBL films at various pH to check the activity of foulant that has not been discussed in detailed earlier.

1.6 Research Framework

The work scheme was expanded into following parts:

1.6.1 Part 1

Part 1 includes successful synthesis of copolymers with different compositions in presence of inert atmosphere. Polymers used were acrylic acid and methyl methacrylate in presence of THF solvent and the AIBN initiator was used by doing Free Radical Polymerization.

1.6.2 Part 2

Prepare LBL thin films by taking different polymer a weak poly cation (PAH), a strong poly cation (PDAC). A weak poly anion PAA (PP50, synthesized polymer composition) at different working pH taking into account.

1.6.3 Part 3

1. Characterization done was FTIR to study functional group present in copolymer and TGA to check the thermal stability of prepared copolymer DSC was done to check the glass transition temperature of copolymers.

2. Characterization techniques chosen for LBL thin films was optical profilometry optical microscopy and contact angle.
3. Antimicrobial was also performed.

1.7 Aims & Objectives.

Aims & objectives of designed research framework was:

- i. Synthesis of Copolymer with different composition.
- ii. Preparation of LBL thin films at various pH
- iii. Antimicrobial testing

Purpose to fabricate copolymers was to increase the

- i. Antifouling character
- ii. Hydrophilicity

CHAPTER 2: LITERATURE REVIEW

2.1 Fouling

Fouling is intricate/unwanted phenomenon which occurs when something from atmosphere like macromolecules, suspended particles, microorganisms (algae, bacteria, proteins) stick to the surface in reversible manner [19].

2.2 Bio Fouling

The interfacial contact between microbes, plants, algae, or animals and organic substrates, followed by their buildup on moist surfaces, is known as biofouling. The major component of biofouling is the presence of bacterial colonies which are incorporated in an organic matrix made of extracellular polymeric materials (EPSs). Bacteria create EPSs which are made up of proteins and other related compounds [20].

2.3 Mechanism of Biofouling

Mechanism of biofouling involved different stages.

1. In first stage nutrient from external environment within few seconds they get attach to surface to form primary biofilm, after passing one hour, the primary colonizer gets attached to surface.
2. The second stage involve the multiplication of cells to produce an EPS. Cells proliferation is useful to enhance their thickness and structural integrity, so they get enter into maturation phase.
3. In last stage cell disperse into external environment again [20]

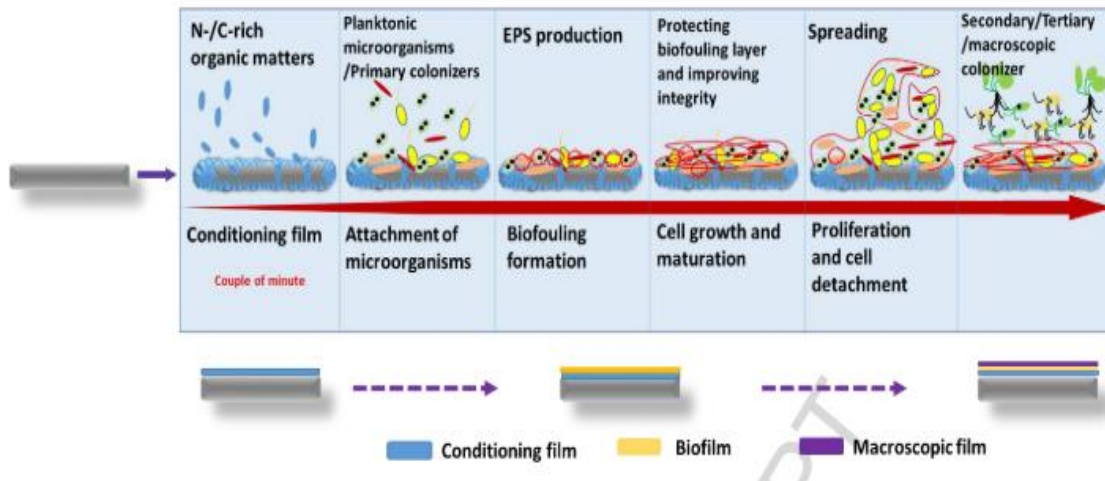


Figure 2.1: Formation of Bio Fouling. Different biofouling layers formation with time is shown with the colour band [20].

2.4 Fields Susceptible to Biofouling

A table is given below which describe the hazards associated with biofouling in different areas.

Table 2.1: Fields Susceptible to Biofouling with Common Examples [5] .

Type	Problem
1. Medical Field Orthopedic implant, Respirator, catheter	Removal owing to infection, Ventilator pneumonia, Urinary tract infection
2. Marine Ship hull, Metals	High fuel expenditure, increased cost & biocorrosion
3. Industrial Membrane, Heat exchanger, Fluid flow, drinking water, metals etc.	Reduced flux, Reduced convection efficiency, contamination, Food spoilage & health risk.

2.5 Main Factors Affecting Biofouling

2.5.1 Surface Condition

Biofilm growth at initial stage in water medium, started more readily as compared to air/solid media [21], [22].when a thin layer is adhered onto material surface .it will lead towards biofilm formation, among other unidentified elements this layer includes some organic macromolecules like amino acids, proteins, polysaccharides [23].

The formation of fouling layer occurs instantaneously by the attachment of microorganism on the surface in a nutrient rich environment while their mechanism of adsorption is still not well understood. As an illustration, the conditioning layer is thought to represent the connection between the surface and the initial adhesion; as a result, the attachment strength determines the biofilm resistance [24].

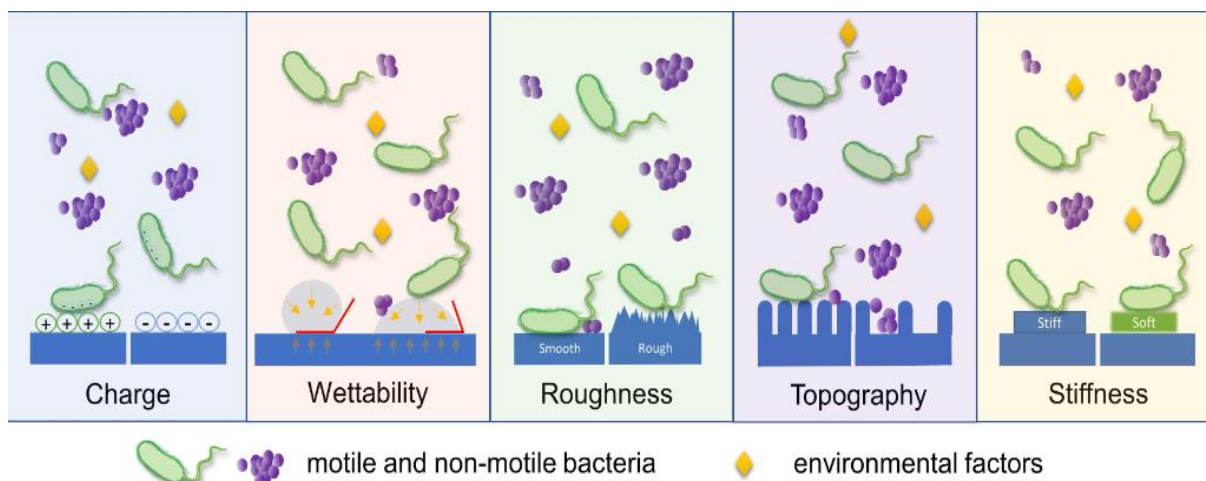


Figure 2.2: Describe Various Surface Parameter That Effect Bacterial Attachment.

Bacterial attachment is driven by various surface properties including surface charge density, wettability, roughness, topography and stiffness. This figure depicts a major reason of bacterial attachment to a single surface parameter[25].

2.5.2 Fouling Settlement

Biofilm spread with two things. first, microbes must align themselves with substrate (less than 1 nm) then they must stick to surface. physical /chemical interactions also play a role in establishment of conditioning layer after once it is formed [26]. Additionally DELVO theory of colloid stability provide idea of microorganism proliferation towards substrate [27].

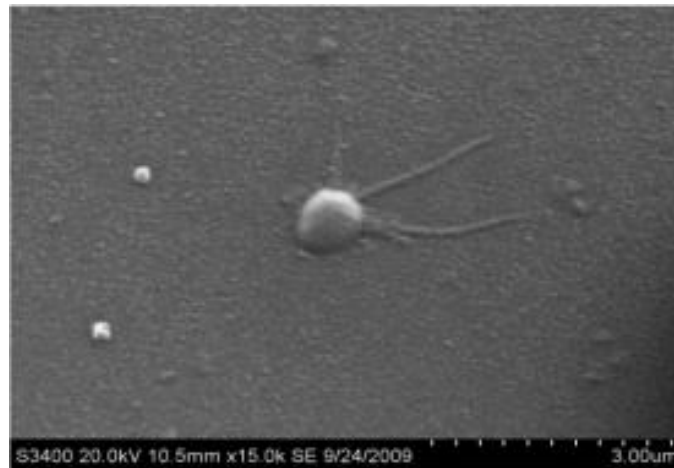


Figure 2.3: Zoospores with flagella on polymeric membrane by scanning electron micrograph at a voltage of 20kv[28].

2.5.3 Biofilm Composition

It is estimated that more than 99 percent of bacteria on earth reside in organized biofilm colonies. Bacterial biofilms are collection of cells affixed to surface encased in extracellular polymeric matrix.

Availability of nutrient, PH & temperature are some examples of environmental factors that greatly affect the biofilm composition[29].

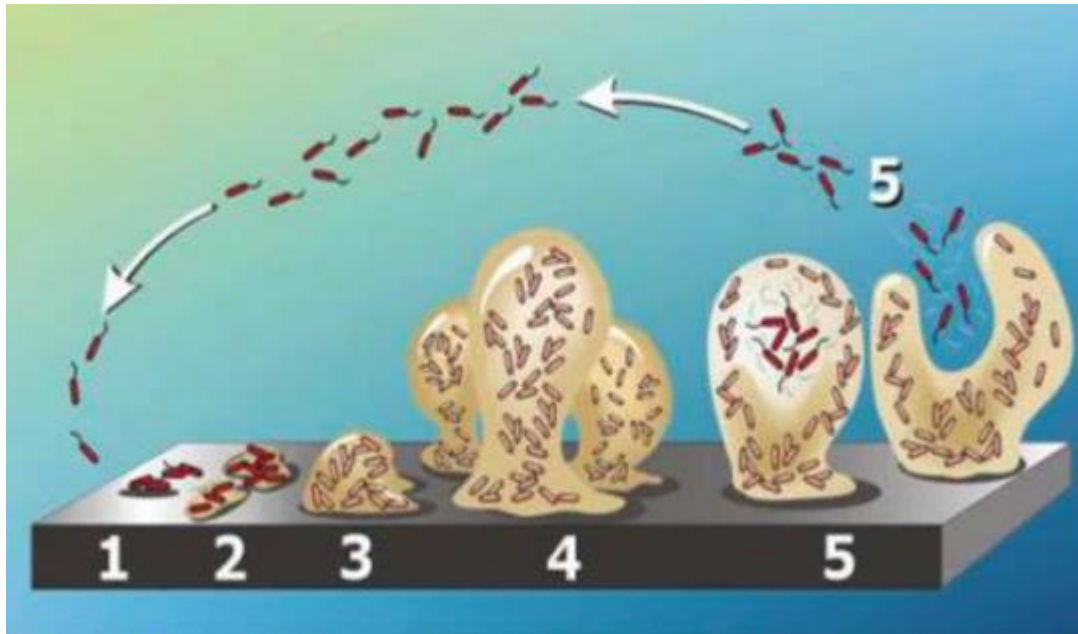


Figure 2.4: The Five Stages of Biofilm Development.

- Stage 1:** Microbes from external environment start to attach to substrate.
- Stage 2:** Bacterial cells aggregate from microcolonies, secret extracellular polymeric substances (EPS).
- Stage 3:** A biofilm produced and matured, and cells form multilayered cluster.
- Stage 4:** maturation of biofilm, providing protection against external environment.
- Stage 5:** The biofilm reaches a critical mass, and planktonic bacteria disperse to colonize another surface [29].

2.6 Antifouling Copolymers

Microorganisms like bacteria, algae are important source of infection, energy waste and financial loss. The food, pharmaceuticals and textiles are major sectors that particularly deals with antimicrobials. An antimicrobial is used to kill or resist the attachment of microbes on a substrate. A significant contributing factor to both academics and industry was the discovery of antibacterial polymer in 1965 [12], [30].

Majority of the polymeric materials are perfect for the use of antimicrobial & are able to meet multiple requirements at once ,including the lowest possible production cost, control over the chemical/physical qualities and a capacity of combine functional groups [13], [31].Antimicrobial peptide works by first breaking down the bacterial cell wall, Heparin has antiadhesive activity and add hydrophilic properties to inhibit the development of microorganisms [32], [33] .

Biofilms are difficult to remove and various biocide don't work on them [12], [34], [35], [36].It is difficult to prevent the growth of biofilm and minimize microbial adhesion than it is to eradicate microorganism in order to stop the spread of disease [37], [38]. There are two types of antifouling polymer one with active mechanism and second with passive mechanism.

This research explains new development in antifouling polymer[39], [40], [41]. furthermore in case of copolymerization, the right monomer is either hydrophilic or zwitterionic in nature which are used to regulate the production of biofilms through hydration cell, hydrophilicity, surface charge energy etc [37], [38].

2.7 Chemical Nature of Antifouling Polymer

2.7.1 Hydrophilic Polymer

Hydration cells are produced by hydrogen bonding which are essential for biofilms.[27] the cross-linkable polymer materials, the additional copolymers, P(VBCTMAM-co-AA 20)/P(DMAM-co-GMA30), was bent in a water medium and cured for 1 day at 120 °C results in formation of acrylic acid moieties of the trimethyl ammonium salt[42]. A table is given below which provide information of fouling resistant functional groups.

Hydroxyl	—OH
Ether	—CH ₂ —O—CH ₃
Amide	$\begin{array}{c} \text{H} \\ \\ \text{—C—N—CH}_3 \\ \\ \text{O} \end{array}$
Peptoid	$\begin{array}{c} \text{H}_2 \\ \\ \text{—C—C—N—} \\ \quad \\ \text{O} \quad \text{R} \end{array}$
β -Peptoid	$\begin{array}{c} \text{H}_2 \\ \\ \text{—C—C—H}_2\text{C—N—} \\ \quad \quad \\ \text{O} \quad \quad \text{R} \end{array}$
Oxazoline (Open Ring)	$\begin{array}{c} \text{—N—CH}_2\text{CH}_2\text{—} \\ \\ \text{R—C=O} \end{array}$

Figure 2.5: Fouling Resistant Hydrophilic Functional Groups[42].

2.7.2 Amphiphilic Polymers

Amphiphilic polymers comprise hydrophobic /hydrophilic constituents in them. Hydrophobic surfaces e.g. poly (dimethyl siloxane) PDMS shows ‘fouling release’ capacity while the surface of hydrophilic polymer like Poly (ethylene glycol) shows resistant to cell adhesion at low water interfaces. On a fluorinated surfaces researcher shows a significant decrease in staphylococcus aureus (p. aeruginosa) adherence as compared to control the surface [43].

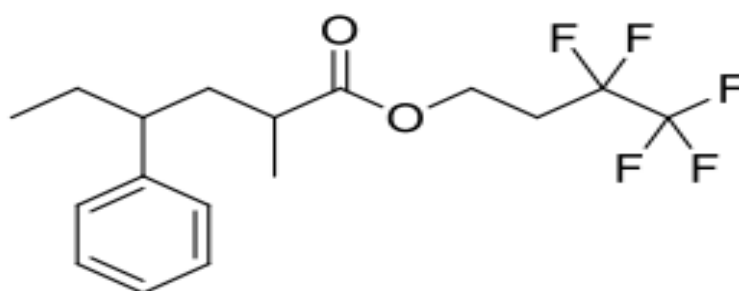


Figure 2.6: Amphiphilic Pegylated Fluoroalkyl Block Copolymer Side Chains With The Antifouling Property [44].

2.7.3 Zwitterionic Polymers

Ionic connection between polymer zwitterionic groups results in limited adherence of proteins and organisms.[45], [46]. Both carboxy betaines and zwitterion hydrophilic amide groups are examples of functional anti-fouling groups found in several anti-fouling polymers. [37], [38], [47].

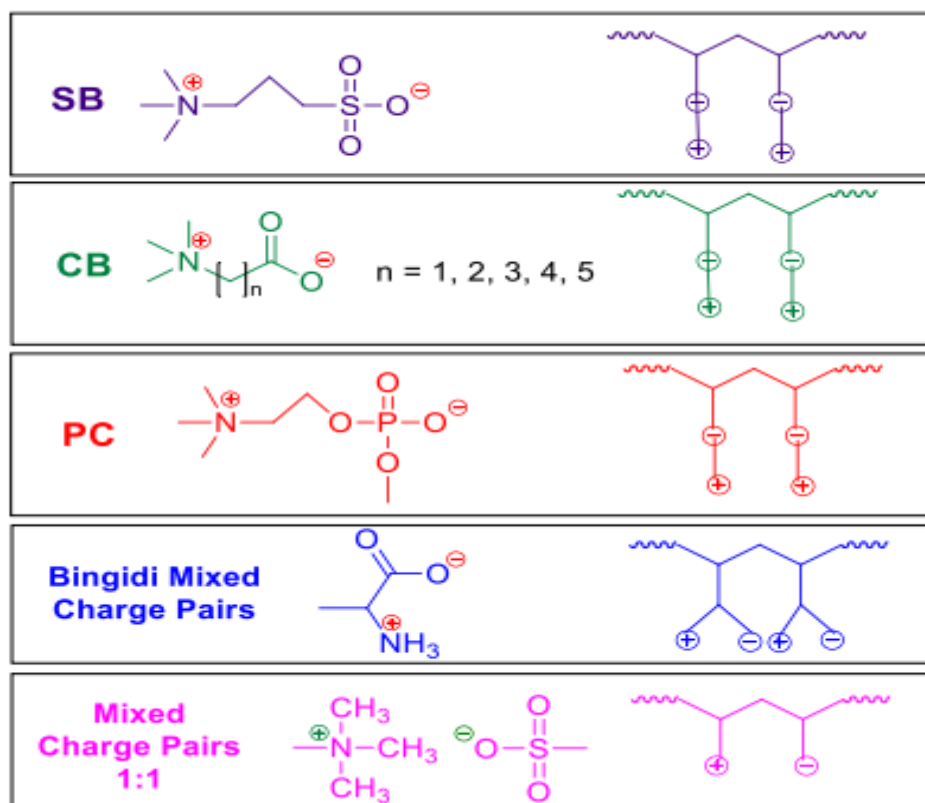


Figure 2.7: Fouling resistant groups of zwitterions[48].

2.8 Free Radical Polymerization

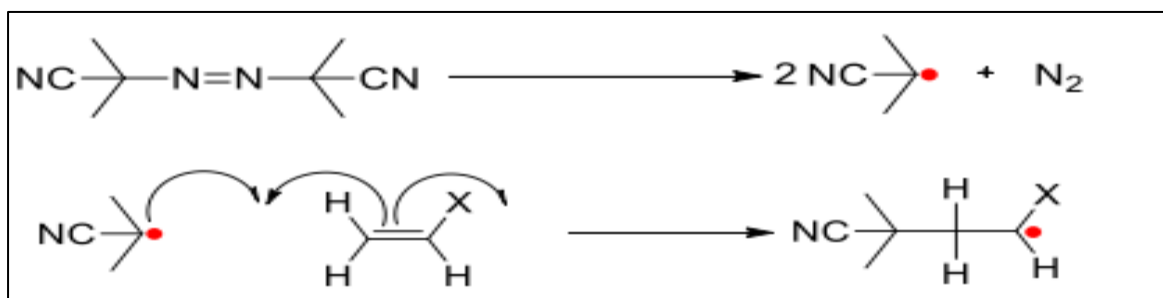
The mechanism of free radical polymerization comprises three steps.

1. Initiation
2. Propagation
3. Termination [49].

2.8.1 Initiation

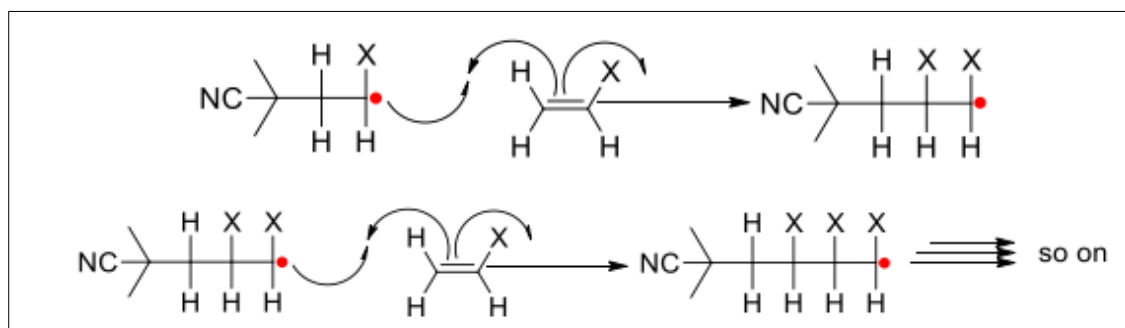
FRP initiation involves two steps.

First is the formation of free radical by thermal decomposition of initiator like AIBN. secondly free radical attack on double bond of carbon atom and starts polymerization[50].



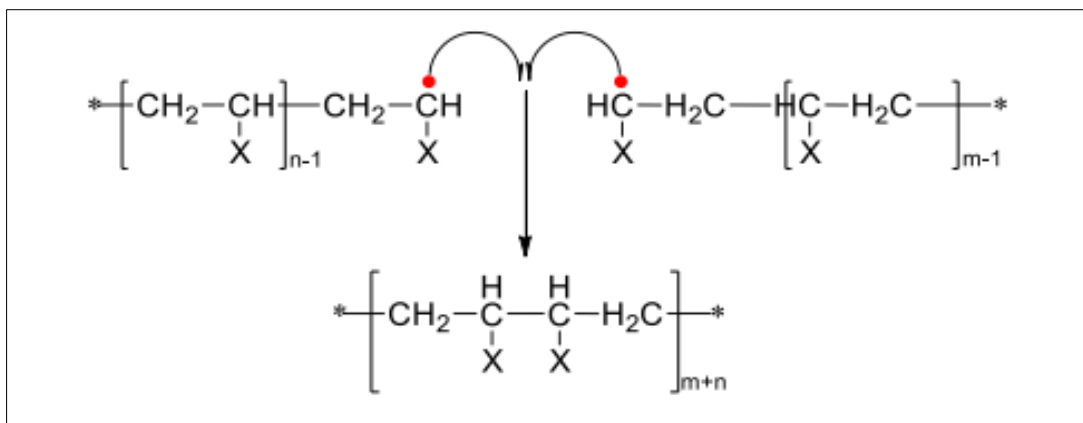
2.8.2 Propagation

Free radical adds other monomers to elongate the chain of monomers [50].



2.8.3 Termination

Two radical meet to form a single bond [50].



2.9 Methods to Incorporate Antifouling Properties

Different methods have developed e.g. change in surface chemistry, topography & architectural changes. Polymer materials are suitable for this purpose because of their low processability, controllable physical chemical properties & due to attain a variety of functional groups at a time [51].

The characteristics of foulant with surface chemistry is hydrophilic /hydrophobic, hydrogen bonding and charge [52]. The formation of a surface of interest's microstructure or nanostructure that restricts the amount of attachment points, lowering foulant adherence and facilitating simple foulant removal during colonization[53].

The most common materials used to create fouling-release coatings are hydrophobic substances like silicon and fluorine, or modelled surfaces like "Sharklet" surfaces. Although interest in the materials has shifted toward zwitterionic polymers, hydrophilic polymers such as poly (ethylene glycol), polyacrylates, and polysaccharides that were resistant to foliage have been utilized most frequently[24], [34].

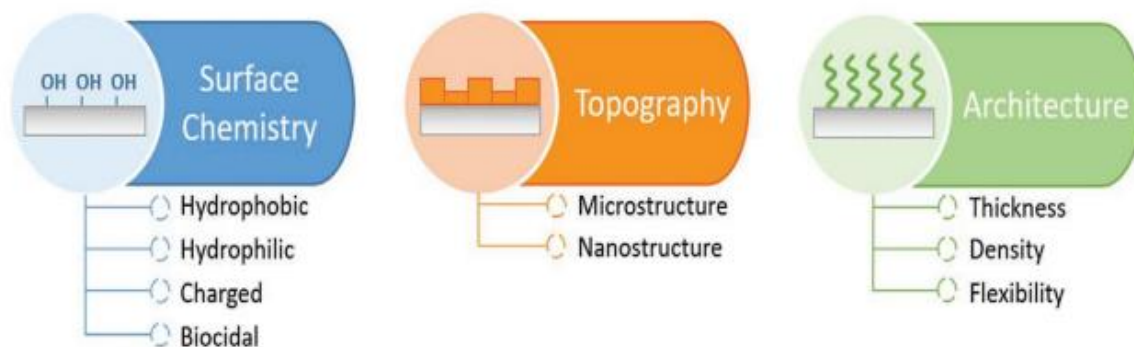


Figure 2.8: Three different approaches to provide a surface with the antifouling properties: 1) surface chemistry modification, 2) topography of surface, and 3) architecture[54].

2.10 Mechanism of Antifouling Polymers

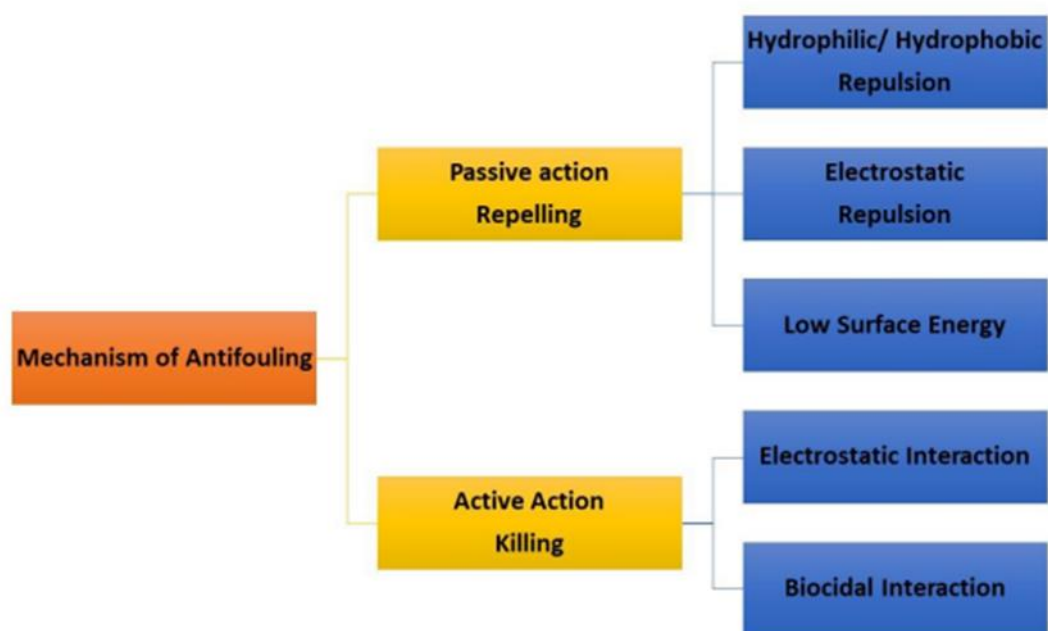


Figure 2.9: The Schematic of The Reaction Mechanisms of Active Action And Passive Action of Antimicrobial Polymer[12].

2.10.1 Bio Passive / Static Copolymer

These are the polymers that do not kill microbes but repel them due to Presence of charges on functional group[55]. Usually microbes have a negative charge, so they repel other

microbes resulting no or reduced biofilm formation [56], [57]. These copolymers/polymers can be formulated as water-soluble soft films, rigid sheets, or semi-rigid sheets either alone or in conjunction with a catalyst[20].

In passive mode of action polymers repel microorganism instead killing[53]. Passive polymers with charge and hydrophobic properties show hydrophilic characteristics that are closely correlated with surface energy and contact angle [12].Some of passive action polymer with antimicrobial properties are given below in the Table 2.

Table 2.2: Examples of Passive Action Polymers for Antimicrobial Applications [12].

Polymer	Microbial types Target	Results and Observations
Polyethylene glycol	<i>E.coli</i> , <i>S. aureus</i>	Can be used to inhibit protein/cells in polymeric systems
Group of Poly(sulfobetaine methacrylate)	<i>p. aeruginosa</i> , <i>S.epidermidis</i>	resist proteins and bacterial attachment
Group of Poly(2-methyl-2-oxazoline)	<i>Escherichia coli</i>	dual-functional antimicrobial surface of positive charge quaternary ammonium
Albumin type polymers	bacillus subtills, <i>Escherichia coli</i>	None of bacterial growth was observed after one day inoculation
polyphenols	streptococcus mitis, Fusobacterium nucleate, Prohormones gingivitis	Effective against periodontal bacteria

2.10.2 Bio Active Copolymer

These polymers kill active bacteria that adhere to their surface and these polymers are utilized to destroy the bacteria like antibiotics, biocides and antimicrobial peptides [24], [58]. Bioactive polymers are the materials based on synthetic polymers that have additional bioactive species fused into the polymer structure, such as proteins, polysaccharides, or peptides, to produce a particular biological reaction.[41], [59].

Mechanism of action of these copolymers depends on the active agents present in them[12], [60]. A table is given below which describe some of the active polymer with their antimicrobial use.

Table 2.3: Active Action Polymers for The Antimicrobial Applications[12].

Polymer	Target	Antimicrobial Substance	Observation
Nisin-immobilized organosilicon	<i>Bacillus subtilis</i>	Nisin	Excellent antimicrobial performance, and resistant to cleaning conditions
Polyurethane containing quaternary ammonium	<i>Bacteria S.aureus, Escherichia coli</i>	Quaternary ammonium	Good antimicrobial performance at low concentrations (5 wt. %)
Poly(n,n-diethylethylendiamine-co-yrosol-based acrylic)	<i>S.epidermidis, S.aureus</i>	Tertiary amine	Combination of two active compounds provide a synergistic action against biofilms and suppress reactive species oxygen
Acrylamide polymers with quaternary ammonium	<i>S.albus, Escherichia coli, Rhizoctonia solani, Fusarium oxysporum</i>	Quaternary ammonium groups	Benzyl group attached to nitrogen atom showed high better inhibitory effect on bacteria and phytopathogenic fungi

2.11 Components used in Copolymerization

Following are the components of Copolymerization method.

2.11.1 Acrylic Acid (AA)

Acrylic acid is colourless, volatile, and less toxic and dissolve completely in water at room temperature .it is used for synthesis of homopolymer and copolymer as well .It is produced from variety of raw materials fossil and renewables[61]. A study conducted to show the antifouling character of membranes based on acrylic acid [62].

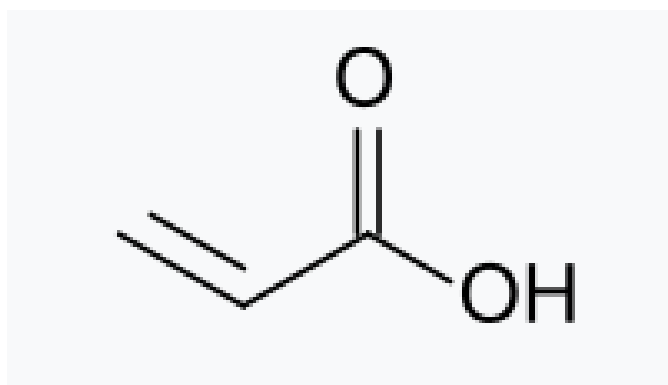


Figure 2.10: Structural Formula of Acrylic Acid (AA)

2.11.2 Methyl Methacrylate (MMA)

Methyl methacrylate is a colorless liquid which is used in copolymerization reactions. Methyl methacrylate also known as Metha acrylic acid. A suitable choice of monomer in polymer is MMA because of its durability, high glass transition temperature & transparency[63].

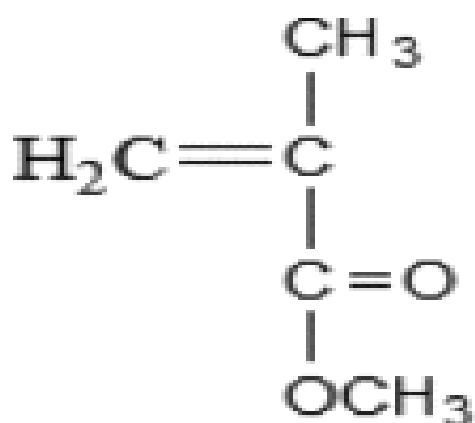


Figure 2.11: Structural Formula of MMA.

2.11.3 Tetrahydrofuran (THF) Solvent

THF is hygroscopic in nature which make it suitable for variety of applications[64]. THF promote acid catalyzed solubilization and it can easily be obtained from sugar solution so it has a less production cost and other advantage is less toxic in nature [65].

2.11.4 2,2-Azobisisobutyronitrile (AIBN)

AIBN is used as initiator in polymerization processes. The process of free radical polymerization is activated with Presence of initiator. The choice of particular initiator depends on template ion stability and electrostatic interaction with monomers[66].

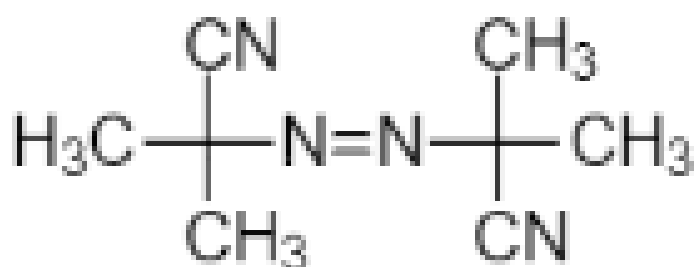


Figure 2.12: Structural Formula of AIBN[66].

2.12 Layer by Layer Self Assembly

LBL self-assembly is a deposition process that grows an ultrathin film on solid substrates by alternating dipping or flip-flopping in positive and negative species [67].

This technology is widely employed in the construction of multilayer structures with regulated Langmuir-Blodgett (LB) phenomena for the adsorption of various charged species by thin films.[67], [68].

Electrostatic interaction is driving force for layer-by-layer self-assembly, but hydrogen interaction also take part in them. In LBL self-assembly multilayers of material can be assembled in 2D support (slides, plastics, silicon wafers) or 3D support including micro/nano templates The resulting film's architecture can be made with nanoscale precision to fulfil various needs such as thickness, biocompatibility, optical / magnetic features etc [15], [17], [67].

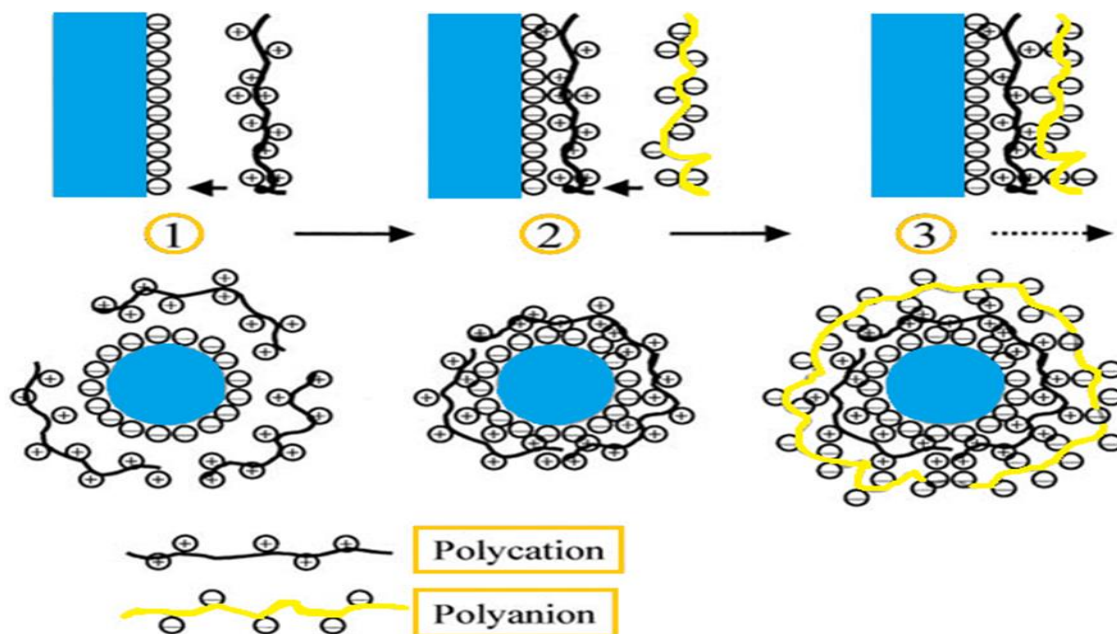


Figure 2.13: The Mechanism of Electrostatic LBL Self-Assembly on 2-D Substrates and 3-D Nano Templates.

2.12.1 Thin Films Properties

The thin film thickness/stability can be change by changing the concentration, pH and ionic strength of polyion solution. By knowing pH of polyelectrolyte solution high degree of polyion ionization is require for LBL process[69].

Pk_a of carbonate group is about 4 and 5 which is used to attain negative charge of polyion solution whereas cationic characteristic of polymer control by amino/imino groups with IEP around 8-9, so to maintain a charge of these poly ions Use of PBS having pH around 7.4 is appropriate [69], [70].

PBS gives physiological ionic strength which is requirement of proteins /enzyme assembly. pH value of coating solutions should not be close to IEP (at least 10% pendant should ionize). High ionic strength provides thicker film formation. Hydrophilic films produced by LBL self-assembly remain stable for about one month in incubation (90⁰C oven) [69], [70], [71].

2.12.2 Advantage of Thin Film

LBL self-assembly presents a number of following advantages in encapsulation, coating or fixation of substances: [69], [71], [72], [73].

- i. Tuneable thickness.
- ii. No sample loss.
- iii. Clean, cheap, easy to handle.
- iv. Tuneable properties (roughness, pattern, surface energy, corrosion resistance, and etc).
- v. Different kind of synthetic and natural colloids are present for LBL.
- vi. The location/sequence of the layers can be controlled.
- vii. Surface labelling with targeting molecules is possible.
- viii. No restriction on substrate size, geometry and topography.
- ix. Mult composite films formation.
- x. LBL do not use of thermodynamically unstable mechanically micronized particles.

2.13 Polyelectrolytes

By definition polyelectrolyte are macromolecules, shows ionization with water or other suitable solvent dissociate into charged polymer species [74]. Different experimentation has been done to understand the root cause of less diluted polyelectrolyte solution contains high number of charges on them. Relationship between polyion and other charge specie/neutral especially adsorption of ionisable polymer is another important part of polyelectrolyte that have been extensively studied & gain attention for numerus industrial purposes. As polyelectrolyte shows dissociation of ionic groups so this dissociation is achieved by small negatively charge counter ion which try to neutralize the charge.[75], [76], [77].

2.13.1 Classification of Polyelectrolyte

Polyelectrolyte classified into strong and weak polyelectrolyte like acid and base.

i. Strong polyelectrolyte:

Strong polyelectrolyte is those which shows complete dissociation for most reasonable pH values.

ii. Weak polyelectrolyte:

Weak polyelectrolyte is those polyelectrolytes that are partially dissociate at intermediate pH values.

2.14 pH Sensitive Behavior of Poly (Acrylic Acid) (PMMA-co-PAA) and Poly (DADMAC) (PAH)

PAA is a weak polyion having pka of 6.5 Poly (acrylic acid) (PAA) and poly (dimethylaminoethyl methacrylate) (PDMAEMA) are commonly used polymers in the development of pH-sensitive materials due to their pH-responsive properties. When combined in a copolymer, such as poly (methyl methacrylate-co-poly (acrylic acid)) (PMMA-co-PAA), and poly (diallyldimethylammonium chloride) (PDADMAC), they can exhibit interesting pH-sensitive behaviour [78],[79].

At low pH values, the carboxyl groups of acrylic acid in PAA are protonated, resulting in a positively charged polymer. On the other hand, the amine groups of PDADMAC are also

protonated under acidic conditions, making it positively charged. This results in electrostatic repulsion between the positively charged polymers, leading to swelling of the polymer network due to osmotic pressure.

Conversely, at higher pH values, the carboxyl groups of PAA become deprotonated, rendering the polymer negatively charged. Similarly, the amine groups of PDADMAC become protonated and positively charged. In this state, electrostatic attraction between the oppositely charged polymers occurs, resulting in collapse or compaction of the polymer [18],[79],[80].

It has been found in the previous studies that pH-sensitive behaviour can be utilized in various applications, such as drug delivery systems, sensors, and controlled release devices. For instance, in drug delivery systems, the swelling and collapse of the polymer matrix in response to changes in pH can be exploited to control the release rate of encapsulated drugs. Additionally, pH-sensitive coatings based on these polymers can be employed in controlled release coatings for agricultural applications or in biomedical devices for targeted drug delivery [16], [78], [81], [82].

2.15 Antimicrobial Coatings

Bacterial adhesion to a substrate can be of different methods such as hydrophobic and may be due to charge interactions. Microbial attachment may lead to cause infection in biological implant. By adjusting surface parameter like hydrophobicity, roughness, wettability bacterial attachment to substrate gets reduced [83].

Coatings are designed to inhibit the growth and spread of microorganisms, including bacteria, viruses, fungi, and algae, on various surfaces. By incorporating antimicrobial agents into coatings, surfaces such as countertops, door handles, medical devices, and even textiles can effectively reduce the risk of infections and cross-contamination [84].

PEG is widely studied polymer having flexible chain that produce high steric repulsive force PEG is a biocompatible polymer that can be modified to exhibit antimicrobial activity through various mechanisms. One approach involves incorporating antimicrobial agents into PEG-based coatings, such as silver nanoparticles or quaternary ammonium compounds, which can effectively inhibit the growth of bacteria and other microorganisms on surfaces [85].

Self-assembled monolayers (SAMs) have emerged as a promising approach for developing antimicrobial coatings with tailored properties and high efficacy. SAMs are formed

by the spontaneous organization of molecules onto surfaces, creating a single layer with well-defined chemical structures and functionalities. Ostenui et al reported the SAMs containing oligo have ability to resist non specific adsorption of protein .according to this study it was reveal that SAMs does not have ability to resist bacterial adhesion on the surface so it was clear that parameter need to build a surface with protein adsorption are not sufficient for bacterial adhesion[85].

Polyelectrolyte multilayers (PEMs) are composed of alternating layers of poly(allylamine hydrochloride) (PAH) and poly(acrylic acid) (PAA) have shown significant potential as antimicrobial coatings. These PEMs take advantage of the electrostatic interactions between the positively charged PAH and the negatively charged PAA to form stable, layer-by-layer assemblies on various substrates. [86].

CHAPTER 3: METHODOLOGY AND CHARACTERIZATION

3.1 Materials

All chemicals were of analytical grade and used in synthesis without further purification.

- i. Methyl methacrylate (MMA, 99%) (Sigma, USA).
- ii. Acrylic acid (AA, 99%) (Sigma Aldrich).
- iii. 2,2-Azobisisobutyronitrile (AIBN, 98%) (Sigma, USA).
- iv. Tetrahydrofuran (THF 99%) (Sigma Aldrich Germany).
- v. Ethanol (Sigma Aldrich Germany).
- vi. NaOH (Sigma Aldrich Germany).
- vii. Diethyl ether.
- viii. H₂O acquired from 18Ωmill pore RO Plant.

3.1.1 For Bacterial Growth

- i. Phosphate Buffer Solution (PBS) (Ameresco, Belgium).
- ii. Mueller-Hinton agar (MHA) (Daejung, Korea).
- iii. Luria Bertani (LB) Agar.
- iv. E. Coli (ATTC 8739) strain
- v. S. Aureus (ATCC 6538) strain.

3.2 Equipment and Characterization Tool for Copolymerization

The following instruments and characterization tools were used during materials synthesis and characterization.

- i. Fume hood.
- ii. Hot plate.
- iii. Schlenk flask 250 ml.
- iv. Glass thermometer.
- v. Glass condenser.
- vi. ATR-FTIR (BRUKER ALPHA II FTIR).
- vii. TGA (TGA/DSC with High Temperature Furnace Metler Toledo).

viii. DSC((DSC Q20 with RCS 90, TA instruments.

3.3 Methods

3.3.1 Synthesis of Copolymer P(MM-Co-AA)

Polymers of acrylic acid ,methyl methacrylate and copolymer having different molar ratios (7:3 , 5:5 , 3:7) were synthesized in Schlenk tube sealed with vacuum grease using THF as solvent and AIBN as free radical initiator by doing free radical polymerization .Reaction was performed in oil bath by maintaining the temperature at 70⁰C and in inert atmosphere(continuous supply of nitrogen gas).For synthesis of first molar ratio feed 7:3 (PP70), took 7 g of AA and 3 g of MMA in 70ml of THF with continuous stirring Then add AIBN initiator (0.2%w/v) and allow to proceed the reaction for 4 hours.

After that rotatory evaporation was performed to remove excess solvent (rotatory evaporation was done under vacuum and at 40⁰c temperature. The obtained polymer then adds dropwise to diethyl ether solvent placed in a liquid nitrogen and then pour onto petri dish for precipitation. after that polymer was dried at constant weight and used. PP50 (5:5), PP30(3:7) was also prepared by doing similar methodology with difference in their monomer concentration [87].

Table 3.1: Concentrations Used for Copolymerization (PP70, PP50, PP30), Solvent & Initiator

Samples Codes	AA (g)	MMA (g)	AIBN (g)	THF (ml)
PP70	7	3	0.02	70
PP50	5	5	0.02	70
PP30	3	7	0.02	70

3.3.2 Work Scheme

Chemical reaction between AA and MMA monomers shown in Fig P(MMA-Co-AA) was done by free radical polymerization, using AIBN as initiator and THF as solvent at 70 °C temperature. Different copolymers were synthesized by varying their concentration of monomers.

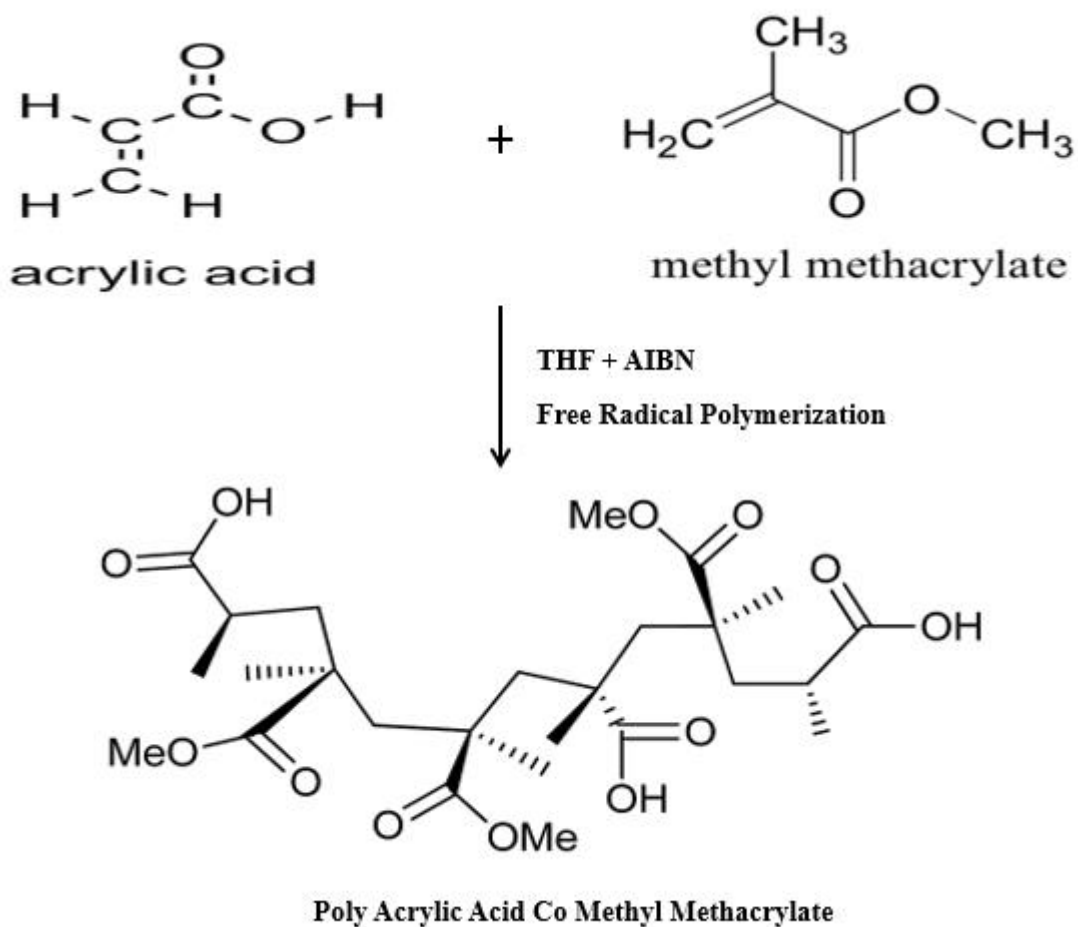


Figure 3.1: Chemical Reaction of Copolymerization between AA and MMA.



Figure 3.2: Polymerization Setup.

3.4 LBL (SAMS) Dip Coating Method

LBL dip coating is a conventional technique to fabricate a thin film and it require less expertise and more economical [88].The process of dip coating occur due to difference in zeta potential or charges of polymer, membranes, and PDAC [73], [89].

Layer by layer is thin film fabrication technique by depositing the oppositely charged alternating layers on material surface with wash steps in between them [79], [90].

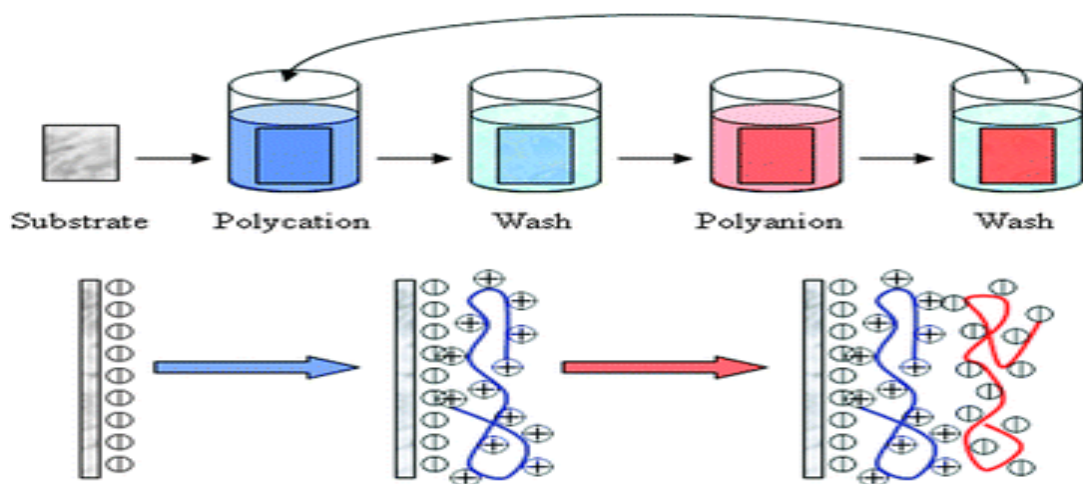
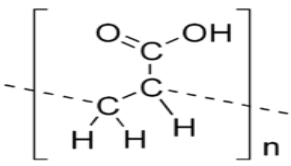
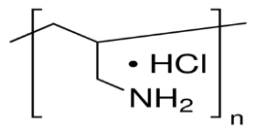
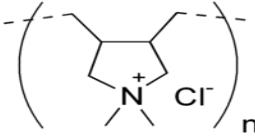
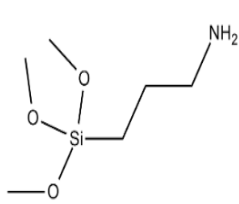


Figure 3.3: General Process Describing the Thin Film Fabrication on Surface Material [68]

3.4.1 Materials used for thin film Fabrication

- Microscopic glass slides .
- (25 x 75 x 1 mm, Globe Scientific Inc., US).
- APTMS (3-aminopropyltrimethoxysilane toluene solution, 10mM) .
- Conc. Sulfuric acid (Sigma-Aldrich, 95-98% purity).
- Potassium dichromate (Scharlau, reagent grade).
- PDADMAC (Polydiallyldimethylammonium chloride).
- PAH (Poly(allylamine hydrochloride)).
- PAA or PP50.
- Ultrapure water (Conductivity=0.0055 μ Siemens, Total dissolved solutes (TDS) =0).

Table 3.2: Depicting the Structural Formulas of Polymers Being Used in Thin Film Fabrication

PAA or PP50(PMMA-co- PAA)	PAH	PDADMAC (PDAC)	APTMS
Weak polyanion	Weak polycation	Strong polycation	Polycation
			

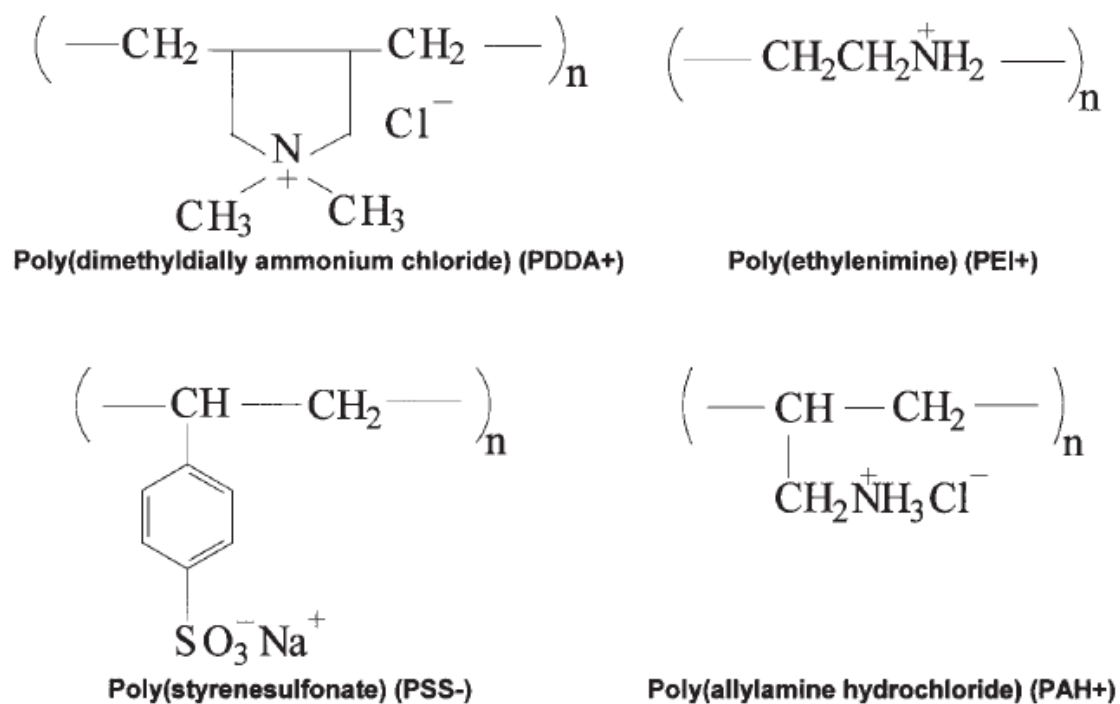


Figure 3.4: Illustrations of Commonly used Polyelectrolyte.

3.4.2 Fabrication of Thin Film

3.4.2.1 Cleaning of Glass Substrate

- Overnight soaking of micro-glass slides in chromic-sulfuric acid solution:
 - 50% sulphuric acid
 - 50% potassium dichromate
- Rinse with tap water and with ultrapure water. The slides dry under ambient conditions.

3.4.2.2 General Process for LBL Assembly

Fabrication of LBL-SAMs by manual dipping of the freshly cleaned glass slides into the desired solutions for a predetermined time.

- A 10BL was prepared by alternating dipping of of the microslides in PDAC (Polycation) and PAA or PP50 (Polyanion). PP50 as the top layer was taken.

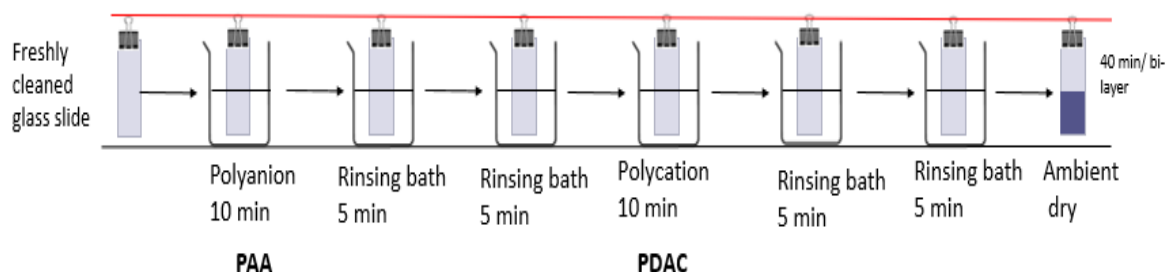
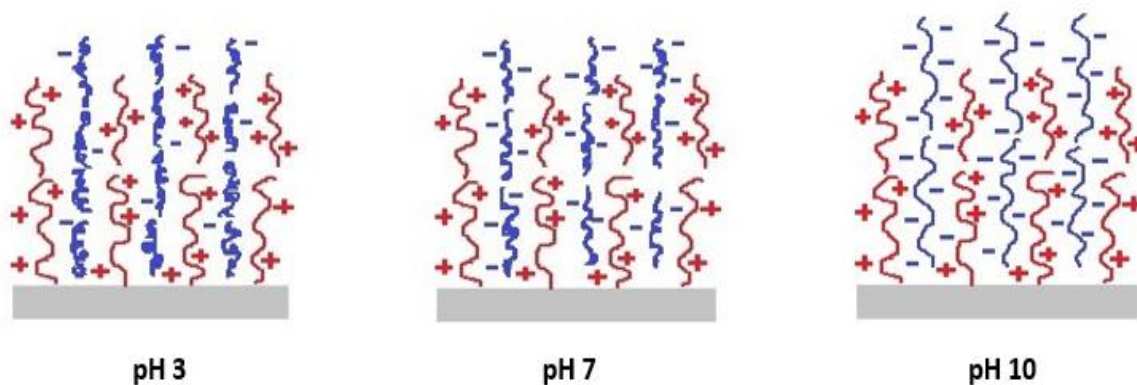


Figure 3.4: General Process of LBL Self Assembly

3.5 pH Responsive Behavior of Model PAA

PAA has a pka value of 6.5 it shows complete ionization at (pH 9.5 or 10) and almost no ionization at pH 3, it has degree of ionization at pH 3 is 10% and at 7 is 60% and at 10 is almost 100%.PAA deposits in loop rich conformations at low pH whereas at high pH the fully charged molecule form thin flat layers[81], [91], [92].



3.6 Sample Preparation for Thin Film Fabrication

1 Step: Three different 10 bilayers samples were prepared using PP50(PAA) & PDAC at:

- pH 3
- pH 7
- pH 10
- With PDAC (polycation) as the top layer

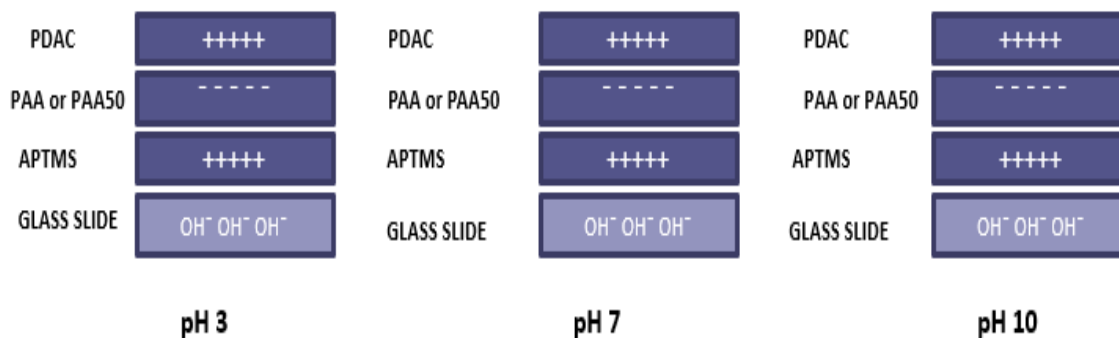


Figure 3.6: LBL Self Assembly at Different (3,7,10) pH with PDAC at Top Layer

2 Step: Three different 10 bilayers samples were prepared using PAA or PP50 & PDAC at:

- pH 3
- pH 7
- pH 10

➤ With PAA or PP50 (Polyanion) as the top layer

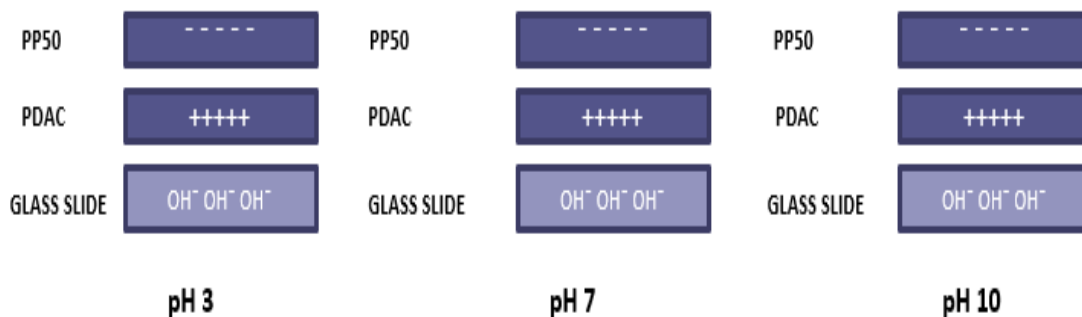


Figure 3.7: LBL Self Assembly at Different (3,7,10) pH with PP50 at Top Layer

3 Step: Four different samples of 1, 5, 10 and 15 bilayers were prepared using PAA or PP50, PDAC and PAH

- PAA or PP50 at pH 10
- PDAC at pH 10
- PAA or PP50 at pH 3 in the penultimate layer
- PAH at pH 7 (top layer)

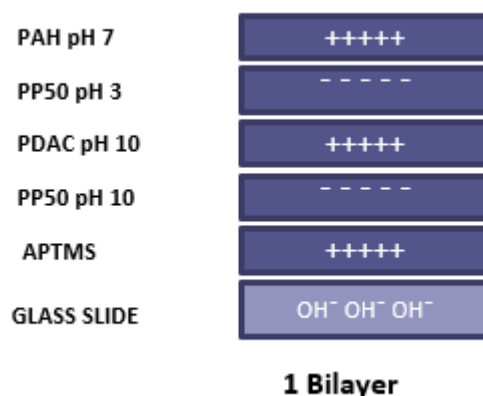


Figure 3.8: 1BL at Different pH (3,7,10) with PAH at Top Layer.

3.7 Characterizations

Table 3.3: Characterizations Done for Copolymer and for Thin Film SAMs.

Characterization of polymer	Characterization of Thin Films
FTIR	Optical microscopy
TGA	Optical profilometry
DSC	Contact angle measurement
	Antimicrobial Testing

3.7.1 Characterization of Copolymer

3.7.1.1 FTIR

FTIR was used to detect the functional groups present in copolymer. The resolution was 1 to 2 cm^{-1} and spectral range was about 500- 4000 cm^{-1} . A BRUKER ALPHA II FTIR spectrophotometer was used for this purpose.

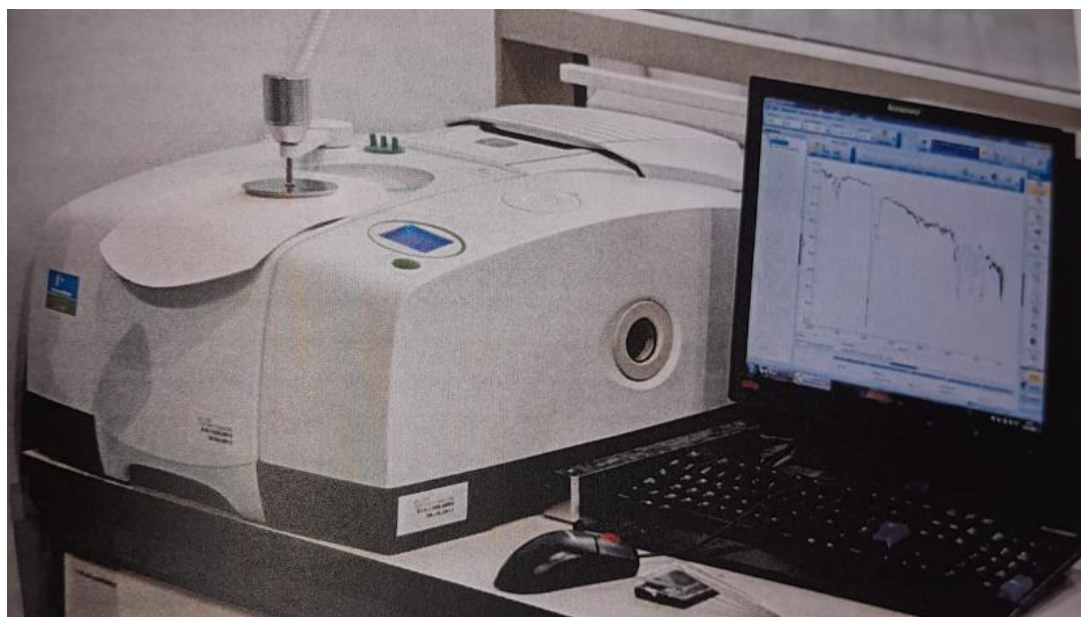


Figure 3.9: ATR-FTIR (BRUKER ALPHA II FTIR).

3.7.1.2 TGA (Thermogravimetric Analysis)

Thermogravimetric analysis is used to observe the changes in weight with respect to temperature or time. The weight changes of polymer material may be due to decomposition and oxidation reaction or may be some of physical parameter like sublimation vaporization etc [93].

Samples were scanned around 250⁰c temperature under inert atmosphere, scan rate was 10 °C per minute and amount of sample used was in mg. For TGA analysis sample preferably in powder form because it is easy to put in sample pan .TGA was done to analyse the sample and graph is plot between temperature and weight loss.

3.7.1.3 DSC (Differential Scanning Calorimetry)

DSC is widely used to test thermal properties of material such as glass transition temperature in case of polymers. DSC provide information of melting crystallisation and transition temperature. Advantage of DSC compared to other calorimetric technique in broad range of heating or cooling state [94], [95].

Sample taken for DSC in mg and scanning rate was 10 Celsius per minute and samples were scanned about 250 Celsius temperatures.

3.8 Characterization of Thin Films

3.8.1 Antimicrobial Testing

Antimicrobial testing was performed by taking two freshly prepared bacterial strain *E. coli* and *S aureus* by cultivated them in bacterial culture of LB broth at 37⁰C. Bacterial culture were prepared before 16 h of harvesting and then bacteria containing broth was centrifuge at about 3000 rpm for about 10 minutes. After cell washing with PBS (pH 7.4), samples were incubated with bacterial suspension for one hour then again wash three times for PBS, fixed with 3% glutaraldehyde for 5 hours and then rinsed with DI water then Dried at 60 °C in the oven for one day [16], [96], [97].

3.8.2 Optical Microscopy

Optical microscopy provides magnified image of objects that are small and cannot be visible with naked eye. Optical microscopy is commonly used to visualize the polymeric films or nanostructure deposited on substrate optical microscope with a features like phase contrast or differential interference contrast (DIC) to enhance the visibility of transparent and low contrast sample like polymer thin films [98], [99].



Figure 3.10: Optical Microscope (Optica B-600 MET) was Used to Analyze the Adsorption of Polymer Chain.

3.8.3 Optical Profilometry

Optical profilometry is non-contact surface measurement technique which is used to analyse the surface parameter of objects .it measure height variations of surface with high precision

Optical microscope is used to evaluate the roughness of surface (Nanovea PS 50), Optical profilometer perform measurement with transparent layer.[100], [101], [102] .

3.8.4 Contact Angle Measurement

Contact angle of the LBL SAMs thin films was measured by placing a 10-20 μ L drop of ultrapure water on the surface of glass slide using a micropipette or syringe (sessile drop method). Then take image of it



Figure 3.11: Contact angle measurement device.

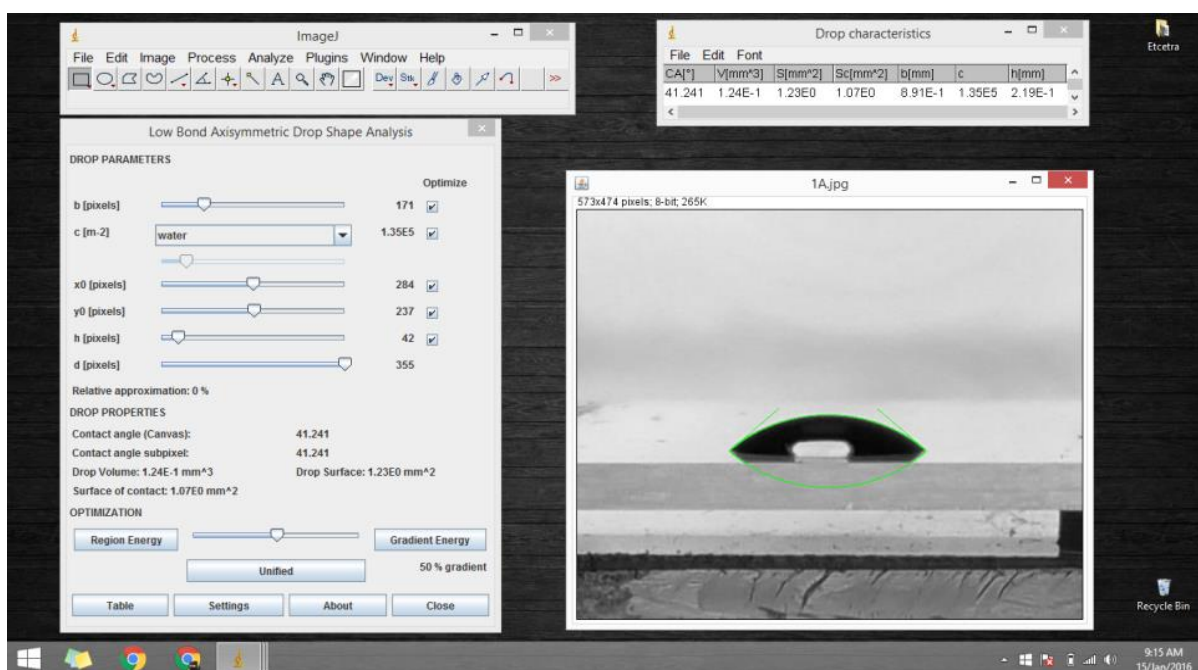


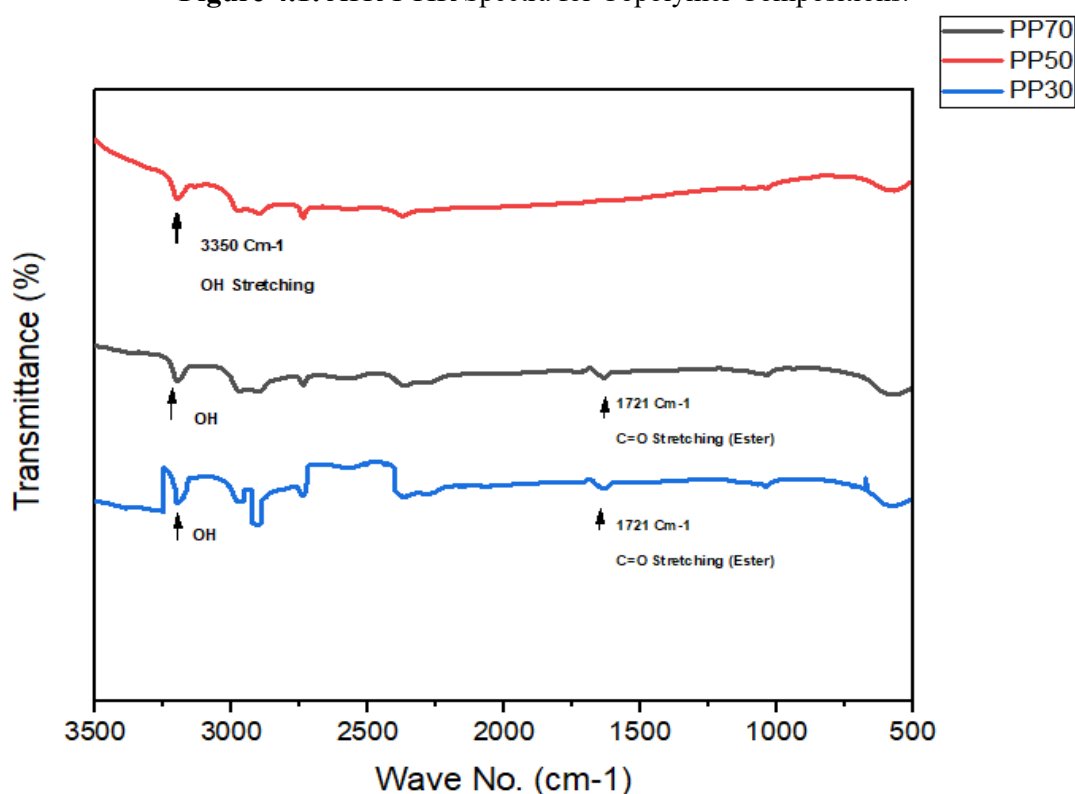
Figure 3.12: Image J* Low Bond Axisymmetric Drop Shape Analysis.

CHAPTER 4: RESULTS AND DISCUSSIONS

4.1 ATR-FTIR

Figure 4.1 represents FTIR analysis of synthesized polymer compositions of PP70, PP50, PP30. FTIR Spectra shows OH stretching at 3350cm^{-1} , C=O stretching of ester group was observed at 1721cm^{-1} , C=C peak is not present at $1400\text{-}1600\text{cm}^{-1}$ shows that polymerization of AA and MMA was successfully completed.

Figure 4.1: ATR-FTIR Spectra for Copolymer Compositions.



The polymerization approach offers a promising solution for enhancing the hydrophilicity of PMMA and expanding its potential uses. Acrylic acid unit are incorporated into MMA that can greatly improve water absorption properties of Copolymer.

These polymerizations typical follow overall rate of polymerization model:

$$R_p = k_p \left(\frac{fk_d}{k_t} \right)^{1/2} [M][I]^{1/2}$$

Where R_p is overall rate of polymerization; (k_p , k_d , k_t) these are the rate constants of propagation, and termination, f_i is the initiator efficiency and M and I are respectively Monomer and initiator concentration. During polymerization M and I are variable and allow to control properties of polymers including degree of hydrophilicity and hydrophobicity. Upon polymerization of monomers through initiation with AIBN initiator, copolymer structure formed which were characterized by FTIR.

The compositional peaks observed in the FTIR spectrum, as illustrated in Figure, provide valuable insights into the distribution of these monomers within the copolymer structure. By analyzing these peaks, it can be determine the optimal ratio that achieves the desired balance between hydrophilicity and hydrophobicity. By studying the FTIR of MMA.

It was observed that characteristic absorption were at 2800–3000 is of C-H stretching and absorption peak at 1728 were of C=O stretching .In case of AA, the stretching peaks were observed at 3550 cm^{-1} and the bending vibrations were observed at 1640 cm^{-1} of –OH groups. . t is noteworthy that the absence of the characteristic absorption peak attributed to C=C bonds in the range of 1620–1680 cm^{-1} indicates that the double bonds in the acrylic acid (AA) molecule have been successfully polymerized or reacted during the copolymerization process.

This suggests that the unsaturated C=C bonds in AA have undergone conversion into other functional groups or have participated in the copolymerization reaction, leading to the formation of the desired copolymer structure.

The prepared copolymers were also used to make composites thin films. By incorporating AA monomers into the compositions of the PMMA(PMMA-co-PAA) composite film, the surface hydrophilicity of the resulting material was enhanced. This improvement in hydrophilicity can be attributed to the presence of polar functional groups, such as -OH, within the acrylic acid units.

These groups have an affinity for water molecules, leading to increased wetting and adhesion properties on the surface of the composite film. It is expected that the absorption

peaks at (3500 cm^{-1} , OH) and (1728 cm^{-1} , C=O) of MMA, become weaker by adding the amount of PAA copolymer. it is may be due to intermolecular hydrogen bonding is present between copolymer.

The emergence of two new absorption peaks at 1548 and 1406 cm^{-1} , corresponding to the symmetric and antisymmetric stretching vibrations of the carboxylate group (-COO-), indicates the successful formation of this functional group on the surface after activation. The detection of these absorption peaks provides valuable insights into the chemical changes occurring at the surface and can aid in understanding the surface modification processes involved in film formation.

The method outlined for constructing hydrophilic PMMA-co-PAA composite films in the current study involves several key steps, starting with the synthesis of the copolymers, followed by the mixing of these copolymers in solution, and adjusting the pH using a sodium hydroxide solution.

As depicted in Scheme 1, the process begins with the pre-polymerization of MMA monomers to form the PMMA backbone, which is then copolymerized with PAA monomers to introduce the desired hydrophilic properties. The subsequent mixing of these copolymers in a solution allows for the preparation of the composite film with controlled composition and structure.

Adjusting the pH using a sodium hydroxide solution is a crucial step in fine-tuning the properties of the composite film, as it can influence the ionization state of the carboxylic acid groups present in the PAA segments.

This pH variation helps optimize the hydrophilicity of the film by promoting interactions between the polymer chains and the surrounding environment. Overall, this method offers a systematic approach to tailor the properties of the PMMA-co-PAA composite films for specific applications requiring enhanced hydrophilicity and surface characteristics.

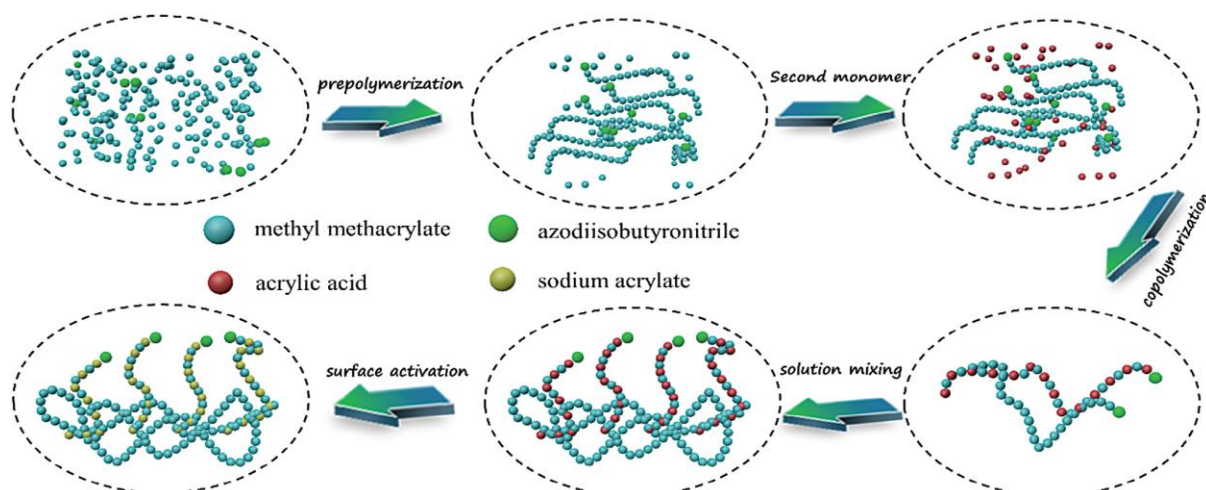


Figure 4.2: Schematic representation of the model formation of hydrophilic PMMA-co-PAAS composite films as adopted from sources.

4.2 Thermo Gravimetric Analysis (TGA)

TGA was done to study the percentage weight loss of polymer composition against temperature change. This method reveals about thermal stability and thermal decomposition of various polymers samples prepared.

Figure 4.2 depict that about 100 °C moisture was present in polymer which is removed and decomposition of copolymer compositions started in the range 100 °C up to 240 °C. Above 190 °C the major weight loss was completed. With the further increase in temperature there was a negligible weight loss was observed.

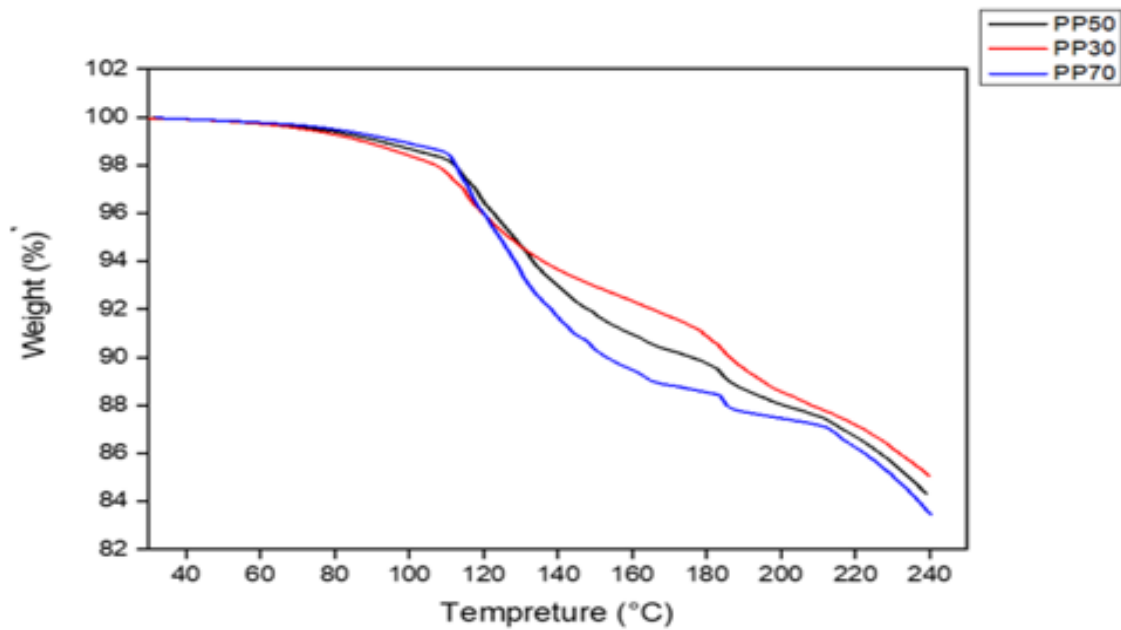


Figure 4.3: TGA Spectra for Copolymer Compositions.

The thermal stability study conducted on PMMA/PMMA-co-PAA aimed to assess how the incorporation of PMMA-co-PAA copolymer affects the degradation behavior of the polymers and their respective films.

The results indicate that the presence of PMMA-co-PAA copolymer led to a decrease in the maximum degradation rate from 15.4% per 10°C to 11.2% per 10°C. This observation suggests that the introduction of PMMA-co-PAA copolymer has a beneficial effect on enhancing the thermal stability of the composite material.

The decrease in the maximum degradation rate implies that the presence of PMMA-co-PAA copolymer helps to mitigate the rate of degradation of the polymer blend at elevated temperatures. This improved thermal stability can be attributed to the specific chemical interactions or structural characteristics introduced by the copolymer, which may enhance the overall resistance of the material to thermal degradation processes.

By influencing the degradation kinetics, the PMMA-co-PAA copolymer contributes to the overall thermal performance and longevity of the polymer blend and its films. This finding

underscores the potential of PMMA-co-PAA copolymer as a valuable additive for enhancing the thermal stability of polymer systems in various applications.

The thermal degradation analysis reveals the presence of two distinct temperature regions associated with degradation processes. The low-temperature region primarily involves the dehydration of carboxylic acid groups to form anhydride moieties.

This initial stage of degradation likely contributes to the early weight loss observed in the polymers, as the carboxylic acid groups undergo structural transformations to yield anhydride functionalities. As the temperature increases, a significant weight loss event occurs after reaching around 200°C, indicating a more pronounced degradation phase characterized by an irregular break of the main polymer chain.

The 10% degradation temperature of PMMA75-co-PAA25 composite film can increase to 250 °C, which is lower than the PMMA polymers. The maximum degradation rate was also affected when the content of PMMA-co-PAA copolymer was increased from 10% to 50%, suggesting that the introduction of copolymer with higher MMA can slightly promote thermostability.

The enhanced thermal stability of the PMMA-co-PAA is directly related to the intermolecular hydrogen bonding present within the copolymer. There is a noteworthy observation that at the low-temperature the process of degradation rises in the pure PMMA film after surface activation, that can be known as partial hydrolysis of MMA units in basic condition.

According to one study, the maximum degradation rate decreased from 23.2%/10 °C to 12.1%/ by 10 °C when the content of PMMA70-co- PAA30 copolymer was increased from 15% to 55%, resulting that by surface activation the copolymer can still improve the thermostability of the composite film through addition of NaOH by adjusting pH.

Furthermore, the carbon residue rises from 2.81% to 27.91% with the PMMA70-co-PAA30 copolymer content increased to 60%. In short, the addition of a copolymer can enhance the thermal stability of the polymers as well as their composite films.

4.3 Differential Scanning Calorimetry (DSC)

DSC was done to check the thermal transition of copolymer compositions (PP70, PP50, PP30) DSC is used to check the T_g like crystallinity, oxidation and melting etc we want to investigate the T_g of polymers. According to literature T_g of PAA was about **106 °C** and of PMMA T_g was 120 °C, so T_g observed in our synthesized compositions of copolymer was about 120 °C. It was also observed that by increasing acrylic acid component the process of degradation decreased.

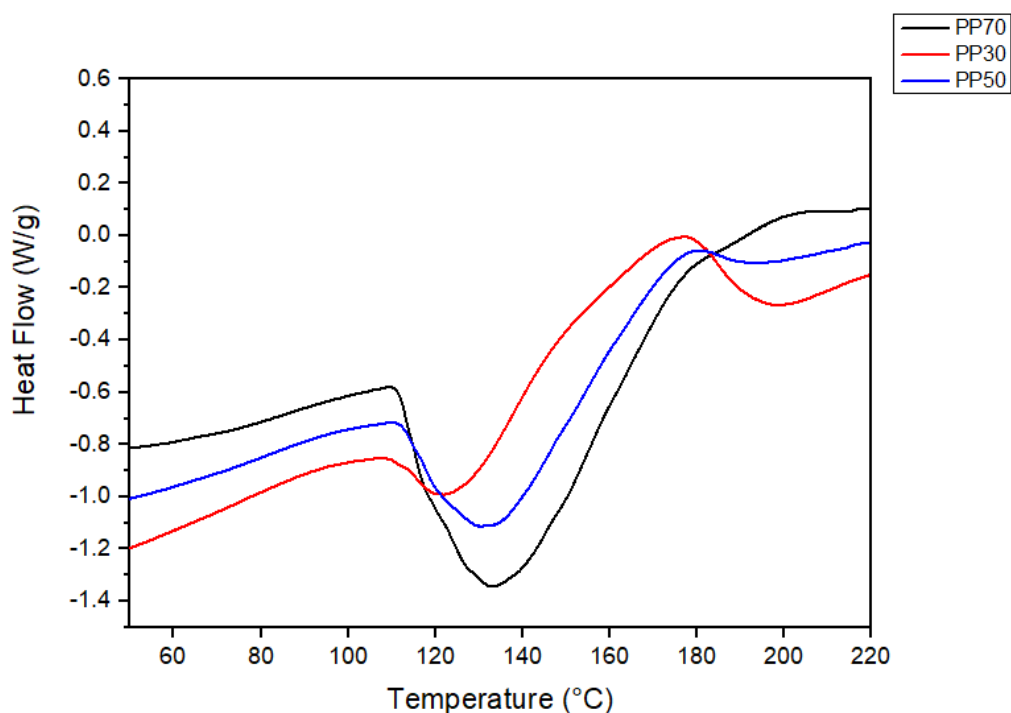


Figure 4.4: DSC Spectra for Copolymer Compositions.

The presence of PAA repeat unit can have influence on chain segmental motion as presented below figure 4.5. If substituted group becomes larger, then chain rotation becomes effected too.

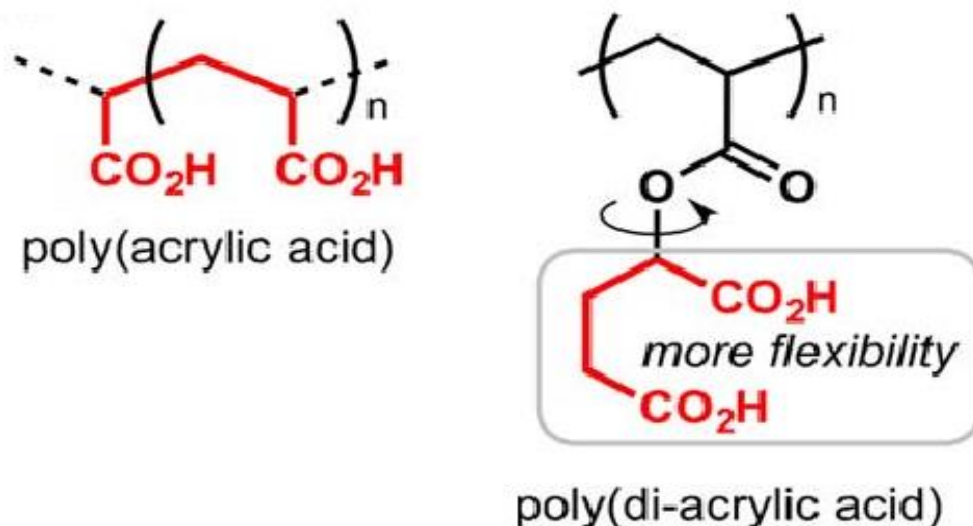


Figure 4.5: Structural Formula of Poly (Acrylic Acid) and Poly (Di-Acrylic Acid).

This is important to understand the melting and glass transition temperatures (T_m and T_g) since both are important parameter in polymer science. For many applications particularly with semicrystalline polymers, they are regarded as the upper and lower temperature limitations, respectively.

The T_g may also define the upper use temperature for glassy amorphous materials. Furthermore, T_m and T_g can affect synthesis procedure for polymers / polymer-matrix composites. Figure 4.6 shows the normal melting and glass transition thermal transitions. It is anticipated that the entire volume will remain constant at T_g and not change.

The PMMA and PMMA-co-AA copolymers' DSC curves have been documented in the literature. When compared to PMMA, the T_g values of PMMA-co-AA copolymers were inconsistent and were impacted by the quantity of AA monomers. Each of these copolymers has a single T_g , suggesting that they are homogenous and primarily in a single block [27].

Consequently, it is possible to see the addition of AA monomers to the PMMA main chain as random and as a single copolymer except blend.

As a result, the bulky MI units significantly affected the segmental movements of the polymer chains, increasing the T_g value of the copolymers. Additionally, link between the T_g values and the AA content of the copolymers can be discovered with further investigation.

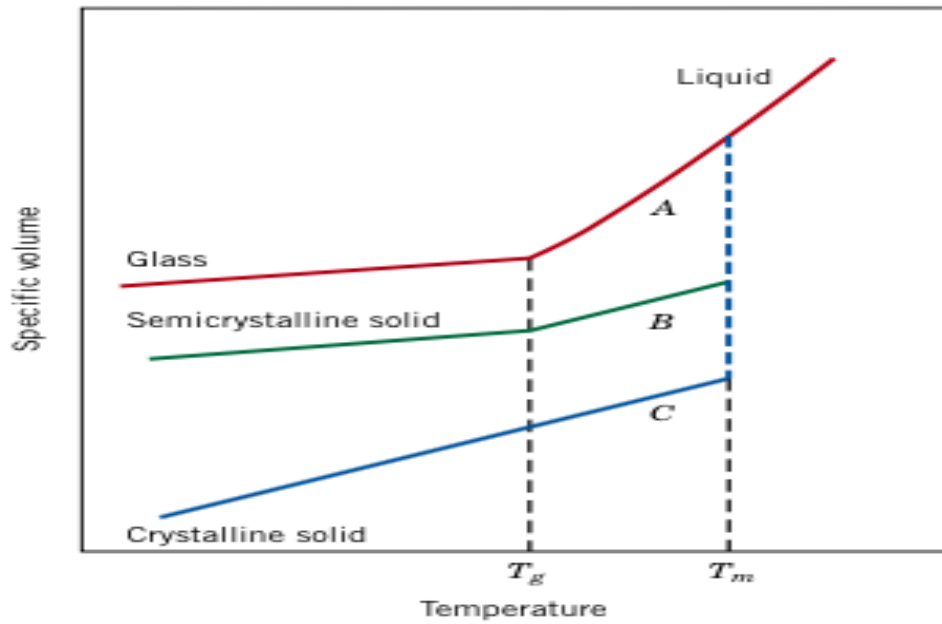


Figure 4.6: Depicting Specific volume w.r.t temperature. On cooling from liquid melt, total amorphous (Curve A), semicrystalline (Curve B), and crystalline (Curve C) polymers observed.

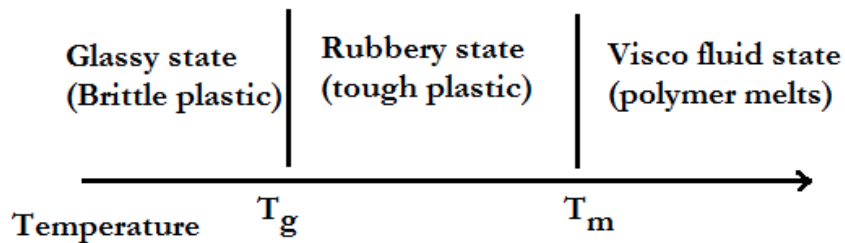


Figure 4.7: Normal Melting and Glass Transition Temperature.

The following elements are crucial to comprehend when analyzing the impact of copolymer composition and structure:

- One prominent impact is chain stiffness, which is determined by how easy it is to rotate about the chemical connections along the chain.
- T_m rises when double bonds and aromatic groups in the polymer backbone are present because they reduce chain flexibility.

- In addition, the kind and amount of side groups affect the flexibility and freedom of chain rotation; big or bulky side groups typically limit molecule rotation and increase T_m .

The significance of the structure-property relationship in the case of copolymers is typically shown by polypropylene, which melts at a greater temperature than polyethylene.

Compared to polyethylene, polypropylene's CH_3 methyl side group is bigger. Similar to this, the presence of polar groups—Cl, OH, and CN—even in small enough amounts increases the value of thermal transition by producing strong intermolecular bonding interactions. By contrasting the melting points of polyvinyl chloride ($212\text{ }^\circ\text{C}$) and polypropylene ($175\text{ }^\circ\text{C}$), this can be confirmed.

The flexibility of the chain is another aspect that determines T_m and T_g overall. Therefore, T_m and T_g will be increased by any factor that decreases chain flexibility.

Table 4.1: Melting Temperature of Common Polymers.

Polymers	Melting Temperature ($^\circ\text{C}$)
PE (LDPE)	110
PE (HDPE)	125
PTFE	327
PP	175
PVC	212
PS	240
PMMA	120 (T_g 106)
PAA	116 (T_g 106)

Chain flexibility in general is affected by following factors:

- Presence of Bulky side groups; (from Table 4.1) T_m for polypropylene is $175\text{ }^\circ\text{C}$ and polystyrene is $240\text{ }^\circ\text{C}$.
- Presence of Polar groups; e.g, T_m of poly (vinyl chloride) is $212\text{ }^\circ\text{C}$ and of polypropylene is $175\text{ }^\circ\text{C}$, respectively.

- Presence of aromatic groups, which tend to stiffen the polymer chain. See Nylon and PET.
- Higher crystallinity led to higher T_m (see LDPE and HDPE).

PAA and PMMA have T_m and T_g values that are reasonably close to one another. In these circumstances, the impact of compositions might not be immediately apparent. The DSC curves shown in Figure 4.3 also show this.

Since the groups in a copolymer structure are identical to those in acrylic and acrylate, their mobility within the structure may not differ significantly enough to significantly affect the temperature transitions of the copolymers that are produced.

4.5 Contact Angle Measurement

The polymer samples and their thin films were examined for surface wettability using contact angle measurement. Equation 1 and the Young Model, which is shown in figure 4.8, can be used to explain surface wettability.

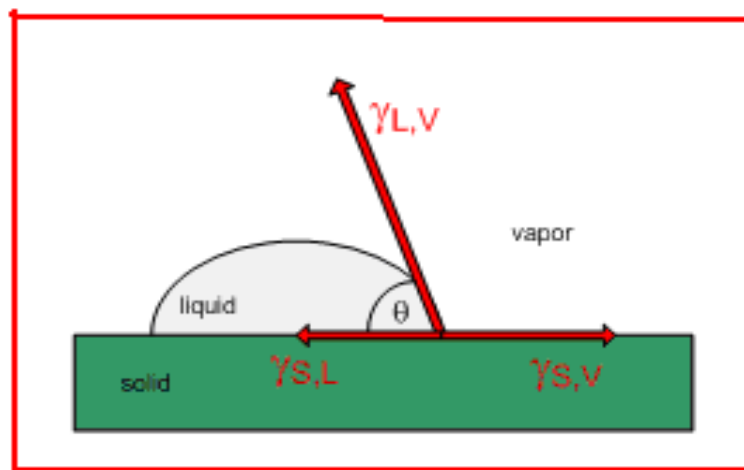


Figure 4.8: The Young Equation Represented on an Ideal Surface, Together with The Equilibrium (Or Static) Contact Angle θ_E

$$\cos \theta_E = (\gamma_{S,V} - \gamma_{S,L}) / \gamma_{L,V} \quad (\text{Equation 1})$$

where θ_E = equilibrium (or static) wetting contact angle;

$\gamma_{S,V}$ = solid-vapor interfacial surface tension;

$\gamma_{S,L}$ = solid-liquid interfacial surface tension;

$\gamma_{L,V}$ = liquid-vapor interfacial surface tension.

and various values of $\cos\theta$ are:

$$\cos^{-1}(0) = 90^\circ; \cos^{-1}(1) = 0; \cos^{-1}(-1) = 180$$

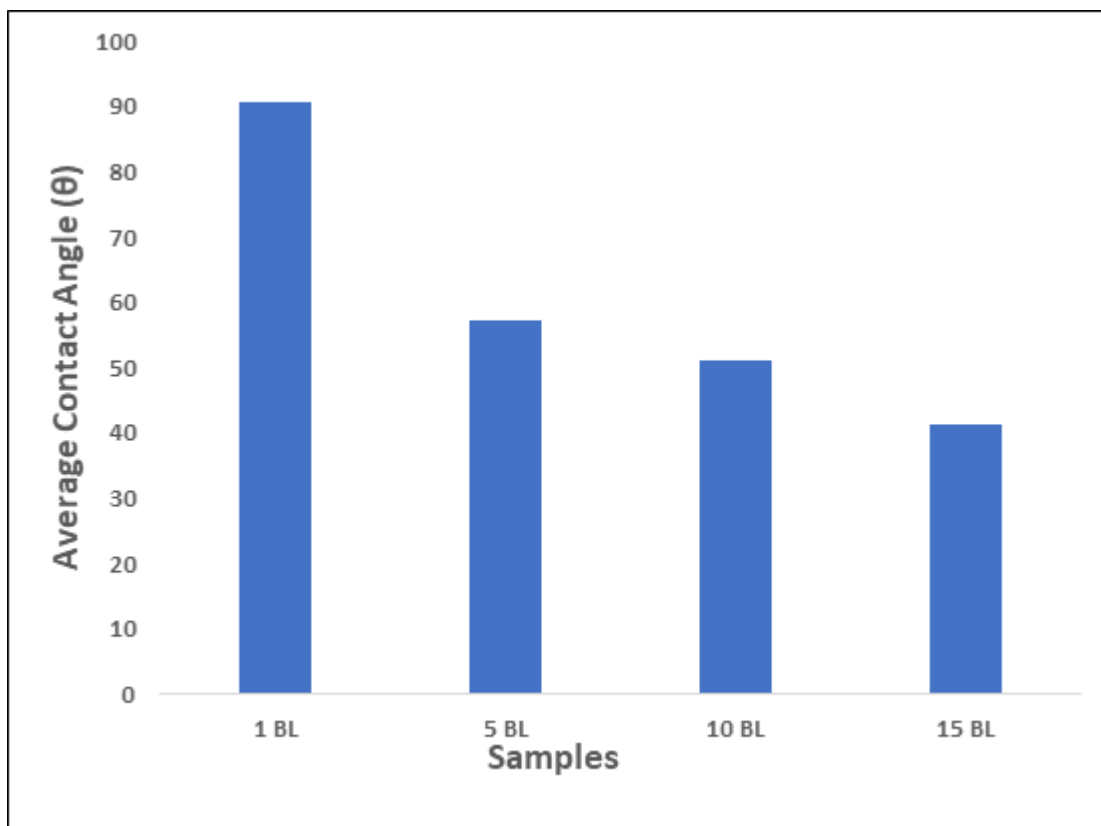


Figure 4.9: Depicting by Increasing No of Bilayers, The Value of Contact Angle Decreased.

Measurement of surface wettability through contact angle for various fabricated thin films is given in Table 4.2 and also presented in Figure 4.9.

It was done by sessile drop method as proposed by Young model and observed the value of contact angle so observation was the lowest contact angle in case of PP50 because it contain

acrylic acid group in it which is more hydrophilic in nature so presence of both hydrophilic and hydrophobic part in them allows them to interact more readily with water and non-polar surfaces.

Resulting in lower contact angle as they spread more easily on surface on contrary positive polymer predominantly have hydrophobic part in them leading to higher contact angle values on polar surface.

It was observed that by increasing the No of bilayers from 1 to 15, the value of contact angle is decreased, making the surface more hydrophilic. By taking pH into account, it was observed that in case of PP50 least value of contact angle was observed.

Table 4.2: 15 BL Samples (PAH Top Layer shows less Hydrophilicity).

Samples	Standard Deviation
1 BL	90.7±4
5 BL	57.1±2
10 BL	51.1±1
15 BL	41.3±0

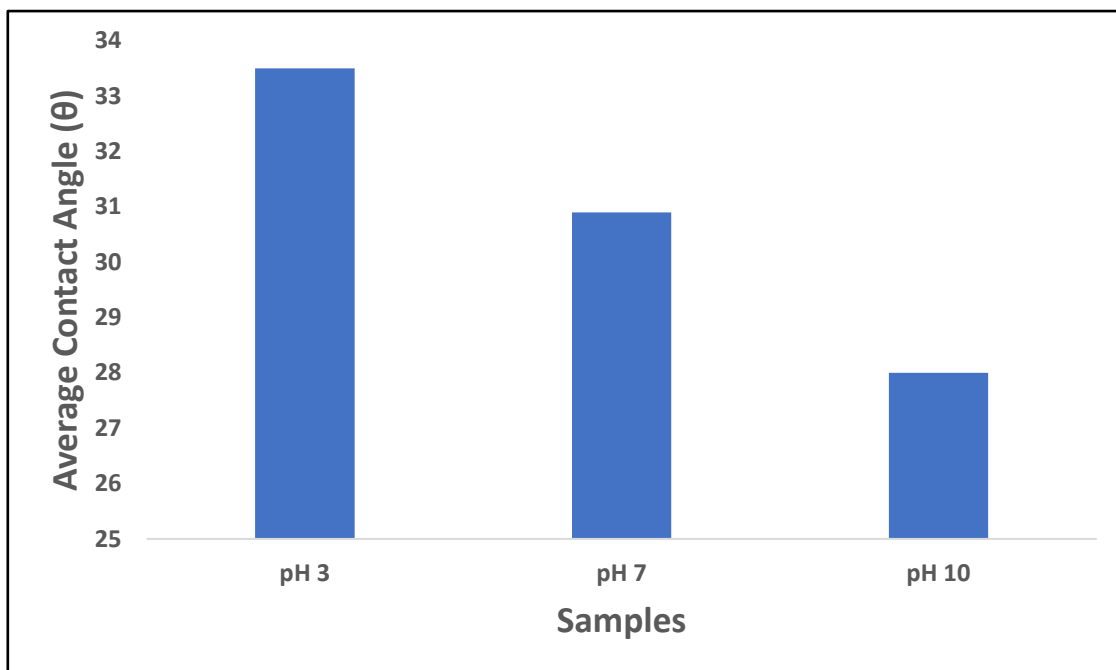


Figure 4.10: Shows Increasing the Value of pH (10) Contact Angle Value Decreased.

Table 4.3: 15 BL Samples (PDAC as the Top Layer).

Samples	Standard Deviation
pH 3	33.5±1
pH 7	30.9±0
pH 10	28.0±1

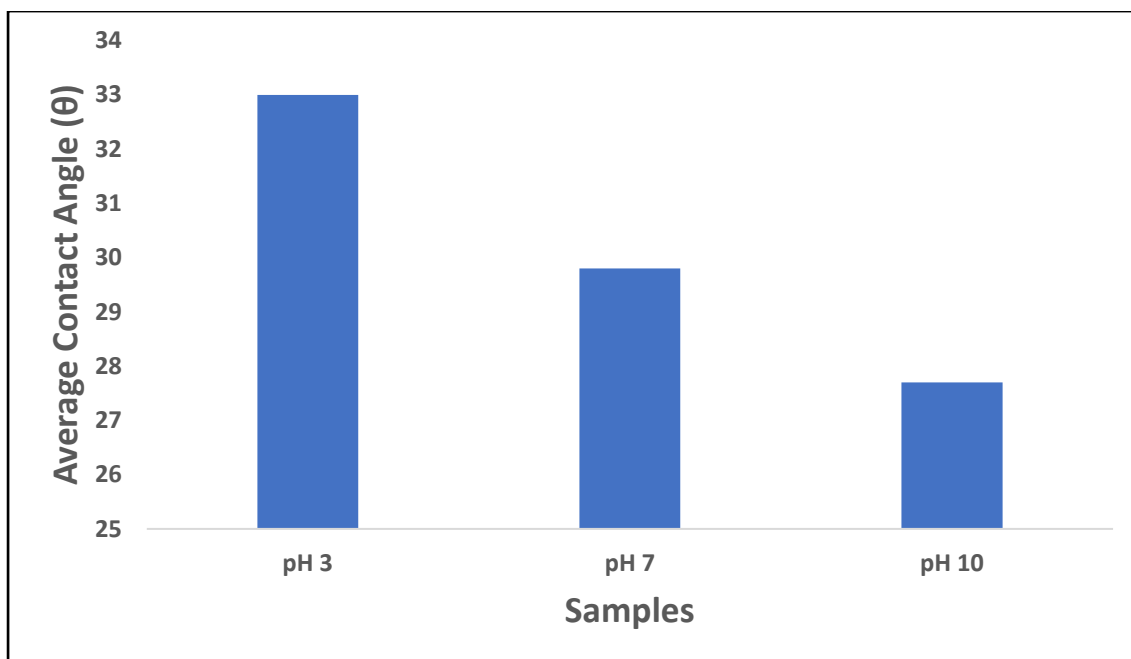


Figure 4.11: Shows Increasing the Value of pH (10) Contact Angle Value Decreased.

Table 4.4: 15 BL Samples (PP50 as the Top Layer provide Lowest Contact Angle Values with more Hydrophilicity)

Samples	Standard Deviation
pH 3	33.0±1
pH 7	29.8±1
pH 10	27.7±1

The following points should be taken into consideration in order to provide an intriguing explanation for contact angle values. A single, distinct contact angle is implied by the Young Model. Owing to its diverse intricacies, models have been utilized to acquire a more profound comprehension of the thermodynamic state of contact angles. Overall, it has been

discovered that the Young contact angle, θ_E (theoretical), and the experimentally observed apparent contact angle, θ^* (experimental), may or may not be equal.

In consideration of above points, various complement models have been proposed such as:

(i) Wenzel Model: chemical homogeneous, but physically rough surface:

$$\cos \theta^* = r \cos \theta_E \quad (\text{Equation 2})$$

(ii) Cassie-Baxter Model: physically smooth, but chemically heterogeneous:

$$\cos \theta^* = \Phi_1 \cos \theta_1 + \Phi_2 \cos \theta_2 \quad (\text{Equation 3})$$

(iii) Composite Hydrophilic Model: Porous surface with liquid fills pores and drop finds itself on mixed solid/liquid surface:

$$\cos \theta^* = 1 + \Phi_S (-1 + \cos \theta_E) \quad (\text{Equation 4})$$

(iv) Composite Hydrophobic Model: Porous surface with air trapped below the drop:

$$\cos \theta^* = -1 + \Phi_S (1 + \cos \theta_E) \quad (\text{Equation 5})$$

Where,

- θ^* is apparent contact angle (experimental);
- surface roughness r is defined as the ratio of the actual area over the apparent surface area of the substrate. For flat surface $r = 1$.
- θ_1 and θ_2 are CA of two different surfaces each has Φ_1 and Φ_2 fractional surface area;
- Φ_S is the fractional areas of the solid relative to fluid area (liquid or air) underneath the drop.

The surface wettability of the prepared films can be explained from the consideration of Young Model as well as above mentioned various surface model given in Equations 1 to 5.

For example, composite Hydrophobic Model: Porous surface with air trapped below the drop:

$$\cos \theta^* = -1 + \Phi_S (1 + \cos \theta_E) \quad (\text{Equation 5})$$

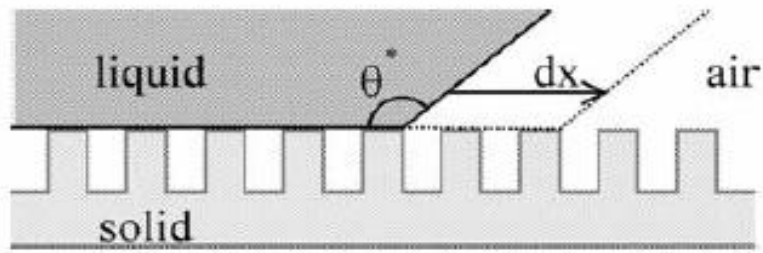


Figure 4.12: A Liquid is Deposited on a Model Surface That has Holes or Spikes. When The Contact Angle is Greater Than 90°, Air is Trapped Beneath The Liquid, Causing The Solid and The Drop to Form a Composite Interface.

It is possible that through increase in hydrophobic part of the polymers, thin films can be developed that results in such surfaces. This is reflected in relatively higher contact angle with lower wettability. Also, due to higher contents of PMMA in polymers which act as polyelectrolytes chain, there is possibility of mor enough films with loopy structures in it, which ultimate enhances the contact angel values.

Upon moving towards acidic pH in PMMA-co-AA copolymer, chains are less ionized and hence lead to relatively less dense but loopy films. Such effect is very subtle and have a significant effect on controlling the hydrophilic to hydrophobic interactions.

Upon increasing the hydrophilic components in the copolymer compositions, With porous surfaces, when liquid fills pores and drops land on surfaces that are partially solid and partially liquid, the hydrophilic model becomes relevant. Figure displays this.

This is presented in Figure X:

$$\cos \theta^* = 1 + \Phi_S(-1 + \cos \theta_E) \quad (\text{Equation 4})$$

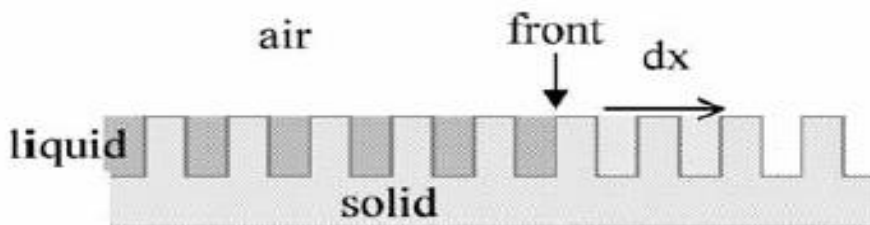


Figure 4.13: Spike-Adorned Solid Surface Being Invaded by Liquid Film (Or Microchannels). An Arrow Points to The Forward.

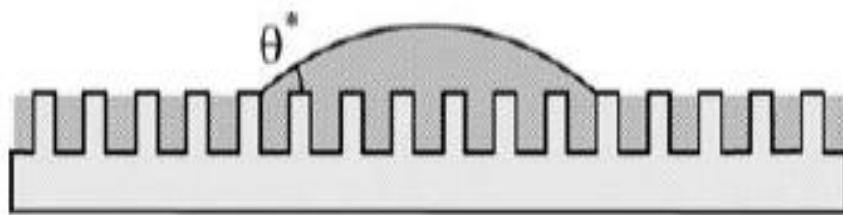


Figure 4.14: Calculation of θ^* on a Composite Surface

Another intriguing scenario is in Figure 4.14, when a drop rests on a composite surface made of both liquid and solid and a film infiltrates the solid roughness.

It is then discovered that θ^* lies in the middle of θ , the contact angle on a flat homogeneous solid, and 0 (which would be observed if the substrate consisted solely of liquid).

The hydrophilic model is relevant when AA monomers in the polymer composition becomes higher. This leads to two factors; First, thin films expect to be more compact and less dense due to strong interaction between oppositely charged counter ions of polycations and polyanions.

Secondly, roughness of films can also be tuned through compositional control via pH variation. It is observed through that at lower pH with AA in structure, chain is less ionized and in general lead to loopy films; However, with higher AA contents, chains are more ionized at basic pH values to lead to more compact with higher ionic interaction films. Thus, allow to control hydrophilic and hydrophobic interactions.

Since hydrophilic and hydrophobic interactions are strongly influenced by surface roughness, and such observation can be explained by Wenzel Model. Contrary to all existing findings, a surface with complete wetting ($\theta^* = 0$) or superhydrophobic de-wetting ($\theta^* = 180$) can be generated by texture, as long as the roughness is sufficiently great ($r > 1$).

The Wenzel relation qualitatively supports the main findings: roughness increases hydrophilicity and hydrophobicity since $\theta^* > \theta > 90^\circ$ and $\theta^* < \theta < 90^\circ$. The Wenzel connection is only applicable to mild roughness factors and is typically non-quantitative.

One final comment needed to be addressed is that in the formation of self-assembled multilayers thin films of PMMA-co-PAA, it is expected that there is hysteresis. The non-equivalent advances and retreating contact angles are what characterize hysteresis. Contact angle hysteresis is present on almost all solid surfaces; H the difference between

$$H = CA(\text{adv}) - CA(\text{rec}) \quad (\text{Equation 6})$$

A solid surface's heterogeneity and roughness may be the cause of contact angle hysteresis. According to Young's equation, the measured contact angles have little significance if roughness is the main contributing factor.

Contact angles are greater on extremely rough surfaces than they are on smooth, chemically equivalent surfaces. It is obvious that interpreting such angles in terms of the Young Model Contact angles are greater on extremely rough surfaces than they are on smooth, chemically equivalent surfaces.

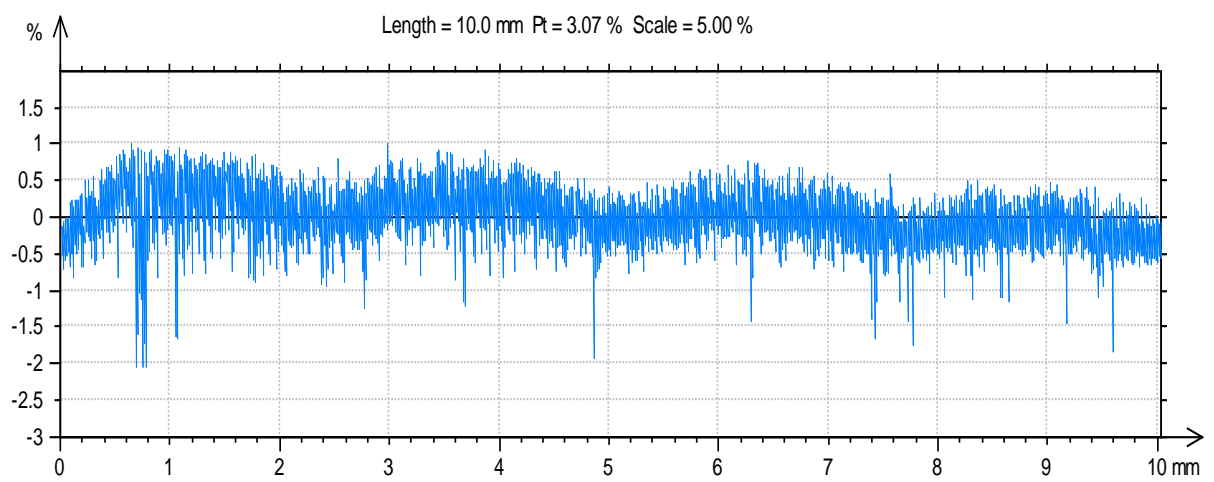
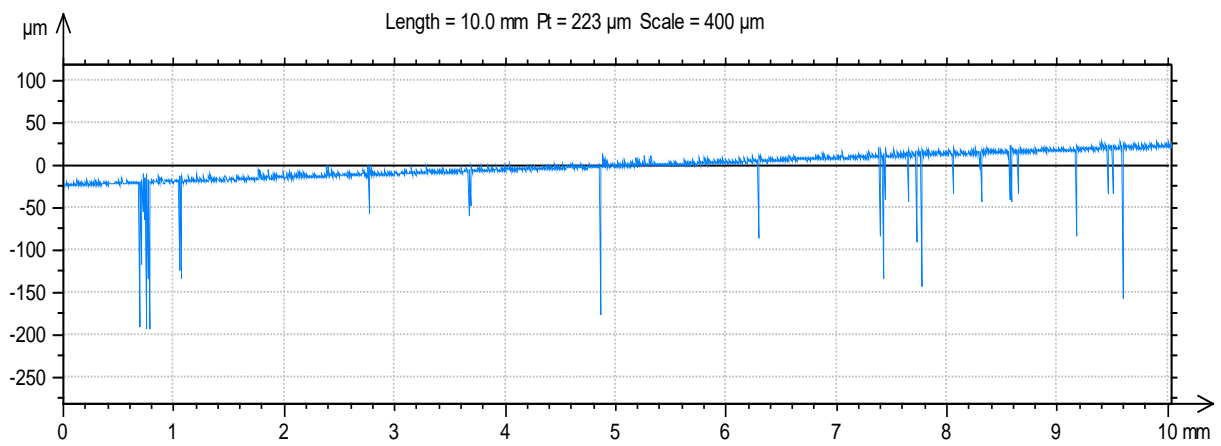
It is obvious that interpreting such angles in terms of the Young Model would produce incorrect findings since, because of ($\gamma_{S,V}$, $\gamma_{S,L}$, $\gamma_{L,V}$), the CA would inexorably reflect surface topography rather than only surface energetics.

4.6 Optical Profilometry

Optical profilometry was used to determine the surface characteristic of thin films, so it was observed that the coated films show less roughness value as compare to control (roughness value decrease after coating).

A general trend in surface roughness was observed with an increase by the number of bilayers and at pH 3, the average roughness was greater due to accumulation of PP50 in loop rick conformation as compare to pH10 where smooth thin layers was formed.

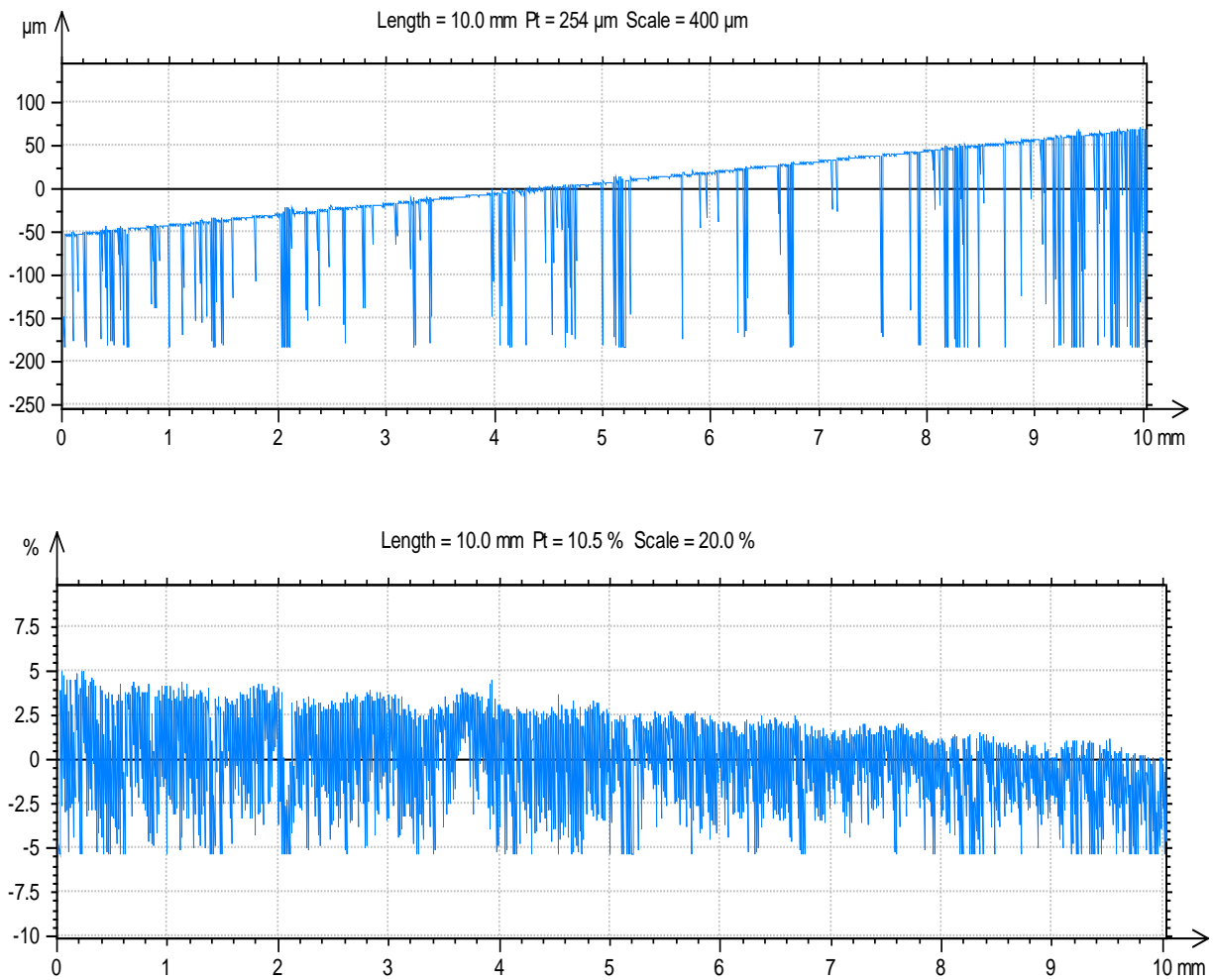
1BL



ISO4287			
Amplitude parameters - Roughness profile			
Rp	10.7	µm	Gaussian filter, 0.8 mm
Rv	82.3	µm	Gaussian filter, 0.8 mm
Rz	92.9	µm	Gaussian filter, 0.8 mm
Rc	35.5	µm	Gaussian filter, 0.8 mm
Rt	199	µm	Gaussian filter, 0.8 mm
Ra	2.17	µm	Gaussian filter, 0.8 mm
Rq	5.91	µm	Gaussian filter, 0.8 mm
Rak	-8.11		Gaussian filter, 0.8 mm
Rku	162		Gaussian filter, 0.8 mm
Material Ratio parameters - Roughness profile			
Rmr	0.026	%	c = 1 µm under the highest peak, Gaussian filter, 0.8 mm
Rdc	2.60	µm	p = 20%, q = 80%, Gaussian filter, 0.8 mm

Figure 4.15: 1 Bilayers Surface Roughness Measures for The Fabricated Thin Films of PMMA-Co-AA Copolymers.

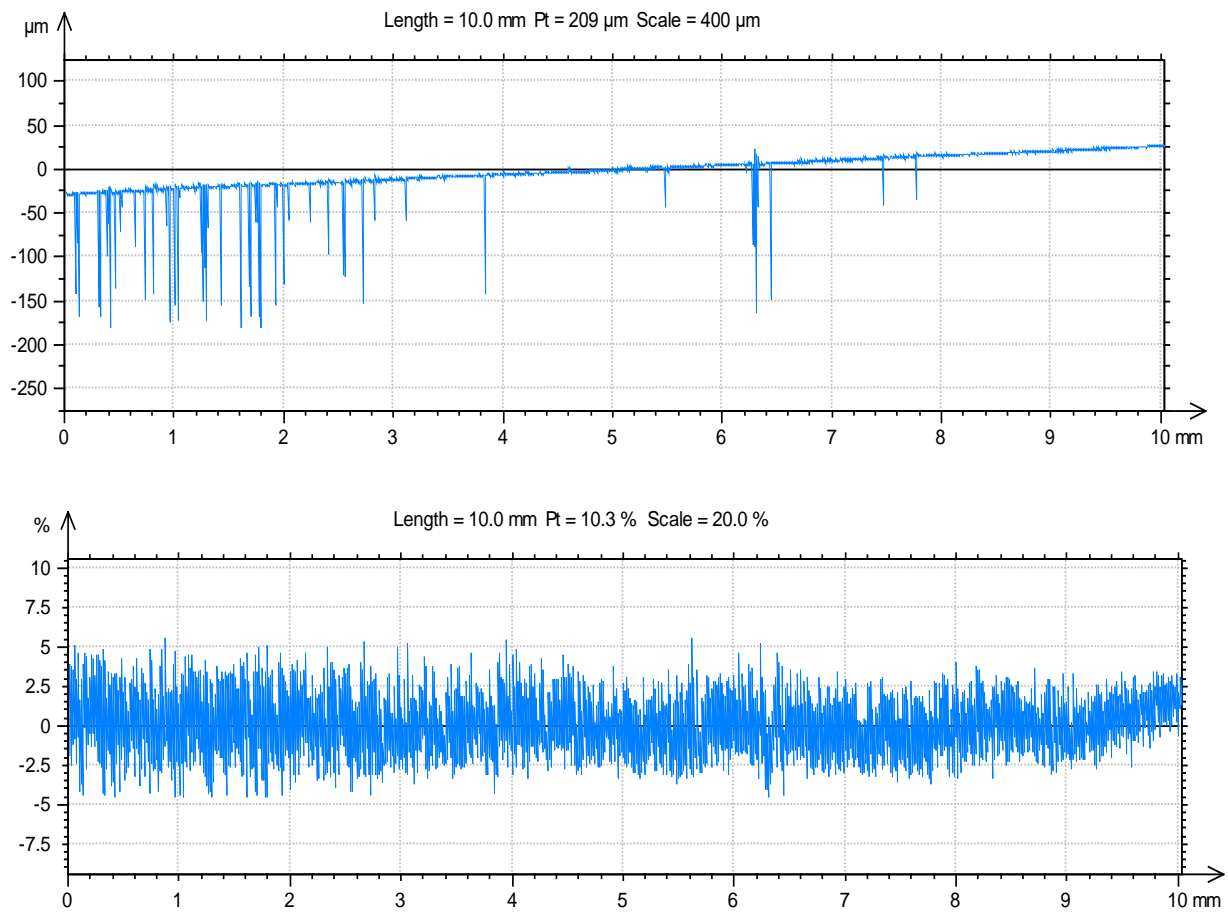
5BL



ISO 4287			
Amplitude parameters - Roughness profile			
Rp	17.4	μm	Gaussian filter, 0.8 mm
Rv	181	μm	Gaussian filter, 0.8 mm
Rz	198	μm	Gaussian filter, 0.8 mm
Rc	148	μm	Gaussian filter, 0.8 mm
Rt	264	μm	Gaussian filter, 0.8 mm
Ra	11.5	μm	Gaussian filter, 0.8 mm
Rq	27.7	μm	Gaussian filter, 0.8 mm
Rsk	-5.76		Gaussian filter, 0.8 mm
Rku	47.1		Gaussian filter, 0.8 mm
Material Ratio parameters - Roughness profile			
Rmr	0.0311	%	c = 1 μm under the highest peak, Gaussian filter, 0.8 mm
Rdc	8.28	μm	p = 20%, q = 80%, Gaussian filter, 0.8 mm

Figure 4.16: 5 Bilayers Surface Roughness Measures for The Fabricated Thin Films of PMMA-Co-AA Copolymers.

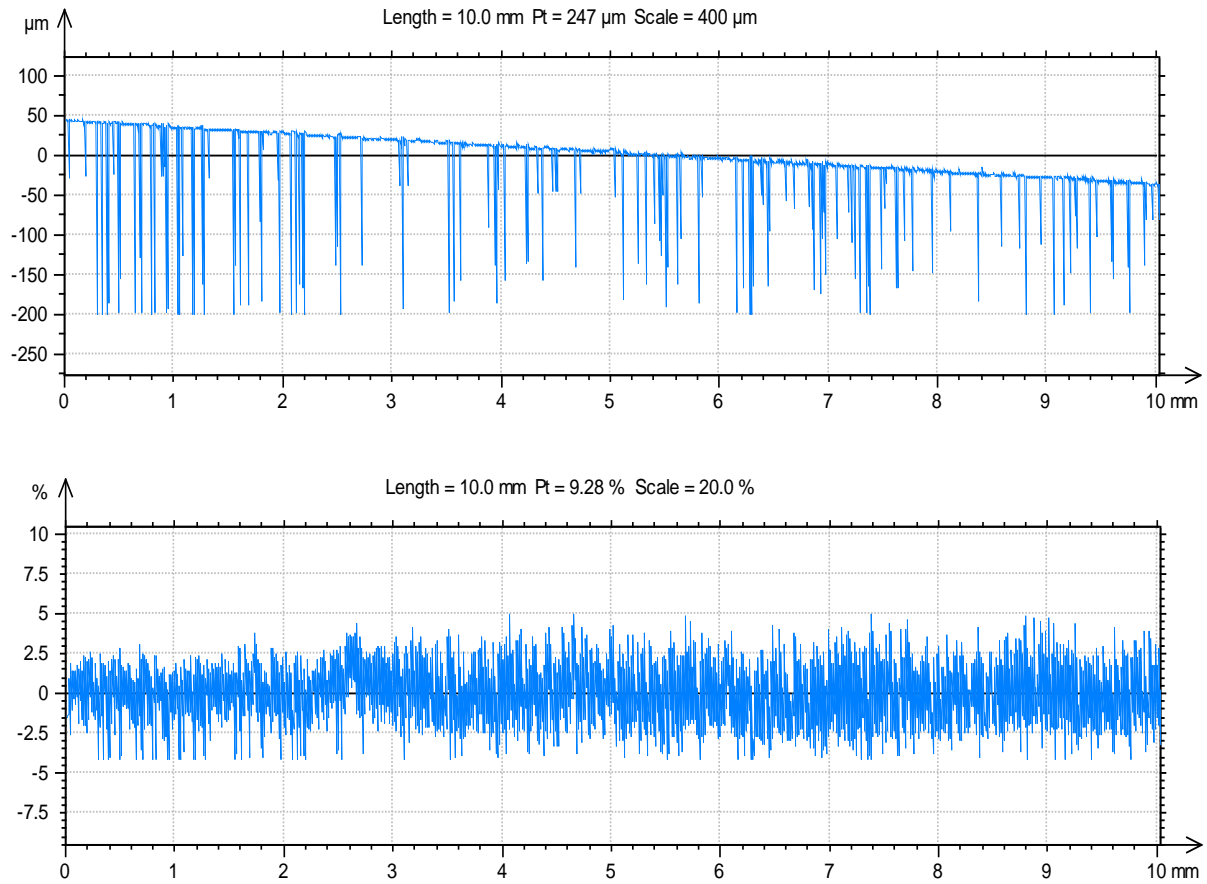
10BL



ISO 4287			
Amplitude parameters - Roughness profile			
Rp	6.48	µm	Gaussian filter, 0.8 mm
Rv	84.4	µm	Gaussian filter, 0.8 mm
Rz	90.9	µm	Gaussian filter, 0.8 mm
Rc	39.5	µm	Gaussian filter, 0.8 mm
Rt	181	µm	Gaussian filter, 0.8 mm
Ra	2.10	µm	Gaussian filter, 0.8 mm
Rq	6.47	µm	Gaussian filter, 0.8 mm
Rsk	-10.2		Gaussian filter, 0.8 mm
Rku	188		Gaussian filter, 0.8 mm
Material Ratio parameters - Roughness profile			
Rmr	0.0114	%	c = 1 µm under the highest peak, Gaussian filter, 0.8 mm
Rdc	2.10	µm	p = 20% q = 80% Gaussian filter, 0.8 mm

Figure 4.17: 10 Bilayers Surface Roughness Measures for The Fabricated Thin Films of PMMA-Co-AA Copolymers.

15 BL



Amplitude parameters - Roughness profile			
Rp	11.6	µm	Gaussian filter, 0.8 mm
Rv	104	µm	Gaussian filter, 0.8 mm
Rz	206	µm	Gaussian filter, 0.8 mm
Rc	100	µm	Gaussian filter, 0.8 mm
Rt	200	µm	Gaussian filter, 0.8 mm
Ra	6.29	µm	Gaussian filter, 0.8 mm
Rq	32.9	µm	Gaussian filter, 0.8 mm
Rsk	-7.41	µm	Gaussian filter, 0.8 mm
Rku	166.2	µm	Gaussian filter, 0.8 mm
Material Ratio parameters - Roughness profile			
Rmr	0.0001	%	0.1 µm filter, 0.8 mm
Rdc	0.99	µm	0.1 µm filter, 0.8 mm

Figure 4.18: 15 Bilayers Surface Roughness Measures for The Fabricated Thin Films of PMMA-Co-AA Copolymers.

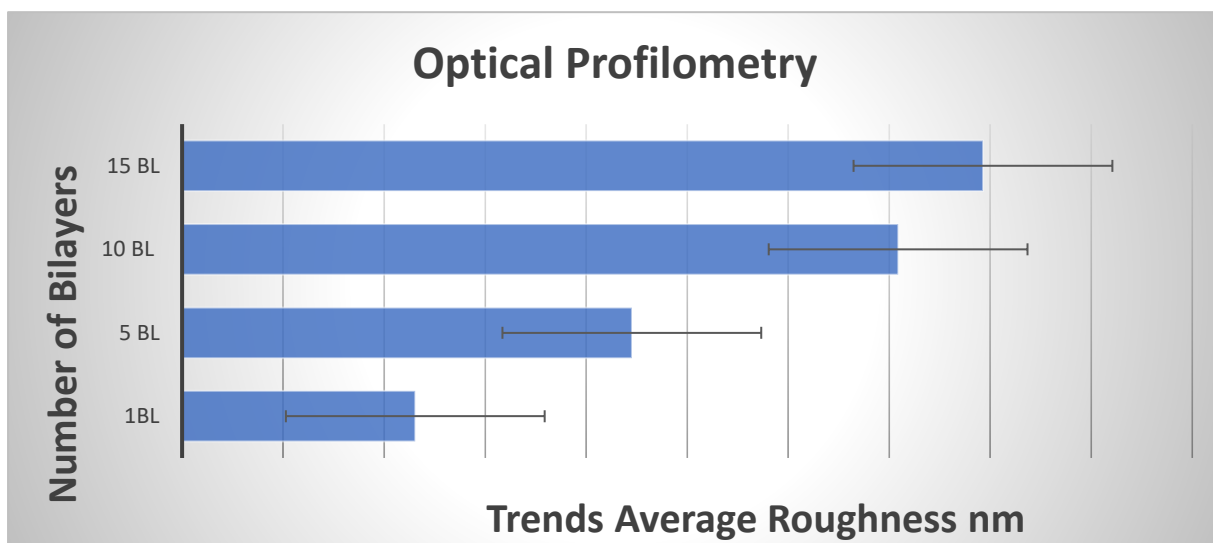


Figure 4.19: By Increasing number of LBL Bilayers, the Average Roughness Value Increased.

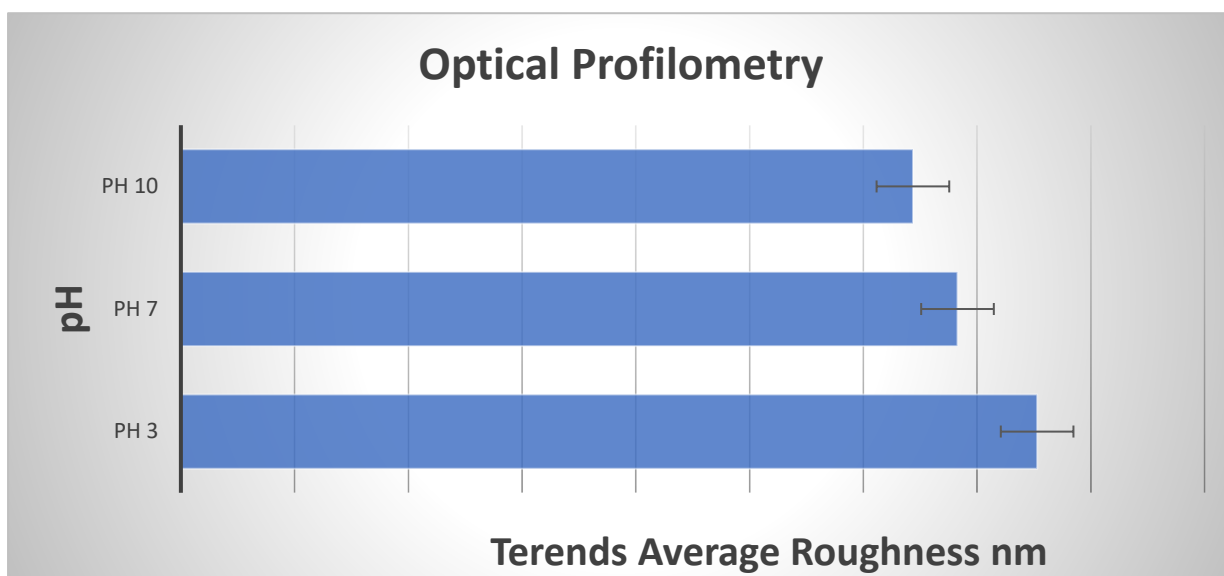


Figure 4.20: 10 BL Samples (PAA50 as the Top Layer)

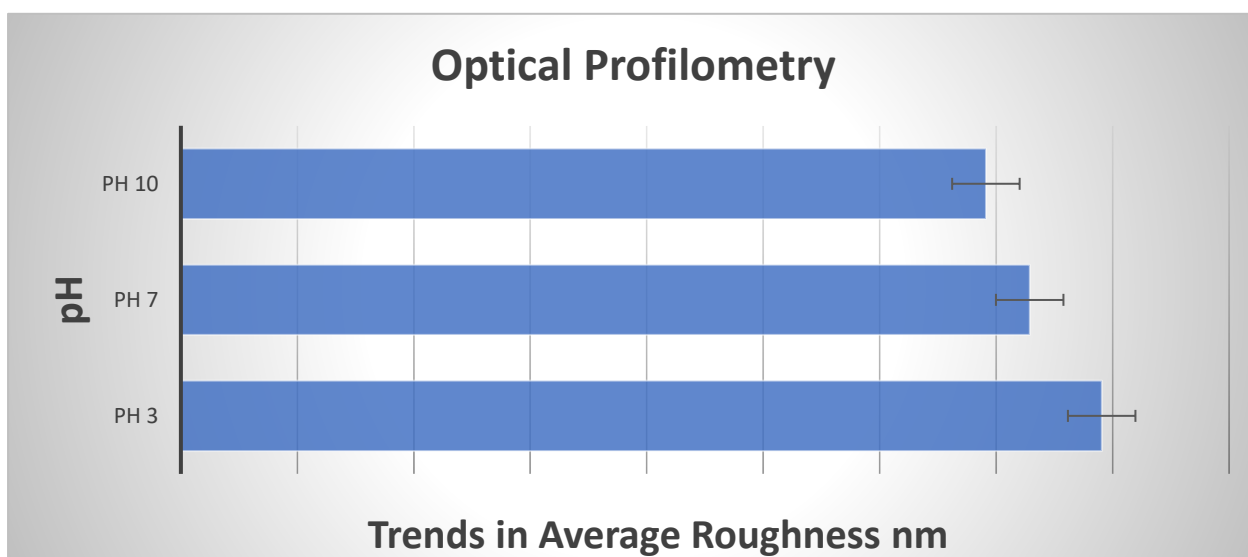


Figure 4.21: 10 BL Samples (PDAC as the Top Layer)

The data and figures presented above for the fabricated films of 1, 5, 10 and 15 are explained and correlated with reported results. Further understanding of the surface morphology can be obtained by tracking the rise in surface roughness with increasing layer count. One way to quantify the variations in surface height is to look at RMS roughness. Features that have similar dimensions in the surface topography are associated with a certain density, which in turn determines the RMS roughness.

The polyelectrolyte film produced on naked glass, as well as the film grown on strongly ionized and loosely ionized polymer chains, exhibit broad trends for the RMS roughness, as shown in figure 4.23. The two curves differ significantly, as would be predicted based on roughness data and topographic photos taken with an optical microscope.

The film applied to bare glass reveals that chains with loosely ionized and pH-tuneable effects have relatively rough surfaces, whereas strongly ionized chains have less rough surfaces. Additionally, it was noted that roughness increased gradually as the number of bilayers increased before somewhat plateauing once more. On the other hand, the film-deposited glass with ionized chain exhibits significantly less surface roughness.

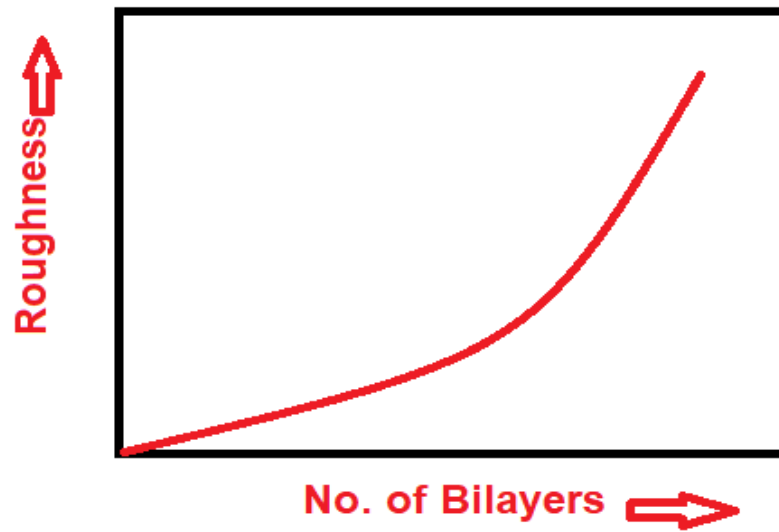


Figure 4.22: Bilayers Effect on Surface Roughness of The Self-Assembled Multilayers Films.

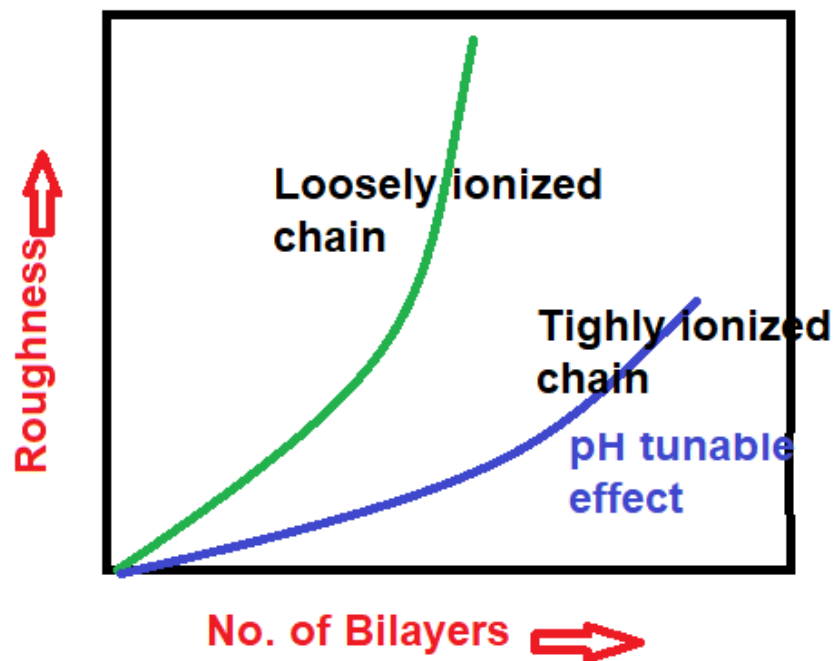


Figure 4.23: Tuneable pH Effect on The Surface Roughness of The Self-Assembled Multilayers Films.

For instance, during the production of two distinct polyelectrolyte films, the root mean-square surface roughness values were determined based on shear force measurements. The surface roughness difference between a film having PEI/PSS(PAH/PSS)_x and a film containing just (PAH/PSS)_x is plotted. By employing the commercial scanning electronics to calculate the RMS roughness at ten distinct locations on the film, surface roughness measurements were made for each growth phase measured.

Once the polyelectrolyte films formed on bare and PEI-treated glass achieve a steady-state value, both their apparent morphology and surface roughness are likely due to the intrinsic morphology of the layers rather than nucleated defects.

This is in sharp contrast to films made via metal phosphonate self-assembly or Langmuir–Blodgett processes, in which the quantity of surface features and surface roughness rise linearly as the number of layers increases, as does the size of surface bumps.

As more layers are deposited, a highly branched polyelectrolyte decreases interface roughness and enhances film adhesion. Since the steady-state surface topography depends on the intrinsic morphology of the polyelectrolytes rather than the substrate topography, these results suggest that the deposition of polyelectrolyte layers has the ability to "smooth-out" or "heal" a rough surface. There have been various earlier organizations that have proposed the "healing" properties of polyelectrolyte layers.

4.7 Optical Microscopy

Optical microscopy of the prepared self-assembled multilayers thin films was observed with the objective to understand surface morphology of the deposited chains and also surface area coverage. The images of the prepared thin films are presented in figure 4.24. Among various observation, it was noted that LBL thin films of polyelectrolytes with water insoluble polyelectrolyte components can undergoes the process of intermolecular association while intramolecular aggregation.

This effect can be observed due to hydrophobic effect when dissolved in aqueous media and from the PMMA part of the polyelectrolytes chains. The images observed suggest the presence of the aggregation of the films during self-assembly as was investigated studying the film morphology using optical microscopy. By doing microscopic analysis it was observed that

more polymer films were deposited to cover surface with higher number of LBL as compare to low no. of LBL.

This is due to presence of a greater number of oppositely charged surfaces adsorbed here in comparison of 1BL or 5BL, so more surface area was covered due to presence of polymer chain in 10BL.

As an illustration, consider a study that used near-field scanning optical microscopy and scanning force to examine the nanoscale morphology of polyelectrolyte self-assembled films. Here are topography pictures of the prepared thin films produced receptively after zero, two, and ten bilayers on naked glass and on a surface coated with PEI. Picture of a raw glass surface that has been cleaned using the appropriate solutions; the picture shows no characteristics at all.

A number of tiny elevated characteristics emerge on the raw glass surface when two bilayers are added. Similar findings were found when LBL was deposited in the current study.

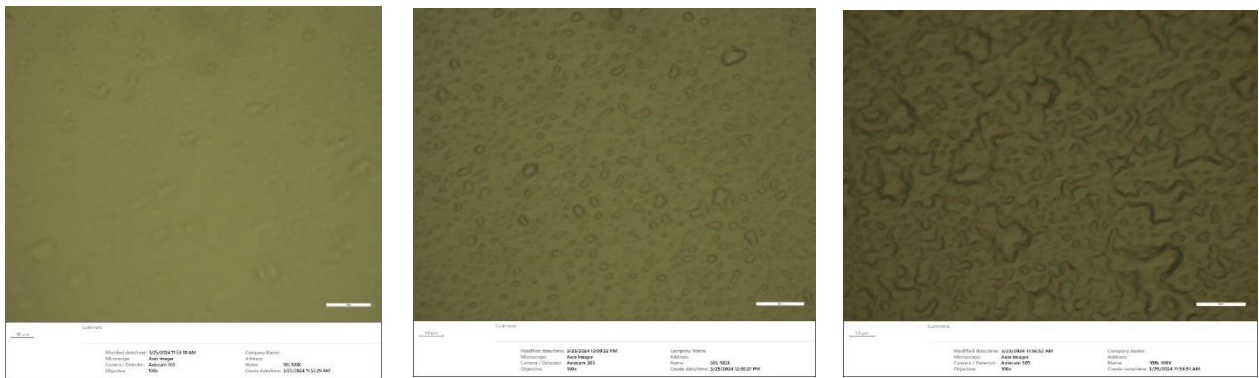
These features' diameter and height are in line with earlier research on a related system that employed cutting-edge microscopic techniques. The density of these features has expanded to cover most of the surface with the addition of 10 bilayers, but their approximate size has not changed.

After the deposition of ten bilayers, there is little change in the surface topography, and images of films with more than ten bilayers are remarkably comparable to those of other LBL. If pH-tuneable conditions are applied to the glass surface during bilayer deposition, a significant shift in the surface topography is seen.

The topography of the glass surface treated with PAHs is depicted in Figures 10 and 15, where the surface seems featureless and remarkably comparable to the naked glass surface. There are much fewer tiny features than in the film without the PAH layers after the deposition of two bilayers. Ten bilayers have been deposited, and while this has improved the density of the microscopic features, their size is still lower than it was in the ten-bilayer film formed on naked glass.

By understanding of surface morphology by tracking the rise in surface roughness in relation to layer count. The rms roughness, as was covered in the preceding section, is a measurement of the surface's height fluctuations. The rms roughness is correlated with the density of features if the surface topography is typified by features of comparable dimensions.

The surface morphological features and coverage of polyelectrolyte films grown on bare glass and glass treated with PAHs are significantly influenced by their respective rms roughness and pH, as demonstrated by optical microscopic pictures. There are noticeable variations, as would be expected based on the topography photos.



OM - 1BL@100X

OM - 5BL@100X

OM - 10BL@100X

Figure 4.24: Optical Microscopic (OM) Images of 1, 5 and 10 BL at 100X Magnification.

4.8 Antimicrobial Testing of the Thin Films

The produced copolymers' antibacterial efficacy against *S. aureus*, *E. coli*, and *P. aeruginosa* demonstrates that activity increases with an increase in PAA content. It was determined that the presence of acrylic acid in copolymers had a bactericidal effect. A few key findings are:

- Bacterial Strain: *Escherichia coli*, SRS, and *P. aeruginosa* were used.
- The antimicrobial activity of the copolymers against *S. aureus*, *E. coli*, and *P. aeruginosa* rises with increasing PAA contents.
- High pH during fabrication of films leads to repulsive effect.

- Presence of high concentration of acrylic acid in the Copolymer produce harsh environment for bacteria consequently leading to the death of the microbes. High pH during fabrication of films leads to repulsive effect.

The observed results are presented below and in good agreement with previous work.

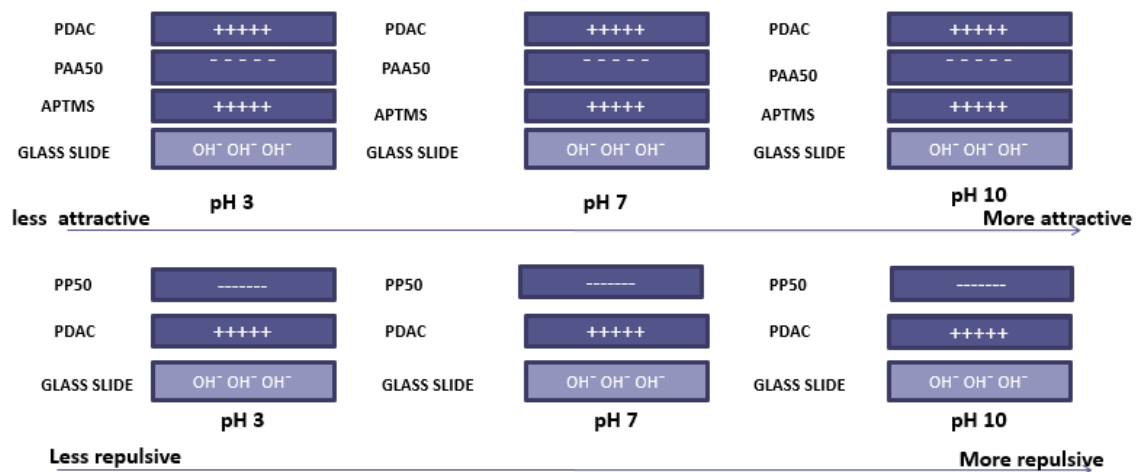


Figure 4.25: More Negative Charge Toward Substrate Produces More Repulsive Substrate for Microbial Attachment and Vice Versa.

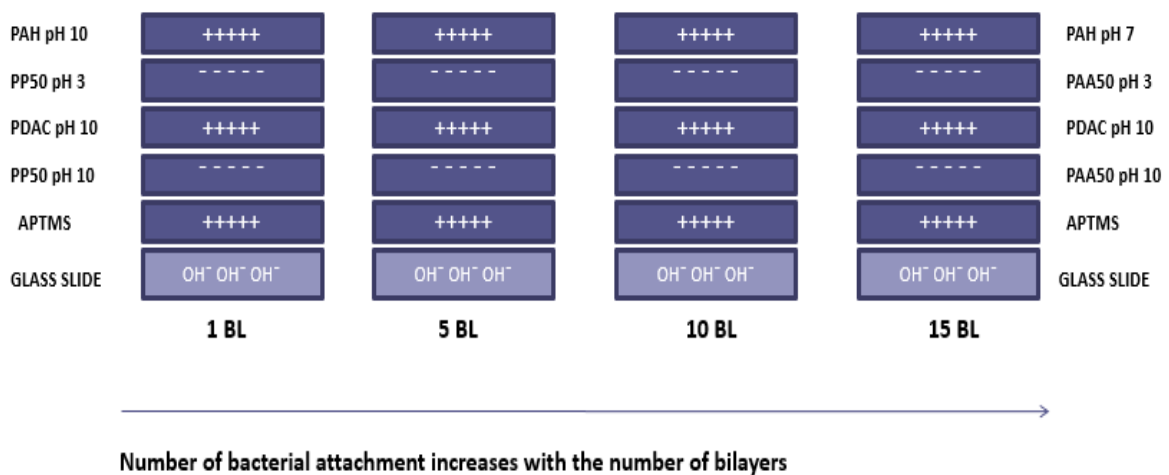


Figure 4.26: Number Of Bacterial Attachments Increases with The Number of Bilayers as Bacterial Get More Surface Area to Attached to Substrate.

4.8.1 Bacteria Repulsion and Attraction Study on Switchable Surface Coatings:

As bacterial fouling is mainly related to biomedical applications, in this study two common bacteria were used living in the physiological environment that is *E. coli* (Gram negative) and *S. aureus* (Gram positive) negatively charged and positively charged films in PBS (artificial physiological environment) at pH 7.4.

The aforementioned microorganisms were subjected to fouling experiments, which were conducted in accordance with a predetermined settlement technique and evaluated accordingly. The bacterial cell surfaces have a net negative electric charge because of the ionized phosphoryl and carboxylate substituents on their outer cell envelope [102].

4.8.2 Bacterial repellent thin films on the basis of surface charge and Ionization degree:

In this study the bacterial repellent thin films were prepared by using PAA and PDADMAC. PAA that is a weak Polyanion and is sensitive to pH was used as the top layer. At pH 10 PAA is fully ionized so greater amount of negative charge is exposed on the surface thus the surface become highly bacteria repellent and no bacterial attachment was found on the surface of glass slides as compared to pH 7 where PAA is not fully ionized and expose less negative charge, resulted in less bacterial attachment on the glass slide and at pH 3 where PAA is almost fully deionized and do not repel bacteria. As a result, large amount of bacterial attachment was found. As shown in figure 4.7.

4.8.3 Bacterial attraction thin films:

The bacterial attractive thin films were prepared using PAA and PDADMAC, where PDADMAC that is a strong Polycation was used as the top layer. At pH 3 large amount of bacterial attachment was found due to the greater load of deionized PAA that as a result attracted large amount of PDADMAC in order to compensate the underlying charge. On the other hand, less, bacterial attachment was found at pH 7 and little bacterial attachment at pH 10 due to fully ionized PAA in the underlying layer. (as shown in the figure 4.8).

Microbicidal properties that are either intrinsic or enhanced by nanotechnology are exhibited by antimicrobial thin films, or ATFs. Due to their many uses in a variety of industries, particularly in textile finishing, food packaging, wound dressing, and anti-fouling water

treatment membranes, they are growing in popularity. By customizing their functionality to target particular microorganisms in different engineering designs, ATFs can be used to stop the growth of dangerous pathogens like fungi and bacteria on a range of surfaces.

A number of factors need to be carefully taken into account when designing an ideal antimicrobial thin film, such as the type of active agent material, stability against external environmental triggers, manufacturing processes, geometric requirements for adhesion to substrate material/surface, physical advantages like breathability,

The current study uses chemical biocides embedded in films as a common antimicrobial action mechanism for nano-enabled antimicrobial thin films in the current work. For example, in thin-film based on PDADMAC, positively charged cationic residues typically first attach themselves to anionic charge group to produce electrostatic repulsion to kill microorganism polymer-based antimicrobial coating design comprises three components; the active layer, the adhesive/repulsive layer, and the polymer backbone.

The physical and chemical states of the substrate have been created by a range of surface treatment and media switchable approaches to explore the mechanism of how the substrate state influences the adhesive.

While active layers, such as those with specific killing mechanisms, impart antibacterial and antifungal properties, the adhesive layer aids in adhering the film. The PMMA-co-AA produced LBL thin films, which exhibit hydrophilic to hydrophobic properties and pH tuneability, are intriguing polymer materials that can showcase inherent antimicrobial activity in ATF systems. Additionally, they can function as a matrix medium to support active agents.

Three primary mechanisms are demonstrated in figure 4.27 for the action of polymer-based antimicrobial thin films: diffusion killing (semi-leaching), contact killing (leaching), and physical barriers (non-leaching).

Physical barriers employ contact angles and surface roughness features to hinder bacterial attachment, whereas contact killing biofilms, when dampened and lit, allow direct killing through leachate release, frequently through ion exchange processes. Finally, diffusion killing systems work with preformed pores and capillaries in the film matrix to allow small amounts of chemicals scattered throughout the layer to slowly seep out over time through thermally induced polymer chain motions upon exposure to light or humidity triggers.

This process reduces transport away from the site and contributes to localized and prolonged efficacy while also minimizing environmental impact.

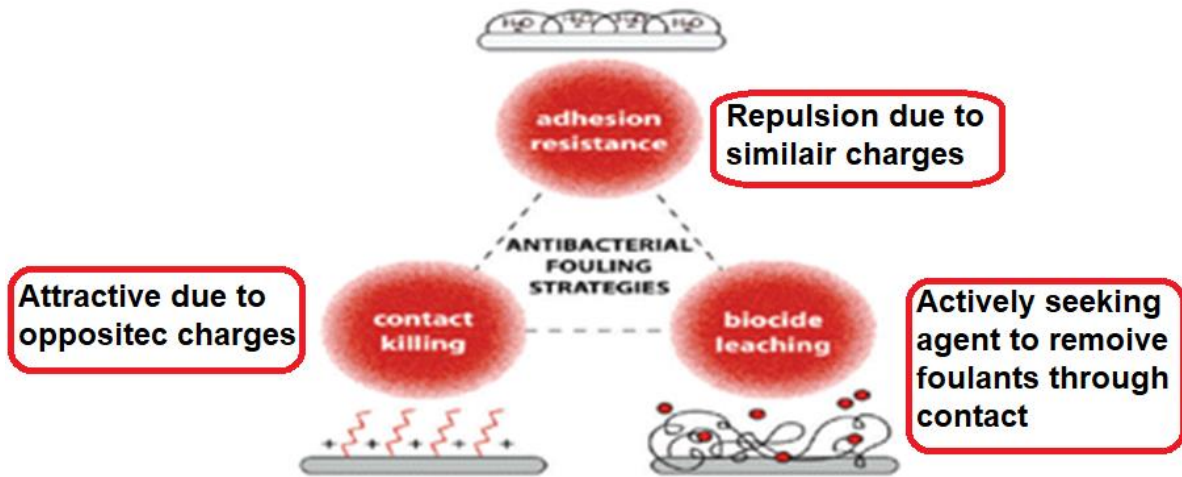


Figure 4.27: PMMA-Co-PAA Polymer-Based Thin Film Antimicrobial Mechanisms Illustrate the Role of Attractive and Repulsive Nature. With Increase in PMMA Amount in Copolymers, There is a Possibility of More Adhesion; At Higher pH with Highly Charged Anionic Chain can Perform Repulsive Action to Foulants.

CHAPTER 5: CONCLUSION AND FUTURE RECOMENDATIONS

5.1 Conclusion

The main conclusions from the current works are mentioned below:

- A general decreasing trend in contact angle was observed with an increase in number of bi-layers which means that more water molecules interact with the surface due to accumulation of a greater number of surface charges.
- Lowest value of contact angle was observed at pH 10 because of greater number of surface charges as compared to pH 3
- However, a general increasing trend in surface roughness was observed with an increase in number of bi-layers
- At pH 3 average roughness was greater due to accumulation of PP50 in loop rich conformations as compared to pH 10 where smooth thin layers were formed
- The slides were coated at pH 10 with PP50 as the top layer following LBL deposition process as an application of the above work and no bacterial attachment was found.

5.2 Future Recommendations

In present work, interesting polymer compositions with variable amount of hydrophilic and hydrophobic structure were prepared. These structures allow to tune many properties and applications. For example, coatings of these films of membranes and materials can eb explored to as the bacterial repellent thin films for water purification purpose.

The prepared polymer compositions can also be used for sterilization purpose in biomedical application such as in a range of applications. The bacterial adhesive thin films can also be used to attach and detect desired bacterial strains in cases when strains are in very minute concentrations.

Coatings can be performed on surgical equipment to understand their efficacy and performance. In future it can be used to fabricate the charge control LBL capsule for drug delivery purpose; it can also be used for selective adsorption or purification of proteins through the exploration of the prepared copolymers.

BIBLIOGRAPHY

- [1] D. Sen, B. Mohite, and N. Kayande, “REVIEW ON POLYMER,” *Int. Journal of Pharmaceutical Sciences and Medicine (IJPSM)*, vol. 4, pp. 1–15, 2019, [Online]. Available: www.ijpsm.com
- [2] “Reviewing of General Polymer Types, Properties and Application in Medical Field,” *International Journal of Science and Research (IJSR)*, vol. 5, no. 8, pp. 212–221, Aug. 2016, doi: 10.21275/art2016772.
- [3] F. Perin, A. Motta, and D. Maniglio, “Amphiphilic copolymers in biomedical applications: Synthesis routes and property control,” *Materials Science and Engineering C*, vol. 123. Elsevier Ltd, Apr. 01, 2021. doi: 10.1016/j.msec.2021.111952.
- [4] S. Mushtaq, N. M. Ahmad, A. Mahmood, and M. Iqbal, “Antibacterial amphiphilic copolymers of dimethylamino ethyl methacrylate and methyl methacrylate to control biofilm adhesion for antifouling applications,” *Polymers (Basel)*, vol. 13, no. 2, pp. 1–13, Jan. 2021, doi: 10.3390/polym13020216.
- [5] G. D. Bixler and B. Bhushan, “Review article: Biofouling: Lessons from nature,” *Philosophical Transactions of the Royal Society A: Mathematical, Physical and Engineering Sciences*, vol. 370, no. 1967. Royal Society, pp. 2381–2417, May 28, 2012. doi: 10.1098/rsta.2011.0502.
- [6] D. A. V. da Silva *et al.*, “Biocide Susceptibility and Antimicrobial Resistance of *Escherichia coli* Isolated from Swine Feces, Pork Meat and Humans in Germany,” *Antibiotics*, vol. 12, no. 5, May 2023, doi: 10.3390/antibiotics12050823.
- [7] Z. K. Zander and M. L. Becker, “Antimicrobial and Antifouling Strategies for Polymeric Medical Devices,” *ACS Macro Lett*, vol. 7, no. 1, pp. 16–25, Jan. 2018, doi: 10.1021/acsmacrolett.7b00879.
- [8] I. A. Jones and L. T. Joshi, “Biocide use in the antimicrobial era: A review,” *Molecules*, vol. 26, no. 8. MDPI AG, Apr. 02, 2021. doi: 10.3390/molecules26082276.
- [9] L. Gu *et al.*, “Construction of antifouling membrane surfaces through layer-by-layer self-assembly of lignosulfonate and polyethyleneimine,” *Polymers (Basel)*, vol. 11, no. 11, Nov. 2019, doi: 10.3390/polym11111782.
- [10] L. Wang, N. Wang, J. Li, J. Li, W. Bian, and S. Ji, “Layer-by-layer self-assembly of polycation/GO nanofiltration membrane with enhanced stability and fouling resistance,” *Sep Purif Technol*, vol. 160, pp. 123–131, Feb. 2016, doi: 10.1016/j.seppur.2016.01.024.
- [11] S. Liu and W. Guo, “Anti-Biofouling and Healable Materials: Preparation, Mechanisms, and Biomedical Applications,” *Advanced Functional Materials*, vol. 28, no. 41. Wiley-VCH Verlag, Oct. 10, 2018. doi: 10.1002/adfm.201800596.

- [12] K. S. Huang, C. H. Yang, S. L. Huang, C. Y. Chen, Y. Y. Lu, and Y. S. Lin, "Recent advances in antimicrobial polymers: A mini-review," *International Journal of Molecular Sciences*, vol. 17, no. 9. MDPI AG, Sep. 20, 2016. doi: 10.3390/ijms17091578.
- [13] R. Hu, A. Qin, and B. Z. Tang, "AIE polymers: Synthesis and applications," *Progress in Polymer Science*, vol. 100. Elsevier Ltd, Jan. 01, 2020. doi: 10.1016/j.progpolymsci.2019.101176.
- [14] Z. Zhou *et al.*, "Amphiphilic triblock copolymers with PEGylated hydrocarbon structures as environmentally friendly marine antifouling and fouling-release coatings," *Biofouling*, vol. 30, no. 5, pp. 589–604, 2014, doi: 10.1080/08927014.2014.897335.
- [15] L. Gu *et al.*, "Construction of antifouling membrane surfaces through layer-by-layer self-assembly of lignosulfonate and polyethyleneimine," *Polymers (Basel)*, vol. 11, no. 11, Nov. 2019, doi: 10.3390/polym11111782.
- [16] X. Zhu *et al.*, "Polyion multilayers with precise surface charge control for antifouling," *ACS Appl Mater Interfaces*, vol. 7, no. 1, pp. 852–861, Jan. 2015, doi: 10.1021/am507371a.
- [17] N. Peng, X. M. Xia, W. T. He, W. M. Liu, S. W. Huang, and R. X. Zhuo, "Fabrication and stability of porous poly(allylamine) hydrochloride (PAH)/poly(acrylic acid) (PAA) multilayered films via a cleavable-polycation template," *Polymer (Guildf)*, vol. 52, no. 5, pp. 1256–1262, Mar. 2011, doi: 10.1016/j.polymer.2011.01.033.
- [18] X. Zhu *et al.*, "Polyion multilayers with precise surface charge control for antifouling," *ACS Appl Mater Interfaces*, vol. 7, no. 1, pp. 852–861, Jan. 2015, doi: 10.1021/am507371a.
- [19] S. Chen, L. Li, C. Zhao, and J. Zheng, "Surface hydration: Principles and applications toward low-fouling/nonfouling biomaterials," *Polymer*, vol. 51, no. 23. Elsevier Ltd, pp. 5283–5293, Oct. 29, 2010. doi: 10.1016/j.polymer.2010.08.022.
- [20] M. T. Noori, M. M. Ghangrekar, C. K. Mukherjee, and B. Min, "Biofouling effects on the performance of microbial fuel cells and recent advances in biotechnological and chemical strategies for mitigation," *Biotechnology Advances*, vol. 37, no. 8. Elsevier Inc., Dec. 01, 2019. doi: 10.1016/j.biotechadv.2019.107420.
- [21] A. Laschewsky, "Structures and synthesis of zwitterionic polymers," *Polymers*, vol. 6, no. 5. Molecular Diversity Preservation International, pp. 1544–1601, 2014. doi: 10.3390/polym6051544.
- [22] T. Iwasaki and J. I. Yoshida, "Free radical polymerization in microreactors. Significant improvement in molecular weight distribution control," *Macromolecules*, vol. 38, no. 4, pp. 1159–1163, Feb. 2005, doi: 10.1021/ma048369m.
- [23] Y. Kakihana *et al.*, "Preparation of positively charged PVDF membranes with improved antibacterial activity by blending modification: Effect of change in membrane surface material properties," *Colloids Surf A Physicochem Eng Asp*, vol. 533, pp. 133–139, Nov. 2017, doi: 10.1016/j.colsurfa.2017.08.039.

- [24] D. Zhang *et al.*, “Micro- and macroscopically structured zwitterionic polymers with ultralow fouling property,” *J Colloid Interface Sci*, vol. 578, pp. 242–253, Oct. 2020, doi: 10.1016/j.jcis.2020.05.122.
- [25] S. Zheng *et al.*, “Implication of Surface Properties, Bacterial Motility, and Hydrodynamic Conditions on Bacterial Surface Sensing and Their Initial Adhesion,” *Frontiers in Bioengineering and Biotechnology*, vol. 9. Frontiers Media S.A., Feb. 12, 2021. doi: 10.3389/fbioe.2021.643722.
- [26] A. Schindler, M. Doedt, Ş. Gezgin, J. Menzel, and S. Schmölzer, “Identification of polymers by means of DSC, TG, STA and computer-assisted database search,” *J Therm Anal Calorim*, vol. 129, no. 2, pp. 833–842, Aug. 2017, doi: 10.1007/s10973-017-6208-5.
- [27] A. Ozkan and H. Berberoglu, “Adhesion of algal cells to surfaces,” *Biofouling*, vol. 29, no. 4, pp. 469–482, Apr. 2013, doi: 10.1080/08927014.2013.782397.
- [28] W. Yandi *et al.*, “Antialgal activity of poly(2-(dimethylamino)ethyl methacrylate) (PDMAEMA) brushes against the marine alga *Ulva*,” *Biofouling*, vol. 33, no. 2, pp. 169–183, Feb. 2017, doi: 10.1080/08927014.2017.1281409.
- [29] G. F. Alotaibi, “Factors Influencing Bacterial Biofilm Formation and Development,” *Am J Biomed Sci Res*, vol. 12, no. 6, pp. 617–626, May 2021, doi: 10.34297/ajbsr.2021.12.001820.
- [30] A. Muñoz-Bonilla and M. Fernández-García, “Polymeric materials with antimicrobial activity,” *Progress in Polymer Science (Oxford)*, vol. 37, no. 2. Elsevier Ltd, pp. 281–339, 2012. doi: 10.1016/j.progpolymsci.2011.08.005.
- [31] F. B. Mamba, T. Ndlovu, S. Mbizana, W. Khan, and N. P. Gule, “Antimicrobial and biodegradable materials based on ϵ -caprolactone derivatives,” *J Appl Polym Sci*, vol. 138, no. 9, Mar. 2021, doi: 10.1002/app.49903.
- [32] R. Yañez-Macías *et al.*, “Combinations of antimicrobial polymers with nanomaterials and bioactives to improve biocidal therapies,” *Polymers*, vol. 11, no. 11. MDPI AG, Nov. 01, 2019. doi: 10.3390/polym11111789.
- [33] L. Timofeeva and N. Kleshcheva, “Antimicrobial polymers: Mechanism of action, factors of activity, and applications,” *Applied Microbiology and Biotechnology*, vol. 89, no. 3. pp. 475–492, Feb. 2011. doi: 10.1007/s00253-010-2920-9.
- [34] R. Almousa, X. Wen, S. Na, G. Anderson, and D. Xie, “A modified polyvinylchloride surface with antibacterial and antifouling functions,” *Polym Adv Technol*, vol. 30, no. 5, pp. 1216–1225, May 2019, doi: 10.1002/pat.4554.
- [35] W. Sun, W. Liu, Z. Wu, and H. Chen, “Chemical Surface Modification of Polymeric Biomaterials for Biomedical Applications,” *Macromolecular Rapid Communications*, vol. 41, no. 8. Wiley-VCH Verlag, Apr. 01, 2020. doi: 10.1002/marc.201900430.
- [36] B. Ran, C. Jing, C. Yang, X. Li, and Y. Li, “Synthesis of efficient bacterial adhesion-resistant coatings by one-step polydopamine-assisted deposition of branched

- polyethylenimine-g-poly(sulfobetaine methacrylate) copolymers,” *Appl Surf Sci*, vol. 450, pp. 77–84, Aug. 2018, doi: 10.1016/j.apsusc.2018.04.184.
- [37] A. L. Z. Lee, V. W. L. Ng, W. Wang, J. L. Hedrick, and Y. Y. Yang, “Block copolymer mixtures as antimicrobial hydrogels for biofilm eradication,” *Biomaterials*, vol. 34, no. 38, pp. 10278–10286, Dec. 2013, doi: 10.1016/j.biomaterials.2013.09.029.
- [38] D. Park *et al.*, “Antimicrobial behavior of semifluorinated-quaternized triblock copolymers against airborne and marine microorganisms,” *ACS Appl Mater Interfaces*, vol. 2, no. 3, pp. 703–711, Mar. 2010, doi: 10.1021/am900748v.
- [39] C. J. Waschinski, J. Zimmermann, U. Salz, R. Hutzler, G. Sadowski, and J. C. Tiller, “Design of contact-active antimicrobial acrylate-based materials using biocidal macromers,” *Advanced Materials*, vol. 20, no. 1, pp. 104–108, Jan. 2008, doi: 10.1002/adma.200701095.
- [40] M. Szkudlarek, E. Heine, H. Keul, U. Beginn, and M. Möller, “Synthesis, characterization, and antimicrobial properties of peptides mimicking copolymers of maleic anhydride and 4-methyl-1-pentene,” *Int J Mol Sci*, vol. 19, no. 9, Sep. 2018, doi: 10.3390/ijms19092617.
- [41] P. Elena and K. Miri, “Formation of contact active antimicrobial surfaces by covalent grafting of quaternary ammonium compounds,” *Colloids and Surfaces B: Biointerfaces*, vol. 169, Elsevier B.V., pp. 195–205, Sep. 01, 2018. doi: 10.1016/j.colsurfb.2018.04.065.
- [42] A. Tsagdi, D. Druvari, D. Panagiotaras, P. Avramidis, V. Bekiari, and J. K. Kallitsis, “Polymeric coatings based on water-soluble trimethylammonium copolymers for antifouling applications,” *Molecules*, vol. 25, no. 7, 2020, doi: 10.3390/molecules25071678.
- [43] E. Chiellini, P. Cinelli, F. Chiellini, and S. H. Imam, “Environmentally degradable bio-based polymeric blends and composites,” in *Macromolecular Bioscience*, Mar. 2004, pp. 218–231. doi: 10.1002/mabi.200300126.
- [44] S. Krishnan, C. J. Weinman, and C. K. Ober, “Advances in polymers for anti-biofouling surfaces,” *J Mater Chem*, vol. 18, no. 29, pp. 3405–3413, 2008, doi: 10.1039/b801491d.
- [45] G. Masci *et al.*, “Atom transfer radical polymerization of potassium 3-sulfopropyl methacrylate: Direct synthesis of amphiphilic block copolymers with methyl methacrylate,” *Macromolecules*, vol. 37, no. 12, pp. 4464–4473, Jun. 2004, doi: 10.1021/ma0497254.
- [46] H. Liu, Z. Ma, W. Yang, X. Pei, and F. Zhou, “Facile preparation of structured zwitterionic polymer substrate via sub-surface initiated atom transfer radical polymerization and its synergistic marine antifouling investigation,” *Eur Polym J*, vol. 112, pp. 146–152, Mar. 2019, doi: 10.1016/j.eurpolymj.2018.07.025.
- [47] A. Debuigne, T. Radhakrishnan, and M. K. Georges, “Stable free radical polymerization of acrylates promoted by α -hydroxycarbonyl compounds,” *Macromolecules*, vol. 39, no. 16, pp. 5359–5363, Aug. 2006, doi: 10.1021/ma060288y.

- [48] L. Liu, W. Li, and Q. Liu, “Recent development of antifouling polymers: Structure, evaluation, and biomedical applications in nano/micro-structures,” *Wiley Interdiscip Rev Nanomed Nanobiotechnol*, vol. 6, no. 6, pp. 599–614, Nov. 2014, doi: 10.1002/wnan.1278.
- [49] H. Günaydin, S. Salman, N. Ş. Tüzün, D. Avci, and V. Aviyente, “Modeling the free radical polymerization of acrylates,” *Int J Quantum Chem*, vol. 103, no. 2, pp. 176–189, May 2005, doi: 10.1002/qua.20480.
- [50] R. J. Young and P. A. Lovell, “Introduction to Polymers INTRODUCTION TO.”
- [51] M. Moreno-Couranjou, R. Mauchauffé, S. Bonot, C. Detrembleur, and P. Choquet, “Anti-biofouling and antibacterial surfaces: Via a multicomponent coating deposited from an up-scalable atmospheric-pressure plasma-assisted CVD process,” *J Mater Chem B*, vol. 6, no. 4, pp. 614–623, 2018, doi: 10.1039/c7tb02473h.
- [52] A. Ziesche, J. Bergelt, H. Deubel, and F. H. Hamker, “Pre- and post-saccadic stimulus timing in saccadic suppression of displacement – A computational model,” *Vision Res*, vol. 138, pp. 1–11, Sep. 2017, doi: 10.1016/j.visres.2017.06.007.
- [53] J. A. Finlay, M. E. Callow, L. K. Ista, G. P. Lopez, and J. A. Callow, “The Influence of Surface Wettability on the Adhesion Strength of Settled Spores of the Green Alga *Enteromorpha* and the Diatom *Amphora* 1,” 2002. [Online]. Available: <http://icb.oxfordjournals.org/>
- [54] A. M. C. Maan, A. H. Hofman, W. M. de Vos, and M. Kamperman, “Recent Developments and Practical Feasibility of Polymer-Based Antifouling Coatings,” *Advanced Functional Materials*, vol. 30, no. 32. Wiley-VCH Verlag, Aug. 01, 2020. doi: 10.1002/adfm.202000936.
- [55] L. Carlsson *et al.*, “Modification of cellulose model surfaces by cationic polymer latexes prepared by RAFT-mediated surfactant-free emulsion polymerization,” *Polym Chem*, vol. 5, no. 20, pp. 6076–6086, Oct. 2014, doi: 10.1039/c4py00675e.
- [56] T. E. Irving and D. G. Allen, “Species and material considerations in the formation and development of microalgal biofilms,” *Appl Microbiol Biotechnol*, vol. 92, no. 2, pp. 283–294, Oct. 2011, doi: 10.1007/s00253-011-3341-0.
- [57] M. E. Callow and R. L. Fletcher, “The Influence of Low Surface Energy Materials on Bioadhesion a Review,” 1994.
- [58] Y. Pu *et al.*, “Synthesis and Antibacterial Study of Sulfobetaine/Quaternary Ammonium-Modified Star-Shaped Poly[2-(dimethylamino)ethyl methacrylate]-Based Copolymers with an Inorganic Core,” *Biomacromolecules*, vol. 18, no. 1, pp. 44–55, Jan. 2017, doi: 10.1021/acs.biomac.6b01279.
- [59] T. Dai, Y.-Y. Huang, S. K. Sharma, J. T. Hashmi, D. B. Kurup, and M. R. Hamblin, “Topical Antimicrobials for Burn Wound Infections,” 2010.
- [60] Y. J. Oh, E. S. Khan, A. Del Campo, P. Hinterdorfer, and B. Li, “Nanoscale Characteristics and Antimicrobial Properties of (SI-ATRP)-Seeded Polymer Brush

- Surfaces,” *ACS Appl Mater Interfaces*, vol. 11, no. 32, pp. 29312–29319, Aug. 2019, doi: 10.1021/acsami.9b09885.
- [61] A. C. Dimian, C. S. Bildea, and A. A. Kiss, “Acrylic Acid,” in *Applications in Design and Simulation of Sustainable Chemical Processes*, Elsevier, 2019, pp. 521–569. doi: 10.1016/B978-0-444-63876-2.00014-0.
- [62] B. Deng *et al.*, “Antifouling microfiltration membranes prepared from acrylic acid or methacrylic acid grafted poly(vinylidene fluoride) powder synthesized via pre-irradiation induced graft polymerization,” *J Memb Sci*, vol. 350, no. 1–2, pp. 252–258, Mar. 2010, doi: 10.1016/j.memsci.2009.12.035.
- [63] N. Deka, A. Bera, D. Roy, and P. De, “Methyl Methacrylate-Based Copolymers: Recent Developments in the Areas of Transparent and Stretchable Active Matrices,” *ACS Omega*, vol. 7, no. 42. American Chemical Society, pp. 36929–36944, Oct. 25, 2022. doi: 10.1021/acsomega.2c04564.
- [64] T. Sychaj and D. Berek, “Thermodynamic and hydrodynamic properties of the systems polymer-tetrahydrofuran-water 1. Solution properties of polystyrene.” [Online]. Available: <https://www.researchgate.net/publication/342690361>
- [65] A. Ghosh, M. R. Haverly, J. K. Lindstrom, P. A. Johnston, and R. C. Brown, “Tetrahydrofuran-based two-step solvent liquefaction process for production of lignocellulosic sugars,” *React Chem Eng*, vol. 5, no. 9, pp. 1694–1707, Sep. 2020, doi: 10.1039/d0re00192a.
- [66] V. V. Kusumkar, M. Galamboš, E. Viglašová, M. Daňo, and J. Šmelková, “Ion-imprinted polymers: Synthesis, characterization, and adsorption of radionuclides,” *Materials*, vol. 14, no. 5, pp. 1–29, Mar. 2021, doi: 10.3390/ma14051083.
- [67] D. Rawtani and Y. K. Agrawal, “ARTICLE Nanobiomedicine Emerging Strategies and Applications of Layer-by-layer Self-Assembly,” 2014.
- [68] Y. Pan *et al.*, “Layer-by-Layer Self-Assembly Coating for Multi-Functionalized Fabrics: A Scientometric Analysis in CiteSpace (2005–2021),” *Molecules*, vol. 27, no. 19. MDPI, Oct. 01, 2022. doi: 10.3390/molecules27196767.
- [69] E. Acosta, “Thin Films/Properties and Applications.” [Online]. Available: www.intechopen.com
- [70] “Thin Film Technology/Physics of Thin Films’ 81 4. Properties and Characterization of Thin Films 4. 1. Film Thickness 4.1.”
- [71] M. Čekada, “PROPERTIES AND CHARACTERIZATION OF THIN FILMS.” [Online]. Available: www.worldscientific.com
- [72] K. L. Materna and L. Hammarström, “Photoredox Catalysis Using Heterogenized Iridium Complexes**,” *Chemistry - A European Journal*, vol. 27, no. 68, pp. 16966–16977, Dec. 2021, doi: 10.1002/chem.202101651.

- [73] M. I. Hossain and S. Mansour, “A critical overview of thin films coating technologies for energy applications,” *Cogent Engineering*, vol. 10, no. 1. Cogent OA, 2023. doi: 10.1080/23311916.2023.2179467.
- [74] M. Criado-Gonzalez, C. Mijangos, and R. Hernández, “Polyelectrolyte multilayer films based on natural polymers: From fundamentals to Bio-Applications,” *Polymers*, vol. 13, no. 14. MDPI AG, Jul. 02, 2021. doi: 10.3390/polym13142254.
- [75] A. Papagiannopoulos, “Current Research on Polyelectrolyte Nanostructures: From Molecular Interactions to Biomedical Applications,” *Macromol*, vol. 1, no. 2. Multidisciplinary Digital Publishing Institute (MDPI), pp. 155–172, Jun. 01, 2021. doi: 10.3390/macromol1020012.
- [76] A. Sill, P. Nestler, A. Weltmeyer, M. Paßvogel, S. Neuber, and C. A. Helm, “Polyelectrolyte Multilayer Films from Mixtures of Polyanions: Different Compositions in Films and Deposition Solutions,” *Macromolecules*, vol. 53, no. 16, pp. 7107–7118, Aug. 2020, doi: 10.1021/acs.macromol.0c01089.
- [77] L. Mhamdi *et al.*, “Study of the polyelectrolyte multilayer thin films’ properties and correlation with the behavior of the human gingival fibroblasts,” in *Materials Science and Engineering C*, Mar. 2006, pp. 273–281. doi: 10.1016/j.msec.2005.10.049.
- [78] Ajaya Bhattarai, “A Review on Polyelectrolytes (PES) and Polyelectrolyte Complexes (PECs),” *International Journal of Engineering Research and*, vol. V9, no. 08, Sep. 2020, doi: 10.17577/IJERTV9IS080112.
- [79] J. Mendez Garza *et al.*, “Polymer Layers as Multicompartment Films,” *Langmuir*, vol. 21, no. 26, 2005, doi: 10.1021/la051465b.
- [80] A. Garg, J. R. Heflin, H. W. Gibson, and R. M. Davis, “Study of film structure and adsorption kinetics of polyelectrolyte multilayer films: Effect of pH and polymer concentration,” *Langmuir*, vol. 24, no. 19, pp. 10887–10894, Oct. 2008, doi: 10.1021/la8005053.
- [81] G. Rydzek *et al.*, “PH-Responsive Saloplastics Based on Weak Polyelectrolytes: From Molecular Processes to Material Scale Properties,” *Macromolecules*, vol. 51, no. 12, pp. 4424–4434, Jun. 2018, doi: 10.1021/acs.macromol.8b00609.
- [82] P. Jagtap, K. Patil, and P. Dhattrak, “Polyelectrolyte Complex for Drug Delivery in Biomedical Applications: A Review,” *IOP Conf Ser Mater Sci Eng*, vol. 1183, no. 1, p. 012007, Sep. 2021, doi: 10.1088/1757-899x/1183/1/012007.
- [83] M. Cloutier, D. Mantovani, and F. Rosei, “Antibacterial Coatings: Challenges, Perspectives, and Opportunities,” *Trends in Biotechnology*, vol. 33, no. 11. Elsevier Ltd, pp. 637–652, Nov. 01, 2015. doi: 10.1016/j.tibtech.2015.09.002.
- [84] C. Maxime, T. Michael, and M. Diego, “Strategies for controlled release of biocidal silver ions from plasma-deposited antibacterial coatings,” *Front Bioeng Biotechnol*, vol. 4, 2016, doi: 10.3389/conf.fbioe.2016.01.02479.

- [85] X. Tian and Y. R. Qiu, “2-methoxyethylacrylate modified polyurethane membrane and its blood compatibility,” *Prog Biophys Mol Biol*, vol. 148, pp. 39–46, Nov. 2019, doi: 10.1016/j.pbiomolbio.2017.10.003.
- [86] C. Chen, J. Illergård, L. Wågberg, and M. Ek, “Effect of cationic polyelectrolytes in contact-Active antibacterial layer-by-layer functionalization,” *Holzforschung*, vol. 71, no. 7–8, pp. 649–658, Jul. 2017, doi: 10.1515/hf-2016-0184.
- [87] S. Vijay, O. P. Sati, and D. K. Majumdar, “Acrylic acid-methyl methacrylate copolymer for oral prolonged drug release,” *J Mater Sci Mater Med*, vol. 21, no. 9, pp. 2583–2592, Sep. 2010, doi: 10.1007/s10856-010-4104-7.
- [88] A. K. Sarkar, D. Sarmah, S. Baruah, and P. Datta, “An Optimized Dip Coating Approach for Metallic, Dielectric, and Semiconducting Nanomaterial-Based Optical Thin Film Fabrication,” *Coatings*, vol. 13, no. 8, Aug. 2023, doi: 10.3390/coatings13081391.
- [89] M. N. Chaudhari, “Thin film Deposition Methods: A Critical Review,” *Int J Res Appl Sci Eng Technol*, vol. 9, no. VI, pp. 5215–5232, Jun. 2021, doi: 10.22214/ijraset.2021.36154.
- [90] S. Javaid, A. Mahmood, H. Nasir, M. Iqbal, N. Ahmed, and N. M. Ahmad, “Layer-By-Layer Self-Assembled Dip Coating for Antifouling Functionalized Finishing of Cotton Textile,” *Polymers (Basel)*, vol. 14, no. 13, Jul. 2022, doi: 10.3390/polym14132540.
- [91] T. Swift, L. Swanson, M. Geoghegan, and S. Rimmer, “The pH-responsive behaviour of poly(acrylic acid) in aqueous solution is dependent on molar mass,” *Soft Matter*, vol. 12, no. 9, pp. 2542–2549, 2016, doi: 10.1039/c5sm02693h.
- [92] T. Swift, L. Swanson, M. Geoghegan, and S. Rimmer, “The pH-responsive behaviour of poly(acrylic acid) in aqueous solution is dependent on molar mass,” *Soft Matter*, vol. 12, no. 9, pp. 2542–2549, 2016, doi: 10.1039/c5sm02693h.
- [93] H. M. Ng, N. M. Saidi, F. S. Omar, K. Ramesh, S. Ramesh, and S. Bashir, “Thermogravimetric Analysis of Polymers,” in *Encyclopedia of Polymer Science and Technology*, Wiley, 2018, pp. 1–29. doi: 10.1002/0471440264.pst667.
- [94] C. Schick, “Differential scanning calorimetry (DSC) of semicrystalline polymers,” *Analytical and Bioanalytical Chemistry*, vol. 395, no. 6, pp. 1589–1611, Nov. 2009. doi: 10.1007/s00216-009-3169-y.
- [95] E. Ghanbari, S. J. Picken, and J. H. van Esch, “Analysis of differential scanning calorimetry (DSC): determining the transition temperatures, and enthalpy and heat capacity changes in multicomponent systems by analytical model fitting,” *J Therm Anal Calorim*, vol. 148, no. 22, pp. 12393–12409, Nov. 2023, doi: 10.1007/s10973-023-12356-1.
- [96] L. Tao, K. Vojnits, M. I. Lam, X. Lu, S. Pakpour, and J. Liu, “Antibacterial Activity of Zinc Oxide Thin Films by Atomic Layer Deposition for Personal Protective Equipment Applications.”
- [97] S. Mushtaq, N. M. Ahmad, H. Nasir, A. Mahmood, and H. A. Janjua, “Transpicuous-Cum-Fouling Resistant Copolymers of 3-Sulfopropyl Methacrylate and Methyl

- Methacrylate for Optronics Applications in Aquatic Medium and Healthcare,” *Advances in Polymer Technology*, vol. 2020, 2020, doi: 10.1155/2020/5392074.
- [98] H. Coceancigh, D. A. Higgins, and T. Ito, “Optical Microscopic Techniques for Synthetic Polymer Characterization,” *Analytical Chemistry*, vol. 91, no. 1. American Chemical Society, pp. 405–424, Jan. 02, 2019. doi: 10.1021/acs.analchem.8b04694.
- [99] A. Diaspro and C. Usai, “Optical Microscopy,” in *Wiley Encyclopedia of Biomedical Engineering*, Wiley, 2006. doi: 10.1002/9780471740360.ebs0869.
- [100] R. Yordanov, M. Ohlidal, O. Salyk, and I. Zhivkov, “Film thickness measurement by optical profilometer MicroProf® FRT,” 2013. [Online]. Available: <https://www.researchgate.net/publication/289136814>
- [101] M. Ledinský *et al.*, “Profilometry of thin films on rough substrates by Raman spectroscopy,” *Sci Rep*, vol. 6, Dec. 2016, doi: 10.1038/srep37859.
- [102] M. F. M. Costa, “Thin Films’ Residual Stress Measurement by Optical Profilometry,” 2001. [Online]. Available: <http://proceedings.spiedigitallibrary.org/>